Characterization of CorS, a histidine protein kinase involved in temperature-dependent synthesis of the phytotoxin coronatine in *Pseudomonas syringae*

Dissertation

zur

Erlangung des Doktorgrades

der Naturwissenschaften

(Dr. rer. nat.)

dem

Fachbereich Biologie

der Philipps-Universität Marburg

vorgelegt von

Angela Vladimirovna Smirnova

aus

Odessa/Ukraine

Marburg/Lahn 2001

Vom Fachbereich Biologie der Philipps-Universität Marburg

Als Dissertation am 13.06.2001 angenommen.

Erstgutachter: **PD Dr. M.S. Ullrich**

Zweitgutachter: **Prof. Dr. R.K. Thauer**

Die öffentliche Disputation der Dissertation erfolgte am 17.07.2001

Meinen Eltern und Lehrern

Моим родителям и учителям

Im Zusammenhang mit der Thematik der vorliegenden Dissertation wurde folgende Publikation erstellt:

Smirnova, A., Wang, L., Rohde, B., Budde, I., Weingart, H., and Ullrich, M. (2001). Control of temperature-responsive synthesis of the phytotoxin in *Pseudomonas syringae* by the two-component system CorRPS. *J. Mol. Microbiol. Biotechnol.*, in press.

CONTENTS

ABBREVIATIONS

A_{xxxnm}	Absorbance at xxx nm
AEBSF	[4-(2-aminoethyl)-benzensulfonyl fluoride hydrochloride
APS	ammonium peroxodisulfate
ATP	adenosine 5'-triphosphosphate
BA	benzyl alcohol
bp	base pair
BSA	bovine serum albumin
CA	catalytic and ATP-binding domain
CHAPS	3-[(3-cholamidopropyl)-dimethylammonio]-1-propanesulfonate
CFA	coronafacic acid
Cfl	coronafacate ligase
CMA	coronamic acid
COR	coronatine
CSPD	disodium 3-(4-methoxyspiro{1,2-dioxetane-3,2'-(5'chloro)tricyclo [3.3.1.1^{3,7}]decan}-4-yl)phenyl phosphate
D	aspartate residue
DHp	dimerization and histidine phosphotransfer domain
DNA	deoxyribonucleic acid
DNase	deoxyribonuclease
dNTP	deoxyribonucleoside 5'-triphosphosphates
DTT	dithiotreitol
DUF5	domain of unknown function
E. coli	*Escherichia coli*
EDTA-Na	ethylenediaminetetraacetic acid, disodium salt
FAME	fatty acid methyl ester
g	gram
GC	gas chromatography
GUS	ß-glucuronidase
h	hour
HABA	4-hydroxyazobenzene 2-carboxylic acid
His/H	histidine residue

HPK	histidine protein kinase
HPLC	high pressure liquid chromatography
HPt	histidine-containing phosphotransfer domain
HSC	Hoitink-Sinden medium optimized for coronatine production
IPTG	isopropyl-ß-D-thiogalactopyranoside
kb	kilo bases
KB	King's B medium
kDa	kilo Dalton
LacZ	ß-galactosidase
LB	Luria-Bertani broth
MBP	maltose-binding protein
MG	mannitol-glutamate medium
mg	milligram
min	minute
ml	milliliter
MOPS	3-(N-morpholino)propanesulfonic acid
MUFA	monounsaturated fatty acid
nm	nanometer
OD_{xxxnm}	optical density at xxx nm
PAS	PER (*Drosophila* period clock protein), ARNT (vertebrate aryl hydrocarbon receptor nuclear translocator), SIM (*Drosophila* single-minded protein)
PCR	polymerase chain reaction
PhoA	alkaline phosphatase
PMSF	phenylmethylsulfonyl fluoride
pv.	pathovar
P. syringae	*Pseudomonas syringae*
RNA	ribonucleic acid
RNAse	ribonuclease
RR	response regulator
rpm	rounds per minute
SB 3-10	N-decyl-N,N-dimethyl-3-ammonio-1-propanesulfonate

SDS-PAGE	sodium dodecyl sulfate – polyacrylamide gel electrophoresis
sec/s	seconds
SFA	saturated fatty acid
TAE	Tris-acetate-EDTA
TCA	trichloroacetic acid
TE	Tris-EDTA
TEMED	N,N,N',N'-tetramethylethylenediamine
TMD	transmembrane domain
Tris	tris(hydroxymethyl)aminomethane
2-DE	two-dimensional protein gel electrophoresis
U	units
uidA	gene encoding ß-glucuronidase from *E. coli*
UV	ultraviolet
v/v	volume per volume
WT	wild type
w/v	weight per volume
X-Gal	5-bromo-4-chloro-3-indolyl-ß-galactoside
X-Gluc	5-bromo-4-chloro-3-indoyl-ß-glucuronic acid
X-PhoA	5-bromo-4-chloro-3-indoyl-phosphate-p-toluidine salt
µg	microgram
µl	microliter

1 SUMMARY

The phytotoxin coronatine (COR) is a major virulence factor of the plant pathogen *Pseudomonas syringae* PG4180. A modified two-component regulatory system consisting of two response regulators and the histidine protein kinase CorS strickly mediates thermoresponsive COR synthesis.

In this study the function of CorS in signal perception and temperature-dependent regulation of COR production was investigated. Complementation analysis of mutants defective in COR production demonstrated that fragments containing the three regulatory genes, *corR, corS,* and *corP*, could restore the thermoresponsive COR production. Biosynthetic proteins involved in the production of the COR precursors, CMA and CFA, were expressed in *Pseudomonas syringae* PG4180 in a temperature-, medium-, and CorRSP-dependent manner. Temperature shift experiments from 28°C to 18°C demonstrated that the expression of COR biosynthetic genes was not a rapid process and was not cold-shock dependent. Our assumption that fluidity of the bacterial membrane might influence the function of the membrane-associated protein CorS was supported by the finding that the fatty acid composition of *P. syringae* membranes differed at 18° and at 28°C in the portions of unsaturated, saturated fatty acids, and a cyclo fatty acid. In addition, the transcriptional activation of COR biosynthetic genes at 18°C was suppressed by addition of a membrane fluidizer. To characterize the fuction of CorS at the biochemical level, it was produced as an N-terminal *Strep*-tag II fusion protein in *E. coli*. Polyclonal antisera directed against two synthetic peptides of CorS were produced and demonstrated to function in detection of $CorS_{Strep\text{-tag}}$. Based on results with translational fusions of hybrid proteins of CorS with either PhoA or LacZ, CorS possesses six transmembrane domains (TMDs). In-frame deletions of the last or all six of these domains gave rise to a non-functional protein. Interestingly, two PhoA fusions located downstream of the sixth TMD, showed a thermoresponsive phenotype suggesting that the actual membrane topology of CorS might be involved in signal perception. The N-terminal region of CorS was randomly altered using *in vitro* ‘entranceposon’ mutagenesis in order to generate temperature-insensitive CorS derivatives.

1 ZUSAMMENFASSUNG

Bei dem Bakterium *Pseudomonas syringae* erfolgt die Bildung des Phytoxins Coronatin in einer temperaturabhängigen Weise. Die Biosynthese von COR wird durch ein modifiziertes Zwei-Komponenten-Regulationsystem kontrolliert. Dieses System besteht aus einer Sensorkinase CorS und den zwei Regulatorproteinen CorR und CorP.

Im Rahmen der vorliegenden Arbeit wurde die Funktion von CorS in der Wahrnehmung des Temperatursignals und der temperaturabhängen Regulation der COR-Biosynthese untersucht. Durch die Komplementation von COR-negativen Mutanten konnte gezeigt werden, daß Fragmente, welche die drei regulatorischen Gene *corR*, *corS* und *corP* tragen, diese Mutanten komplementieren können. Außerdem wurde nachgewiesen, daß Proteine, welche an der Biosynthese der COR-Vorläufer CMA und CFA beteiligt sind, in einer temperatur-, medium- und CorRSP-abhängigen Weise exprimiert werden. Mit Temperaturshift–Experimenten konnte gezeigt werden, daß die Genexpression bei niedriger Temperatur, jedoch nicht bei Kälteschock, relativ langsam induziert wurde. In unserer Hypothese spielt die Membranfluidität eine zentral Rolle für die Detektion des Temperatursignals durch CorS. Diese Hypothese wird durch gaschromatographische Analyse von Fettsäureprofilen von *P. syringae* bestätigt. Bei 18°C werden mehr ungesättigte Fettsäuren produziert während bei 28°C mehr gesättigte Fettsäuren, und – interessanterweise – eine zyklische Fettsäure in die Membranen eingebaut werden. Außerdem, wurde die transkriptionelle Aktivierung des *cmaABT* Promoter nach Zugabe eines Membranfluidizers bei 18°C unterdrückt. Für die weitere biochemische Charakterisierung wurde CorS heterolog in *E. coli* überproduziert. Polyklonale Antikörper, die gegen zwei synthetische Peptide von CorS gerichtet sind, wurden erzeugt und zum Nachweis von $CorS_{Strep\text{-tag}}$ verwendet. Anhand translationaler Fusionen von CorS mit alkalischer Phosphatase (PhoA) und ß-Galactosidase (LacZ) konnte gezeigt werden, daß CorS sechs membranspannende Domänen besitzt. Die in-frame Deletion von vier bzw. allen sechs membranspannenden Domänen führte zur Inaktivierung von CorS. Interessanterweise zeigen zwei PhoA-Fusionen stromabwärts der letzten membranspannenden Domäne einen temperaturabhängigen Phenotyp. Es wird vermutet, daß die Wahrnehmung des Temperatursignals durch Konformationsänderungen von CorS erfolgt. Zur Überprüfung dieser Hypothese wurde eine Mutagenese des N-Terminus von CorS im Bereich der transmembranalen Domänen durchgeführt.

2 INTRODUCTION

2.1 Bacterial thermoregulation

2.1.1 Temperature as a global environmental factor influencing cellular functions at the molecular level

Among environmental factors influencing the growth and survival of organisms, such as carbon source, osmolarity, pH, oxygen availability, and iron concentration, temperature is one of the most important. In order to survive, bacteria have to adapt to changes in temperature which often are not optimal for their growth. Following a temperature change, cells compensate for stress-induced disturbances through physiological and biochemical mechanisms of *homeoviscous* or *homeophasic* adaptation (Vigh *et al*., 1998). *Homeoviscous* adaptation implies an natural phenomenon where an organism subjected to different growth temperature adjusts its membrane lipid composition to maintain fluidity. Growth at low temperature, for example, causes changes in membrane lipid composition, including the increase of fatty acid desaturation, changes in the proportions of lipid classes and changes in the lipid:protein ratio. The modification of the fatty acid composition of the bacterial membrane is achieved by modifying the expression and the activity of enzymes such as Δ^9-desaturase, which incorporate double bonds into saturated fatty acids (Macartney *et al*., 1994). The activities of many membrane-associated enzymes also change dramatically. Changes in local lipid composition, charge, or mechanical stress can shift bilayers out of the normal functional state, thereby altering diffusion rates and many membrane-linked reactions. Living cells are in a perpetual state of dynamic biochemical activity, so a variation in any given reaction rates can have global effects on cell behavior (Jin *et al*., 1999). Maintaining the membrane at or near a fluid critical point is a significant advantage to a cell.

Because temperature has profound effects on many cellular processes, bacteria must possess molecular thermosensing devices in order to adjust to changes in temperature. For example, the low temperature inducible expression of genes for fatty acid desaturases in cyanobacteria is mediated by the coordinated action of two histidine protein kinases, Hik33 and Hik19, sensing the temperature and activating the response regulator protein Rer1 which in turn activates transcription of desaturase genes (Suzuki *et al*., 2000).

Generally, temperature-mediated molecular regulation can occur at levels of transcription, translation, or enzymatic activity and details for this will be given in 2.1.3. Specialized cases

of bacterial thermosensing are heat or cold shock responses. They are characterized by the sudden but transient accumulation of heat or cold shock proteins in the bacterial cell. One of those, the Hsp70-like chaperone DnaK has been proposed to serve as a cellular 'thermometer' (Craig & Gross, 1991). Temperature-mediated regulation of heat shock genes is controlled at the level of synthesis and stability of the alternative sigma factor σ^{32}, which recognizes heat shock promoters (Gamer *et al*., 1996). Heat-induced synthesis of σ^{32} encoded by the *rpoH* gene occurs at the translation level by melting the mRNA secondary structure formed within the 5' non-coding sequence of *rpoH* including the translation initiation region (Morita *et al*., 1999). Some heat shock proteins function as DNA-binding proteins (i.e. H-NS) while others serve as chaperons or proteases either maintaining the correct folding of protein or degrading missfolded proteins at elevated temperatures (Nakahigashi *et al*., 1999). A subset of small acidic proteins, termed cold-shock proteins, is transiently synthesized when bacterial cells are abruptly exposed to low temperature. This phenomenon was originally found in *E. coli* and later confirmed to be a cold-shock response common to many bacterial species (Graumann & Marahiel, 1996). Transient synthesis of cold-shock proteins is mediated by increased stabilization of mRNA at low temperatures. It has been proposed that some cold-shock proteins function as a RNA chaperone in the regulation of translation in the bacterial adaptation to low temperatures (Fukunaga *et al*., 1999).

2.1.2 Influence of temperature on bacterial pathogenicity

For human and animal pathogenic bacteria, temperature is a key environmental factor for colonization and invasion of their respective warm-blooded hosts. Temperatures of 37-41°C, which represent the host millieu, are important signals for these bacteria for the regulation of virulence gene expression. As examples, *Shigella flexneri*, *Yersinia* spp., *Bordetella perstussis*, *Escherichia coli*, and *Vibrio cholerae* all coordinately produce virulence factors such as pili, adhesins, invasins, or toxins optimally at these temperatures (Mekalanos, 1992). The transcription of the invasion genes in *Shigella flexneri* and enteroinvasive *Escherichia coli* is induced at 37°C and repressed at 30°C (Berlutti *et al*., 1998). Lipoproteins of *Borrelia burgdorferi*, which are a major virulence factor of these bacteria, are preferentially expressed at 35°C compared to 24°C (Haake, 2000).

In contrast, low temperature favors virulence expression in plant pathogenic bacteria. Horizontal gene transfer such as the transfer of the tumor-inducing T-DNA from *Agrobacterium tumefaciens* into the plant cell is optimal at temperatures around 22°C and

does not occur at temperatures above 29°C (Fullner *et al*., 1996). Low temperature is a favorable factor for the secretion of extracellular proteins such as pectinases, cellulases and proteases in *Erwinia catovora* and *Erwinia chrysanthemi* (Starr & Chatterjee, 1972; Lei *et al*., 1985; Lanham *et al*., 1991; Hugovieux-Cotte-Pattat *et al*., 1992). A type III protein secretion system, the *hrp* (hypersensitive response and pathogenicity) system, in *Pseudomonas syringae* and *Erwinia amylovora* is also strongly influenced by temperature: transcription of *hrp* genes of *Erwinia amylovora* is increased by low pH, nutrient starvation, and low temperature (Wei *et al*., 1992 & 2000). Avirulence proteins (Avr) which are effector proteins injected into plant cells by *P. syringae*, were secreted at maximum levels when the temperature was 18 to 22°C (van Dijk *et al*., 1999). Biosyntheses of three phytotoxins: coronatine (COR) (Palmer & Bender, 1993; Ullrich *et al*., 1995), phaseolotoxin (Rowley *et al*., 1993 & 2000) and persicomycin (Barzic, 1999), are positively regulated by low temperature in *P. syringae* species.

2.1.3 Molecular mechanisms for thermoregulation of bacterial gene expression

Thermosensing mechanisms are far from well elucidated. However, ongoing research with human pathogenic bacteria has identified at least three processes that are involved in thermoregulation: DNA supercoiling, changes in mRNA conformation, and changes in protein conformation (Hurme & Rhen, 1998).

Supercoiling is the superhelical tension adopted by chromosomal or plasmid DNA, a process regulated by the balancing activities of the two enzymes topoisomerase I and DNA gyrase (topoisomerase II). Topoisomerase I, DNA gyrase, and proteins capable of binding to curved DNA may act as direct sensors to detect temperature changes. The structure of superhelical DNA may also be affected by the presence of histone-like proteins. The histone-like protein H-NS was shown to be involved in the temperature-dependent regulation of Pap pilus production in *E. coli* by repressing *pap* gene transcription at low temperatures (Göransson *et al*., 1990). H-NS, which has the ability to bind DNA and to affect its supercoiling, can either be directly influenced by temperature (White-Zieger *et al*., 1998) or can bind to DNA when temperature causes changes in the DNA topology (Falconi *et al*., 1998). An example of the latter case is a promoter fragment of the *Shigella* regulatory gene *virF*, that is required for activation of several operons encoding invasion functions. This promoter sequence comprises two H-NS binding sites and undergoes a specific and temperature-dependent conformational change (Falconi *et al*., 1998).

Secondly, thermoregulation of cellular functions can result either from mRNA conformational changes or synthesis of antisense RNA. In *Yersinia pestis*, virulence gene regulation is mediated by the transcriptional activator LcrF. A loop structure in the Shine-Dalgarno region of *lcrF* mRNA is melted at high temperature, allowing *lcrF* translation to proceed (Hoe & Goguen, 1993). In *E. coli*, the expression of two porin proteins, OmpF and OmpC, is regulated at the transcriptional level by osmolarity, temperature, and growth phase. At high temperatures, a decrease in *ompF* expression is mediated through the binding of antisense RNA to the complementary 5´ end of the *ompF* mRNA (Anderson *at el*., 1989).

A third mechanism of thermoregulation can occur at the level of protein conformational changes. In *Salmonella* strains the gene product of *tlpA* is an autoregulatory repressor. TlpA in its dimeric, coiled-coil folded conformation is able to bind to its target DNA and repress transcription (Hurme *at el*., 1997). Temperature increase leads to a shift in equilibrium between folded oligomers and non-functional unfolded monomers.

In many other cases it remains unknown how temperature changes influence gene expression. Two-component regulatory systems consisting of an environmental sensor kinase and a response regulator are often used by pathogenic bacteria to regulate virulence gene expression. The BvgSA two-component regulatory system in *Bordetella pertussis* responds to signals such as temperature, SO_4, and nicotinic acid (Melton & Weiss, 1989). Constitutive mutations in the sensor kinase BvgS affected the response to all of these stimuli, suggesting strongly that temperature is an environmental signal sensed by this system (Knapp & Mekalanos, 1988). However, the actual temperature sensing mechanism of the BvgSA system remains unclear.

Although there are many examples for thermoregulation of virulence in plant pathogenic bacteria, little is known about the detailed molecular mechanisms of temperature sensing and temperature signal transduction. The expression of virulence (*vir)* genes of the *Agrobacterium tumefaciens* Ti-plasmid which are essential for tumor formation is mediated by three gene products: VirA, VirG, and ChvE (Stachel & Zambryski, 1986; Cangelosi *et al*., 1990). VirA and VirG form a two-component regulatory system. VirA is the environmental sensor kinase sensing phenolic compounds produced by wounded plants. Both the autophosphorylation of VirA and the subsequent transfer of phosphate to its cognate response regulator, VirG, were shown to be repressed by temperatures above 32°C (Jin *et al*., 1993). This finding correlated with the reduced *vir* gene expression observed at these temperatures. Additionally, it was demonstrated that the assembly of the products of the *virB* operon to a type IV-like pilus

structure contributes to the temperature-sensitivity of the export of oncogenic T-DNA from *Agrobacterium tumefaciens* (Lai & Kado, 1998; Banta *et al*., 1998).

Temperature-dependent expression of the gene for phaseolotoxin-resistant ornithine carbamoyltransferase (ROCT), *argK*, and phaseolotoxin production in *P. syringae* pv. phaseolicola is negatively regulated by binding of an as yet unknown protein(s) to a upstream DNA region of *argK* (Rowley *at al*., 1993 & 2000). This unknown protein is produced only at 28°C.

In the case of the phytotoxin coronatine produced by *P. syringae* pv. glycinea, a modified two-component regulatory system consisting of an environmental sensor kinase CorS and two response regulators, CorR and CorP, regulates thermoresponsive COR production (Ullrich *et al*., 1995). The histidine protein kinase CorS responds to a temperature change, presumably via autophosphorylation of its conserved histidine residue, and transduces the signal to its cognate response regulators CorR and CorP via phosphorylation of their conserved aspartate residues. *In vitro* results indicated that CorR was able to bind to COR biosynthetic promoter regions in a temperature- and CorS-dependent manner (Peñaloza-Vázquez & Bender, 1998; Wang *et al*., 1999).

2.2 Signal transduction by two-component regulatory systems

2.2.1 Bacterial signal transduction

Like all living organisms, pathogenic bacteria have developed efficient systems to scout their surrounding and adapt their life according to the signals they sense. These signals can be divided into three main categories: those derived from the physical environment (abiotic), those derived from other organisms (biotic), and intra-species signals (population signals). The signals perceived from the environment can be of physical or chemical nature, such as temperature, osmolarity, pH, light, CO_2, ammonia, oxygen, metal ions, or nutrients. Biotic signals usually are of wide range. Intra-species signals usually are diffusable molecules produced by bacteria which accumulate in the growth environment and rise in concentration as the bacterial cell density increases (Hellingwerf *et al*., 1998).

The basic mechanism of signal transmission by two-component systems is a phosphorylation cascade that involves histidine and aspartate residues (Swanson *et al*., 1994). A classical two-component system consists of a histidine protein kinase (HPK) and a response regulator (RR), both of which are characterized by a receiver and a transmitter domain. A one-step phosphotransfer occurs between the HPK and the RR. However, the first reaction in the

signalling cascade is autophosphorylation of a highly conserved histidine residue of the HPK's transmitter module. This reaction is under the control of the HPK's sensory or receiver domain which responds to environmental signals. The phosphate group is subsequently transferred from the HPK to an aspartyl residue of the conserved N-terminal receiver module of the RR. This induces activation of the transmitter domain, which often contains a conserved helix-turn-helix DNA binding motif. The transmitter domain subsequently binds specifically to target DNA regions in order to activate the signal-dependent gene expression (Hoch, 2000).

There are numerous examples of 'classical' two component regulatory systems. The best studied systems in *E. coli* are EnvZ/OmpR for regulation of porin expression in response to osmolarity and CheA/CheY for regulation of the flagellar switch in response to chemotactic signals. Unorthodox systems are characterized by a multistep phosphorelay that alternates between several histidine and aspartate residues (His-Asp-His-Asp). Examples are ArcB/ArcA of *E. coli* for control of aerobic respiratory enzymes and BvgS/BvgA of *Bordetella pertussis* for regulation of virulence genes (Perraud *et al*., 1999). The complexity of phosphorelay transfer in unorthodox systems might be required for the efficient adaptation to changing environmental conditions where the adaptive response must proceed in both directions; that is, the response reactions must not only be inducible, but also must be switched off immediately under divergent conditions. In the case of pathogenic bacteria this might be essential for successful invasion and growth in susceptible hosts.

2.2.2 Structure and function of histidine protein kinases

Most HPKs are intrinsic membrane proteins with two or more N-terminal transmembrane α-helices. The C-terminus forms an independently folded domain, extends into the cytoplasm, can bind ATP, and displays autokinase activity. This C-terminal autokinase domain, which is also called the 'transmitter' domain, is approximately 250 amino acyl residues in size and functions in all members of the sensor kinase family in the same manner (Hellingwerf *et al*., 1998). Within this domain a conserved histidyl residue (H box) and several signature sequences can be detected. These are termed the N, D, F, and G boxes (**Fig. 1**) and together are summarized as the catalytic and ATP-binding domain (CA) (Bilwes *et al*., 1999). Glycine-rich sequences of the G boxes are important for ATP-binding. When the N-terminal receiver domain of the bifunctional HPK for nitrogen regulation (NtrB) was deleted, NtrB exhibited a constitutive positive phenotype (Kramer & Weiss, 1999). Additional deletion of the G box from NtrB resulted in a constitutive negative phenotype. It was demonstrated *in vitro* that

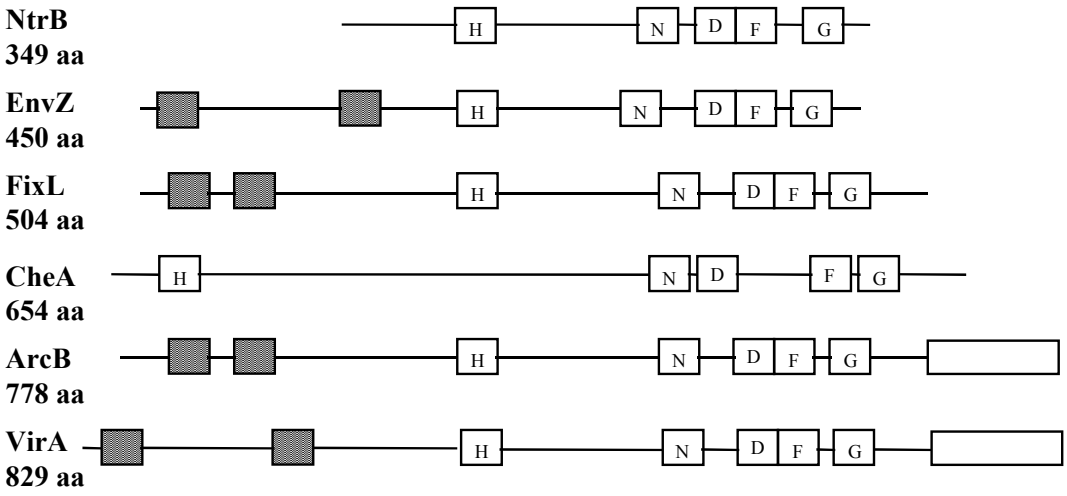

Fig.1. Organization of sequence motifs designated as H, N, D, F and G boxes in various HPKs. C-terminally attached RR domains are indicated by white boxes, and hydrophobic sequences are indicated by gray boxes.

the constitutive negative phenotype of NtrB fragments lacking the G box was caused by stimulation of dephosphorylation of the cognate response regulator, NtrC-P. The function of the N box is still unresolved. It was speculated that this domain might stabilize the H domain and possibly represents a hinge domain necessary for proper alignment of the H and G domains (Kramer & Weiss, 1999). However, mutations in the N box of EnvZ gave rise to a kinase-negative, phosphatase-positive phenotype suggesting the crucial role of the N box in kinase activity (Hsing *et al*., 1998). Moreover, as shown by UV-cross-linking experiments, a mutant in the N box did not bind ATP, as opposed to the wild type EnvZ. This was consistent with the prediction that the N box is involved in nucleotide binding (Hsing *et al*., 1998). The D box contains a conserved DXG motif. Mutations in the conserved D and F boxes of EnvZ resulted in a kinase-negative, phosphatase-positive phenotype confirming the importance of the D and F boxes for kinase activity (Hsing *et al*., 1998). Based on the comparison of three-dimensional structures of two histidine kinases (EnvZ and CheA) and three ATPases (Hsp90, DNA gyrase B, and MutL), remarkable structural homology was found among CA domains (Dutta *et al*., 1999). However, a conserved glutamate residue in the N box of GyrB which had been identified as a catalytic residue of ATPases (Jackson & Maxwell, 1993) is substituted by an asparagine residue in most HPKs. It has been suggested that this substitution may account for the difference in enzymatic activity of the two domains (Bilwes *et al*., 1999).

Dimerization was shown to be essential for the activity of the HPKs CheA and NtrB (Surette *et al*., 1996; Jiang *et al*., 2000). Recent progress in the three-dimensional structure determination of EnvZ and CheA has revealed common features as well as a difference in the position of their dimerization domains (Dutta *et al*., 1999). Based on this finding, HPKs can be divided into two classes. In class I HPKs, which are exemplified by EnvZ, the H box is directly linked to the region that contains the CA domain (D, G, F, N boxes). In contrast, in class II HPKs like CheA, the H box is separated from the CA domain by insertion of distinct domains (**Fig. 2**). The histidine kinase segment of EnvZ consists of two complementary functional domains: a 67-residues substrate and dimerization domain containing the H box, which is henceforth referred to as the DHp domain (Dimerization and Histidine phosphostransfer), and a 161-residues CA domain. The substrate domain for autophosphorylation in EnvZ itself functions as the dimerization domain, forming a four-helix core (DHp domain). Each of the two CA domains within a dimer flanks this central core in such a way that its ATP-binding pocket faces the histidine-presenting α-helix of the twin subunit. In this way a conserved His on the partner subunit within a dimer can be phosphorylated in trans. However, in CheA, the dimerization domain still forms the central four-helix core, but here it does not serve as the substrate domain. Moreover, it became evident from the crystal structure that the ATP-binding pocket of the CA domain faces away from the dimerization domain. It appears that CheA has three independent four-helix bundles, one at the center for dimerizing, the other two HPt (Histidine-containing Phosphotransfer)

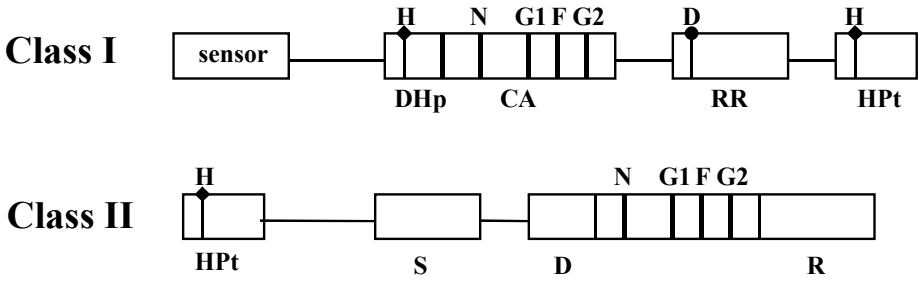

Fig. 2. Schematic diagram of the two classes of HPKs. In class I HPKs, the conserved His residue (H) in the H box of the DHp domain is the primary autophosphorylation site. For some class I HPKs the phosphoryl group is then sequentially transferred to the conserved Asp residue (D) in the covalently-linked response regulator domain (RR) and then to the conserved His residue (H) in the H box of the HPt domain. In class II HPKs, the conserved His residue is in the H box of the HPt domain. S, substrate-binding domain; D, dimerization domain; R, regulatory domain.

domains, for presenting the substrate His residues. Each HPt domain in CheA is likely to be juxtaposed to the catalytic domain of the partner subunit in the homodimer to form an active center for trans-autophosphorylation. Such differences in dimerization ability and domain distribution might be related to the fact that among the characterized HPKs there exists a large class of bifunctional enzymes, including EnvZ, which possess both kinase and phosphatase activities. In contrast CheA, a class II HPK lacking a DHp domain, lacks phosphatase function and instead an independent protein, CheZ, is thought to dephosphorylate phospho-CheY (Levit *et al*., 1998). For most HPKs the three-dimensional structure has not been resolved yet. However, there are features among all HPK primary structures additional to those mentioned above that allow given HPKs to be assigned to either class I or class II. For class I HPKs, the residue downstream of the conserved His residue in the DHp domain is acidic, whereas in the HPt domain of class II HPKs it is either a basic residue or a serine or a threonine residue. Also, the fifth residue after the conserved His residue in DHp is always proline, whereas the fourth residue in HPt is always glycine. Another important fact is that the dimeric DHp domain has two histidine residues which can be phosphorylated, whereas the monomeric HPt domain has only one of those (Dutta *et al*., 1999). It is also important to note that the region around the conserved His residue in the DHp domain of EnvZ is flexible (Tomomori *et al*., 1999), whereas the corresponding region in CheA has been described as fairly rigid (Zhou *et al*., 1995).

2.2.3 Structural determinants for signal perception by class I histidine protein kinases

Although numerous two-component regulatory systems have been described in prokaryotic and eukaryotic organisms, little is known about their actual signals and perception mechanisms. The diversity of environmental signals implies very different ways of signal perception. However, some sub-domains have been identified in HPKs which might play a role in signal perception (**Fig. 3**). One of the best studied is the so-called PAS domain that binds heme or FAD and serves as an oxygen or redox sensor (Taylor & Zhulin, 1999). The PAS domain is directly involved in oxygen sensing by the FixL/FixJ pathway in the plant-symbiotic bacteria, *Sinorhizobium meliloti* and *Bradyrhizobium japonicum*, where the expression of nitrogen fixation genes is induced under low oxygen concentrations (De Philip *et al*., 1990).

In many cases, HPKs respond to multiple environmental stimuli. Diverse structural motifs are likely to be involved in sensing them. However, the most common structural feature of the N-terminal part of HPK is a periplasmic loop flanked by two transmembrane helices. This

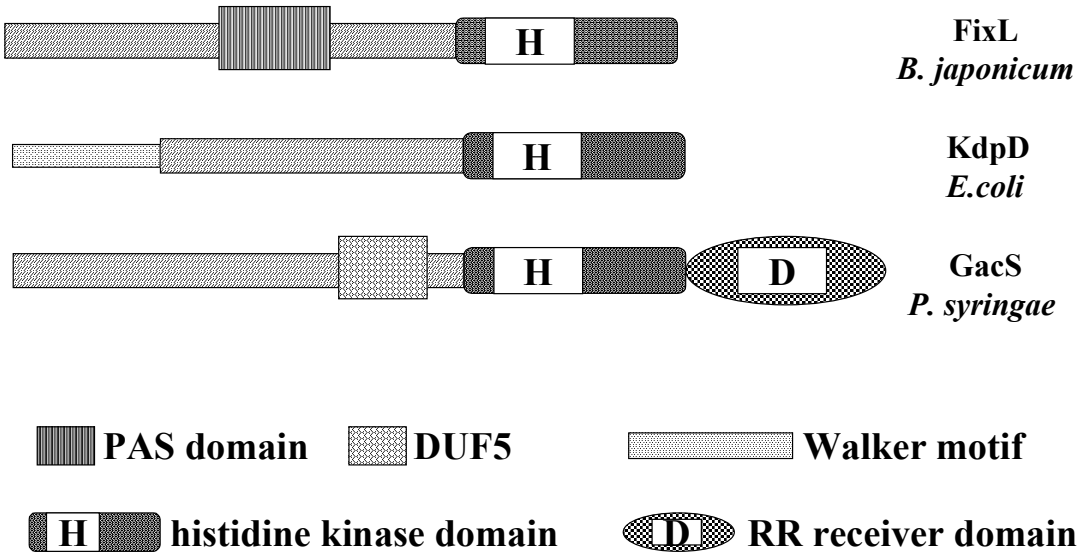

Fig. 3. Schematic representation of some structural determinants in HPKs.

architecture enables the proteins to sense external stimuli. This region presumably is involved in osmolarity sensing by EnvZ of *E. coli* (Waukau & Forst, 1999). Moreover, the periplasmic loop of CitA, the HPK of the CitAB two-component system required for induction of citrate fermentation genes in *Klebsiella pneumonae*, binds citrate as the environmental stimulus with high affinity (Kaspar *et al*., 1999). Additionally, it was proposed that Na^+ and oxygen affect the citrate metabolism by *Klebsiella pneumonae* via the CitA (Bott, 1997). The PAS domain of CitA may play a role in sensing oxygen levels (Taylor & Zhulin, 1999). The DcuSR two-component regulatory system of *E. coli* regulates the anaerobic fumarate respiratory system (Golby *et al*., 1998). The HPK DcuS possesses a periplasmic domain and senses C_4-dicarboxylate concentration externally rather than internally (Golby *et al*., 1999). Other examples for HPKs with periplasmic sensory domains are NarX, NarQ, TorS, and PhoQ in *E. coli* (Lee *et al*., 1999; Jourlin *et al*., 1996; Garcia *et al*., 1997; Castelli *et al*., 2000). In our model system, *P. syringae*, global regulation of pathogenicity is believed to be mediated by the GacSA two-component system (Hrabak & Willis, 1992). Interestingly, the unorthodox GacS HPK possesses a periplasmic sensing domain, however the substrates which able to bind to this region remain to be identified. The presence of a RR receiver domain in GacS suggests a complex signal transduction pathway mediated by this HPK.

Substrate binding to the periplasmic sensing domain of HPKs induces a conformational change which must be transduced to the respective C-terminal transmitter domain. It was proposed that a linker region between the transmembrane helices and the transmitter domain functions in signal transduction. This region is called a type P linker (periplasmic signal

transducing) or DUF5 (domain of unknown function) according to the Pfam nomenclature (Protein families database of alignments and hidden Markov model profiles). Alignment of HPKs with periplasmic sensing domains indicated that most of them contain DUF5-like domains. This domain was first identified in methyl-accepting chemotaxis proteins. Point mutations just downstream of the conserved linker region in TorS and EnvZ resulted in less responsive proteins biased towards their signalling modes (Harlocker *et al*., 1993; Park & Inouye, 1997; Jourlin *et al*., 1996). However, in many other HPKs, the importance of DUF5 domain for signal transduction remains speculative. Within the DUF5 domain two amphipathic sequences, ASI and ASII, could be identified (Williams & Stewart, 1999). It was hypothesized that as a result of signal-transducing axial movement of the second transmembrane span, ASI reorients from these membrane contacts to form new protein-protein contacts. The conserved ASII region is a reasonable candidate for making transient, signal-responsive sensor interactions with ASI. ASII is considered to be the receiver helix of the transmembrane signal transduction process. It accepts the conformational 'signal' from ASI and its conformational change ultimately regulates the downstream transmitter domain.

Walker motifs were found in two HPKs, KdpD involved in the regulation of K^+ uptake in *E. coli* (Jung & Altendorf, 1998), and ChvG involved in the regulation of virulence in *Agrobacterium tumefaciens* (Trevor & Eugene, 1993). Walker motifs represent additional ATP-binding sites. It was suggested that the phosphatase activity of KdpD is controlled by ATP binding to this site (Jung & Altendorf, 1998).

Finally, there are some HPKs which do not possess any of the above mentioned structural determinants. These sensor kinases often have multiple membrane-spanning domains in their N-terminal regions (**Fig. 4**). Such membrane integration might be necessary for signal perception since the physical state of the bacterial inner membrane might directly influence the activity of such a sensor kinase. The HPK DivJ is a member of the phosphorelay pathway regulating CtrA, a global response regulator required for multiple cell cycle events in *Caulobacter crescentus* (Ohta *et al*., 1992). DivJ has an extremely hydrophobic N-terminus, however, the relevance of this structure remains ambiguous. VirS of *Clostridium perfringens*, which is involved in regulation of virulence and pathogenicity (Cheung & Rood, 2000), and PlnB of *Lactobacillus plantarum*, which is involved in regulation of the bacteriocidal plantaricin A production (Diep *et al*., 1994) are examples of HPKs with six membrane-spanning domains. A *Pseudomonas stutzeri* HPK and the *Pseudomonas aeruginosa* HPK PilS Ethier & Boyd, 2000), both of which are involved in regulation of type IV pilus biogenesis,

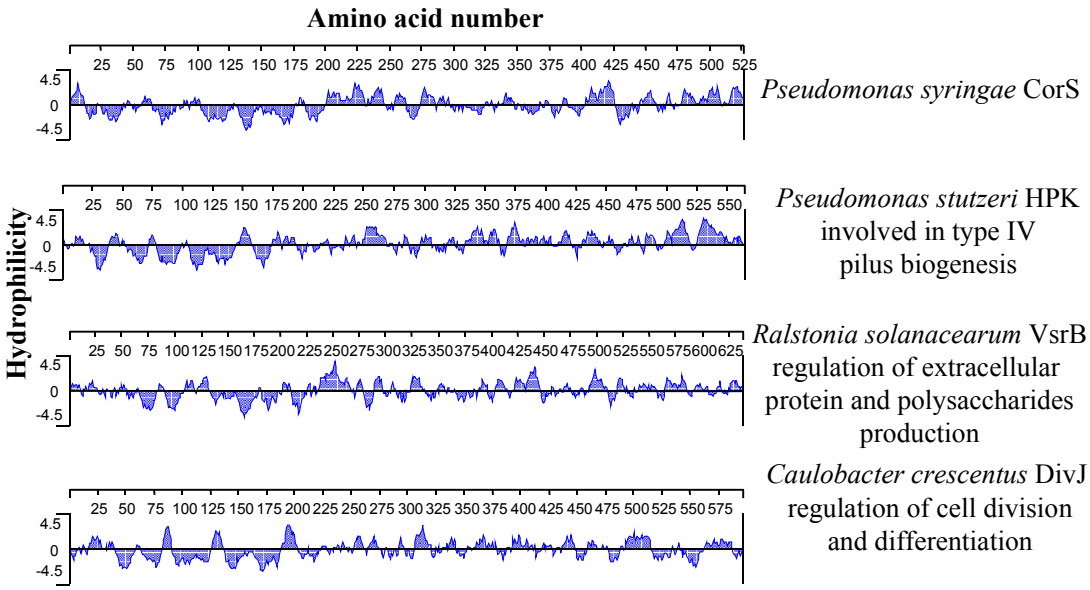

Fig. 4. Hydrophilicity plots of HPKs having multiple membrane-spanning domains in their N-terminal regions.

are additional examples of sensory proteins with six membrane-spanning domains. Moreover, highly hydrophobic N-termini have been identified in HPKs of gram-negative plant pathogenic bacteria such as VsrB of *Ralstonia solanacearum* (Huang *et al*., 1993) and RpfC of *Xanthomonas oryzae* pv. oryzae (Tang *et al*., 1996), both of which are involved in regulation of extracellular protein and polysaccharide production, and in the HPK CorS, which is involved in regulation of themoresponsive coronatine production in *Pseudomonas syringae* and which is the subject of this thesis.

2.3 The plant pathogenic bacterium *Pseudomonas syringae*

2.3.1 General characteristics of *Pseudomonas syringae*

The plant pathogenic bacterium *Pseudomonas syringae* is gram-negative, obligatory aerobic, and forms straight or slightly curved rods with polar flagella. According to the 16S rRNA classification, it belongs to the group of the γ-proteobacteria. Its genome is about 6 Mb in size and its GC-content between 56-58%. *P. syringae* can possess various indigenous plasmids of sizes ranging from 5 to 120 kb, which can mediate many virulence or fitness factors such as phytotoxins (Bender *et al*., 1991; Alarcón-Chaidez *et al*., 1999), ethylene production (Weingart *et al*., 1999), exopolysaccharide biosynthesis (Li & Ullrich, 2001), conjugative

transfer (More *et al*., 1996) and tolerances towards ultraviolet light (Sundin *et al*., 1996; Gibbon *et al*., 1999) and copper (Bender & Cooksey, 1986).

P. syringae induces a variety of symptoms on diverse host plants, including blights (rapid death of tissue), leaf spots, and galls. The species is divided into pathogenic variants (pathovars) according to their host range (Huynh *et al*., 1989; Gardan *et al*., 1999). Two distinct reactions are possible when *P. syringae* enters the plant tissue. One potential outcome is a compatible, susceptible interaction which is characterized by water soaking, a reaction which is followed by pathogen proliferation and advanced symptom development. In contrast, resistant host cells undergo a reaction known as the hypersensitive response. A cluster of genes termed the *hrp* region (for 'hypersensitive response and pathogenicity') is conserved in phytopathogenic bacteria and affects the ability of a bacterium to induce a hypersensitive response in non-host plants, the pathogenicity in host plants, and the ability to grow within plants (Collmer *et al*., 2000). The *hrp* genes are known to encode genes for the regulation and biosynthesis of a type III secretion pathway that is common to plant and animal pathogens and is used to secrete virulence proteins.

However, in addition to the *hrp* genes, phytopathogenic pseudomonads encode gene products that significantly enhance their virulence, including polysaccharides, plant hormones, phytotoxins, and cell-wall degrading enzymes. Bacterial polysaccharides are found either as a dense layer of more regularly arranged polymer structures attached to the bacterial cell walls or as loosely associated exopolysaccharides (EPSs). EPSs are thought to act as protective shields the bacterial cell, preventing desiccation and recognition by the plant, and functioning as detoxifying barriers against plant defense compounds (Rudolph & Sonnenberg, 1997). *P. syringae* produces two types of EPSs, alginate and levan. Alginate is an unbranched ß-(1,4) polysaccharide consisting of two uronic acids, β-D-mannuronic acid and its C5-epimer, α-L-glucuronate. Levan is a β-(2,6) polyfructan with extensive branching through β-(2,1) linkages (Hettwer *et al*., 1998; Li & Ullrich, 2001).

Although many phytotoxins are not required for pathogenicity, they generally function as virulence factors for this pathogen, and their production results in increased disease severity (Bender *et al*., 1999). Most toxins produced by *P. syringae* lack host specificity and cause symptoms on many plants, including some plants which cannot be infected by the toxin-producing pathogen. Toxins produced by *P. syringae* are structurally diverse and include monocyclic ß-lactams (tabtoxin), sulfodiaminophosphinyl peptides (phaseolotoxin), lipodepsinonapeptides (syringomycin), and polyketides (coronatine) (Bender, 1999). Several *P. syringae* phytotoxins show structural analogies to antibiotics that are produced via non-

ribosomal mechanisms in *Streptomyces* and *Bacillus* spp. (Stachelhaus & Marahiel, 1995; Kleinkauf & von Döhren, 1996). The modes of action of these toxins differ widely. Syringomycin targets host plasma membranes and forms ion channels in the lipid bilayers, thereby causing cytolysis (Hutchson *et al*., 1995). The syringomycin pores are freely permeable to a variety of monovalent and divalent cations. This K^+/H^+ exchange generates an electrochemical gradient and a collapse of the pH gradient of the plasma membrane, resulting in acidification of the cytoplasm. Tabtoxin irreversibly inhibits glutamine synthetase (Thomas *et al*., 1983). The inhibition of glutamine synthetase interferes with at least two major processes mediated by the enzyme: glutamine synthesis in plants and detoxification of ammonia (Turner & Debbage, 1982). Phaseolotoxin competitively inhibits ornithine carbamoyl transferase (OCTase), a critical enzyme in the urea cycle which converts ornithine and carbamoyl phosphate to citrulline. Inhibition of OCTase causes an accumulation of ornithine and a deficiency in intracellular pools of arginine, leading to chlorosis (Mitchell & Bieleski, 1977). The mode of action and biosynthesis of the polyketide phytotoxin coronatine will be discussed in 2.3.3.

2.3.2 *Pseudomonas syringae* pv. glycinea PG4180

P. syringae pv. glycinea PG4180 causes bacterial blight disease of soybean plants. The typical symptom is water-soaked lesions that develop into necrotic leaf spots surrounded by chlorotic halos. Like most *P. syringae* strains, it possesses native plasmids. Five of these were identified in strain PG4180 (Bender *et al*., 1991; Ullrich *et al*., 1993). The largest plasmid (plasmid p4180A, 95 kb) encodes all enzymes involved in the biosynthesis of the phytotoxin coronatine (**Fig. 5A**). Production of COR by PG4180 is maximal at 18°C, whereas no toxin formation can be detected at 28°C, the optimal growth temperature of *P. syringae* (**Fig. 5B**) (Budde *et al*., 1998). However, COR production is not the only virulence factor regulated by temperature. PG4180 produces significantly more slime (levan) at low temperature as compared to the optimal growth temperature (Hettwer *et al*., 1998). Recently, a miniTn*5* transposon mutagenesis revealed new thermoresponsive loci in *P. syringae* pv. glycinea (Ullrich *et al*., 2000).

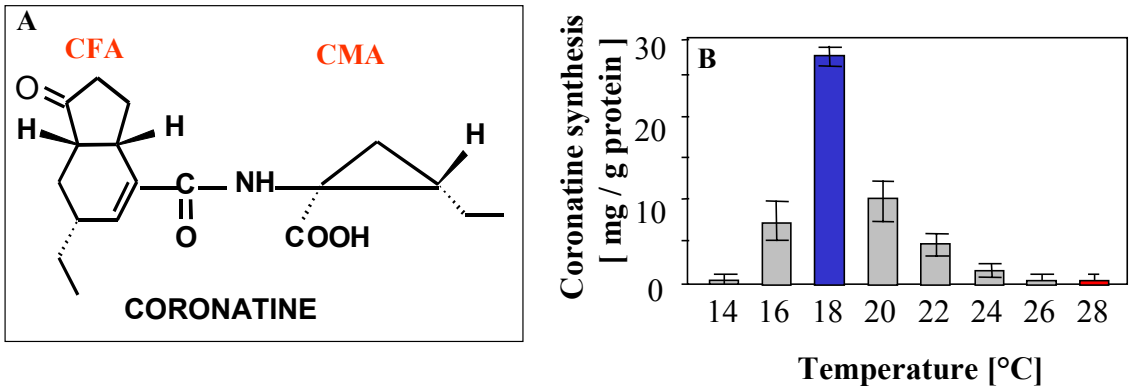

Fig. 5. Structure of coronatine (A) and temperature-dependent coronatine production (B).

2.3.3 Phytotoxin coronatine

P. syringae pv. glycinea and the closely related pathovars atropurpurea, morsprunorum, maculicola, and tomato produce the non-host specific polyketide phytotoxin COR (Mitchell, 1982). However, *P. syringae* pv. glycinea PG4180 produces significantly more COR as compared to other pathovars. The biological effects of COR include the induction of leaf chlorosis (**Fig. 6**), hypertrophy of plant storage tissue, compression of thyllakoids, thickening of plant cell walls, and accumulation of plant-borne protease inhibitors (Sakai *et al*., 1979; Mitchell, 1982; Palmer & Bender, 1995). The final step of COR production is presumed to be the coupling of the polyketide coronafacic acid (CFA) and coronamic acid (CMA) by an amide bond formation (**Fig. 5A)** (Mitchell, 1982). The enzyme(s) catalyzing this reaction is

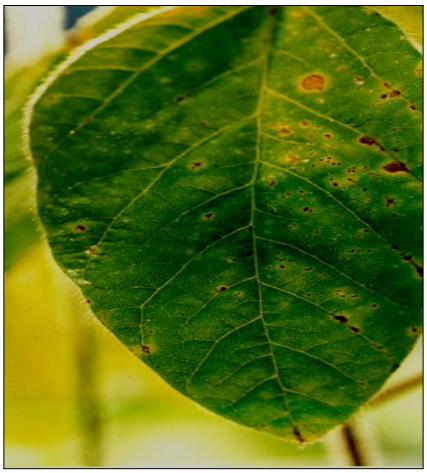

Fig. 6. Typical symptoms of bacterial blight disease caused by *Pseudomomas syringae* pv. glycinea on a soybean leaf.

thought to lack rigid specificity for the amino acid substrate since a variety of coronafacoyl-amino acid conjugates have been isolated, including CFA-L-isoleucine, CFA-L-*allo*isoleucine, CFA-L-valine, norcoronatine, CFA-L-serine and CFA-L-threonine (**Fig. 7**) (Mitchell, 1985; Mitchell & Young, 1985; Mitchell & Ford, 1998). Before CFA and various amino acids are fused together, they have to be synthesized from initial substrates. Precursor feeding studies with ^{13}C-labeled substrates demonstrated that CFA is a novel polyketide synthesized from one unit of pyruvate, one unit of butyrate, and three acetate residues (Parry *et al*., 1994). Furthermore, it was proposed that L-*allo*isoleucine is the precursor of CMA (**Fig. 8, 9**) (Parry *et al*., 1991).

Enzymes involved in COR biosynthesis are encoded by a plasmid-borne 32-kb DNA region (**Fig. 10A**) consisting of two biosynthetic gene clusters, required for synthesis of CFA and CMA respectively, and a 3.4-kb regulatory region (Bender *et al*., 1996). Based on the nucleotide sequence analysis of CMA biosynthetic genes, it was suggested that CMA is synthesized via a mechanism similar to the biosynthesis of non-ribosomal peptides (Ullrich & Bender, 1994; Budde *et al*., 1998). CFA synthesis resembles the biosynthesis of antibiotics with a polyketide structure in *Streptomyces* and *Bacillus* spp. (Rangaswamy *et al*., 1998a) (**Fig. 9**). Interestingly, CFA is synthesized by both types of polyketide synthases (type I and II) (Rangaswamy *et al*., 1998b). Type I polyketide synthases are large multifunctional proteins containing catalytic sites necessary for carrying out all reactions. Type II polyketide synthases are protein complexes consisting of individual proteins with distinct functions in the biosynthetic pathway (Katz & Donadio, 1993).

The 6.9-kb DNA region required for CMA biosynthesis comprises four distinct open reading frames which share a common orientation of transcription: *cmaA, cmaB, cmaT*, and *cmaU*. Transcriptional fusion of the *cmaABT* operon to a promoterless ß-glucuronidase (*uidA*) gene indicated that CMA biosynthesis is regulated by temperature at the transcriptional level, with maximal promoter activity at 18°C (**Fig. 10B**) (Ullrich & Bender, 1994; Budde *et al*., 1998). Subsequently, nine genes (*cfa1* to *cfa9*) were identified that are required for CFA biosynthesis. Finally, the coronafacate ligase-encoding gene (*cfl*) is required for the amide linkage of CFA and CMA (**Fig. 10A**) (Liyanage *et al*., 1995a and 1995b). A transcriptional fusion of the *cfl*/CFA operon with *uidA* was also affected by temperature and showed maximal promoter activity at 18°C (**Fig. 10B**) (Liyanage *et al*., 1995b).

Furthermore, transcription of both biosynthetic operons depended on a modified two-component regulatory system encoded within the COR biosynthetic gene cluster (Ullrich *et al*., 1995). A 3.4-kb DNA fragment from the COR biosynthetic gene cluster restored

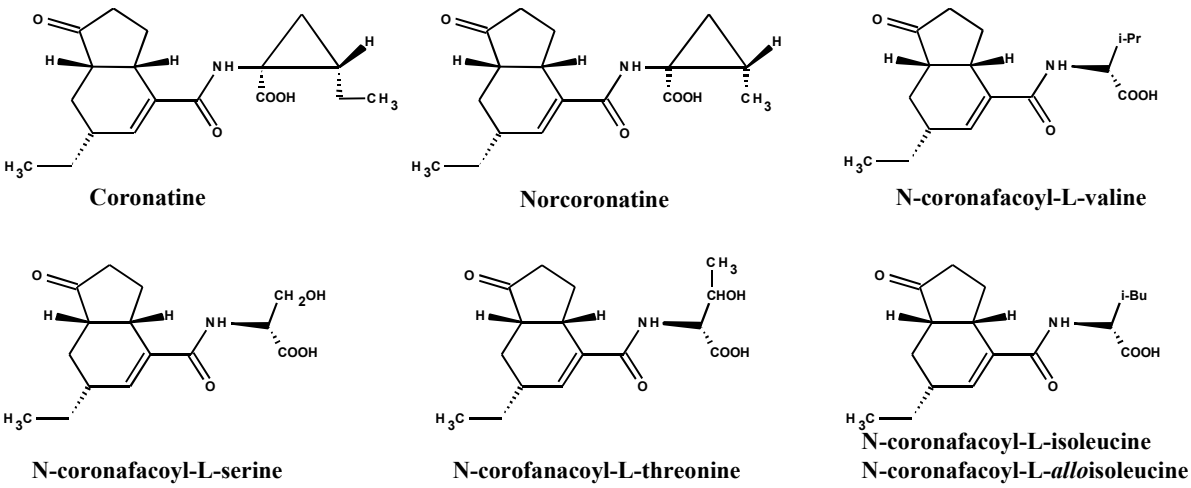

Fig. 7. Structures of coronatine and coronafacoyl compounds produced by *P. syringae*. i-Pr and i-Bu indicate isopropyl and isobutyl substituents.

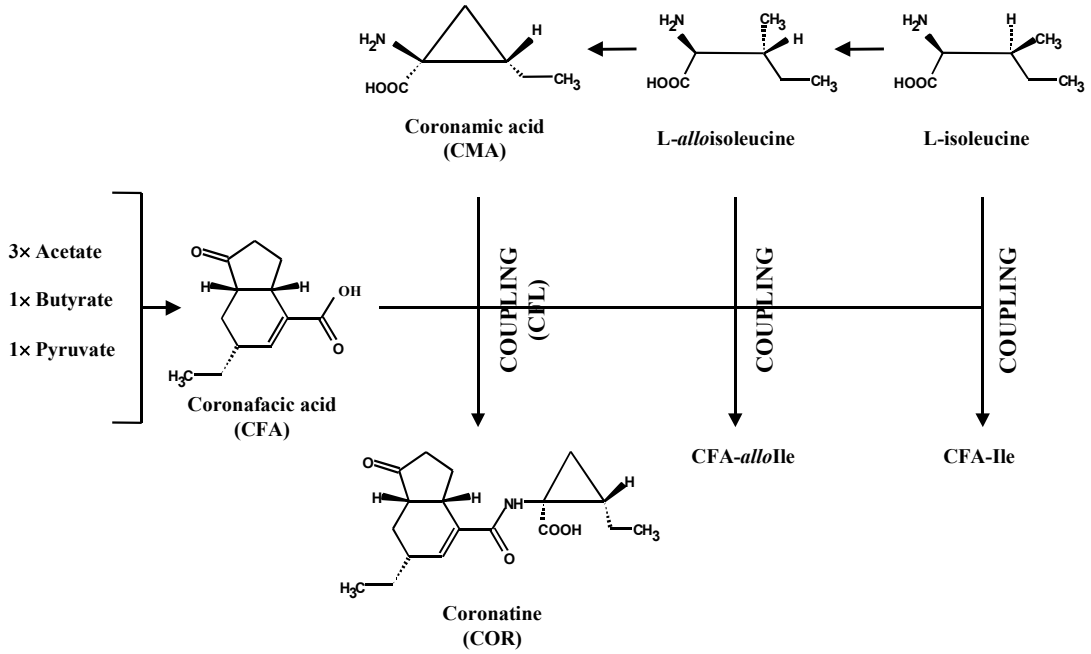

Fig. 8. Biochemical pathways involved in the synthesis of COR and coronafacoyl compounds in *P. syringae* pv. glycinea PG4180. COR consists of a polyketide component, CFA, coupled (CPL) via amide-bond formation to an amino acid component, CMA. CFA is synthesized as a branched polyketide from three acetate units, one pyruvate unit, and one butyrate unit via an unknown sequence of events. CMA is derived from isoleucine via *allo*isoleucine and cyclized by an unknown mechanism. The coronafacoyl analogues, CFA-Ile and CFA-*allo*Ile result from amide bond formation between CFA and isoleucine and *allo*isoleucine, respectively, and are not utilized further in the synthesis of COR.

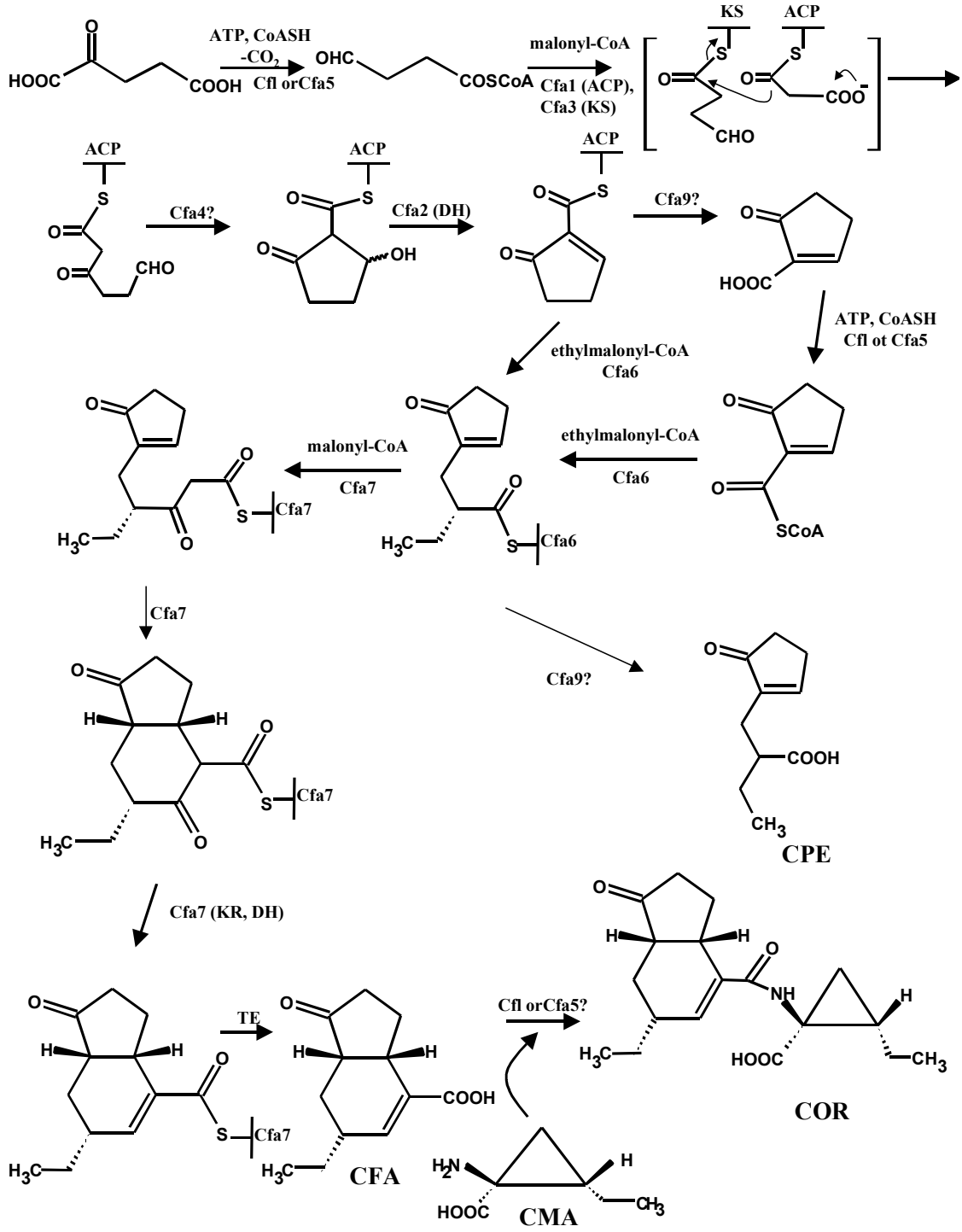

Fig. 9. Hypothetical scheme for the biosynthesis of CFA and COR. Abbreviations: ACP, acyl carrier protein; AT, acyl transferase; CFA, coronafacic acid; Cfa1-9, *P. syringae* polyketide synthases (type I and II) involved in the CFA biosynthesis; CMA, coronamic acid; COR, coronatine; CPE, 2-[1-oxo-2-cyclopenten-2-ylmethyl]butanoic acid; DH, dehydratase; KR, ketoreductase; KS, ketosynthase; TE, thioesterase.

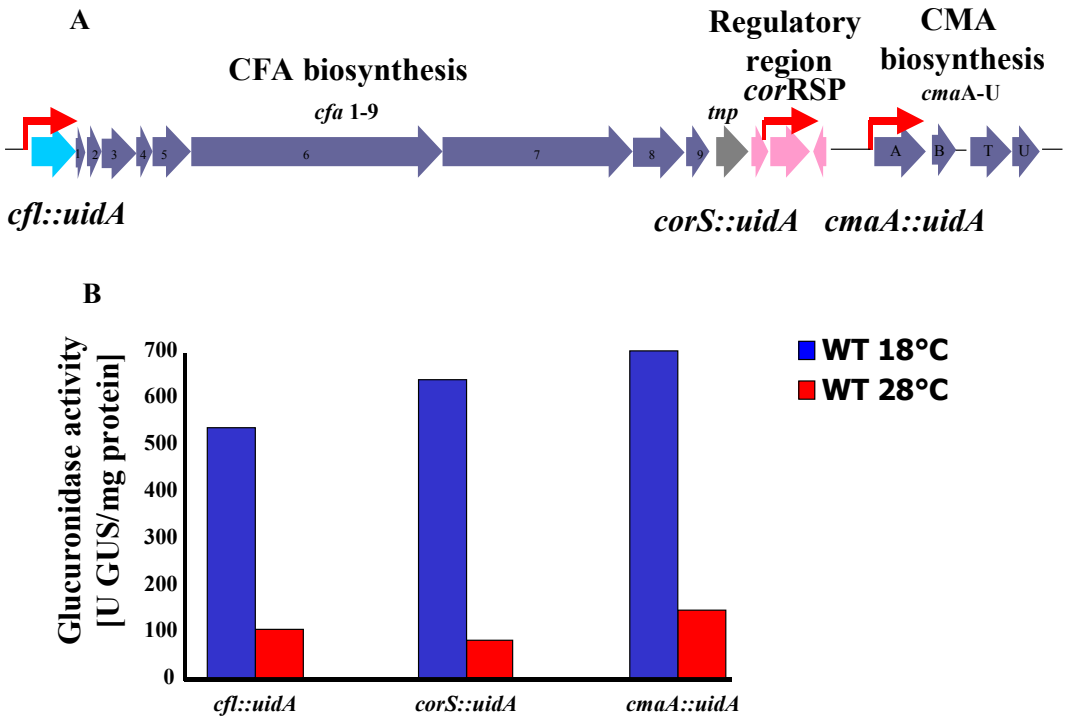

Fig. 10. (A) Schematic representation of the COR biosynthetic gene cluster of *P. syringae* pv. glycinea. Biosynthetic regions for the CMA and CFA syntheses as well as a regulatory region are indicated. Arrows indicate thremoresponsive, *cfl*, *corS*, and *cmaABT*, promoter regions. (B) Effects of temperature on *cfl::uidA*, *corS::uidA*, and *cmaA::uidA* promoter activities.

temperature-regulated phytotoxin production to Tn*5* mutants that were defective in production of both, CFA and CMA (Ullrich *et al*., 1995). Nucleotide sequence analysis of this DNA fragment revealed three genes, *corS*, *corP*, and *corR*, which encode for members of a modified two-component system consisting of an environmental sensor, the HPK CorS, and two response regulators, CorR and CorP. Despite the great similarity between CorR and CorP, only CorR contains a typical C-terminal DNA-binding motif (Ullrich *et al*., 1995). Moreover, it was shown that CorR but not CorP was able to bind specifically to a DNA region upstream of *cfl* (Peñaloza-Vázquez & Bender, 1998) and to a 218-bp DNA fragment corresponding to positions -841 to -623 bp upstream of the transcriptional start of *cmaABT* (Wang *et al*., 1999). Transcriptional fusions of the promoters of *corP* and *corR* to *uidA* indicated that these genes are expressed constitutively. In contrast, a *corS::uidA* fusion exhibited a temperature dependence previously observed for COR biosynthetic promoters and exhibited maximal transcriptional activity at 18°C (**Fig. 10B**) (Ullrich *et al*., 1995). Analysis of GUS activities for the *corS::uidA*, *cmaABT::uidA*, and *cfl::uidA* transcriptional fusions in *corP*, *corR*, and *corS* mutants analyzed at 18°C revealed that they were negligible as compared to the levels

observed for the wild type at the same temperature. This fact clearly highlighted the importance of the regulatory genes *corS, corR,* and *corP* for thermoresponsive COR biosynthesis. Interestingly, thermoregulation of COR gene expression also proceeds *in planta*. Transcriptional fusion of the *cmaABT* promoter region to a promoterless *egfp* gene encoding the enhanced green fluorescent protein showed that it is thermoresponsive *in vitro* as well as *in planta* (Weingart & Ullrich, unpublished results).

Recently, it has been shown that in other *P. syringae* pathovars producing COR there are some additional factors influencing COR production. Mutants of *P. syringae* pv. tomato DC3000 defective in *hrpV*, which encodes a negative regulator for type III or *hrp*-mediated protein secretion, produced significantly more COR as compared to the wild type (Peñaloza-Vázquez *et al*., 2000). It was proposed that HrpV might negatively regulate COR synthesis, although the *hrp* secretion is not required for COR production. It is interesting to note that strain DC3000 does not produce COR in a temperature-dependent manner. Additionally, the *rpoN* gene encoding for the σ^{54} transcription factor was shown to be essential for COR production and for expression of the *cmaABT* operon in *P. syringae* pv. maculicola (Hendrickson *et al*., 2000).

2.4 Aim of this work

The phytotoxin coronatine is produced by *P. syringae* in a temperature-dependent manner. The thermoresponsive COR production is controlled by a modified two-component regulatory system, consisting of the HPK CorS and two RR, CorR and CorP. CorS is thought to respond to a temperature signal, and the signal perception is presumed to result in autophosphorylation of a conserved His residue of CorS. CorS is believed to be membrane-associated with a highly hydrophobic N-terminus that may function as the sensor domain in signal perception. The cognate RR of CorS, CorR, binds to COR biosynthetic promoters (Peñaloza-Vázquez & Bender, 1998; Wang *et al*., 1999) and to the *corS* promoter (Ullrich *et al*., 1995), and thus activates transcription. Since CorR is binding to the *corS* promoter, an enhancement of CorS biosynthesis might occur. Thus, the system is believed to be autoinducible, and a better understanding of the function(s) of CorS may provide a clue to understanding the temperature sensing mechanism.

Consequently, the main goal of this work was to find out how CorS responds to temperature changes. Our working hypothesis was that the physical state (fluidity) of the bacterial membrane might influence CorS, since temperature markedly affects the membrane lipid

composition. Fatty acid analysis at the two respective temperatures, 18°C and 28°C, was a primary step in order to find physiological evidence for this. A second step was to artificially modify the fatty acid composition of the membrane and to simultaneously check the transcriptional activation within the COR biosynthetic gene cluster.

Another main approach was to show that CorS is indeed membrane-associated and to elucidate its membrane topology. For this, a genetic approach based on the construction of translational fusions of CorS with either alkaline phosphatase or ß-galactosidase was used. The activities of both reporter enzymes depend on the side of the cytoplasmic membrane to which they are exposed. Based on the assumption that the membrane association of CorS might be linked to its function as a temperature sensor, the N-terminal part of CorS was subjected to a deletion analysis. Additionally, pentapeptide random mutagenesis of the N-terminus of CorS was used to identify regions of special importance for the thermosensing process. Ultimately, overproduction of CorS, which naturally occurs at very low copy numbers in the cell, was an important pre-requisite for the future biochemical and enzymatic characterization of this interesting protein.

3 MATERIAL

3.1 Equipment

Tab. 1. Equipment used in this study.

Equipment	Name	Company
Refrigerated Incubator Shaker	Innova 4230	New Brunswick Scientific (Nürtingen)
Centrifuges	Centrifuge 5415 C Biofuge pico EBA 8S	Eppendorf (Engelsdorf) Heraus (Hanau) Hettich Zentrifugen (Tuttlingen)
Centrifuge with rotors	$RC5B^{+}$ with SS34 20,500 rpm max, SLA-3,000 12,000 rpm max	SORVALL (Bad Homburg) SORVALL (Bad Homburg)
Speed-vacuum centrifuge	Concentrator 5301	Eppendorf (Hamburg)
SDS-PAGE apparatus	Mini Protean II; Prortean II xi	BioRad (München)
Electrotransfer apparatus	Mini Trans-Blot Electrophoretic Transfer Cell	BioRad (München)
2-D electrophoresis apparatus	Model 175 Tube Cell Multiphor II electrophoresis unit	BioRad (München) Pharmacia Biotech (Freiburg)
Power supply	Power Pack P200/Pack P3000	BioRad (München)
Dryer	Slab Gel Dryer (SGD 2000)	Savant (Frankfurt)
DNA electrophoresis chambers	MINI SUB DNA CELL WIDE MINI SUB CELL	BioRad (München) BioRad (München)
Polaroid Camera	MP 4+	AGS (Heidelberg)
Electroporation apparatus	GenePulser II	BioRad (München)
Thermocyclers	Hybaid Touchdown GeneAmp PCR System 2400	Hybaid (Middlesex, England) Perkin Elmer (Norwalk, USA)
Sequence apparatus	LICOR Model 4000	MWG Biotech (Ebersberg)
French Press Cell	20K-Cell FA-073	SLM Aminco (Rochester, USA)
Ultrasonic apparatus	Type UW 70	BANDELINelectronic (Berlin)
Fluorometer	Fluorolite 1000	Dynatech Laboratories (Denkendorf)
Spectrophotometer	MRX Microplate Reader	Dynatech Laboratories (Denkendorf)
HPLC system	Sykam 2000	Sykam (Fürstenfeldbruck)
HPLC column	250×4 mm, Spherisorb, C18-reversed-phase column	Sykam (Fürstenfeldbruck)
Gas chromatograph	GC 6000 VEGA Series	Carlo Erba Strumentazione (Milan, Italy)
GC column	DB-5ms (5% phenyl nonpolar), 30 m × 0.25 mm	J & W Scientific Products (Köln)
Thermomixer	Eppendorf Thermomixer 5436	Eppendorf (Hamburg)

3.2 Chemicals, antibiotics and enzymes

Chemicals and antibiotics were purchased from BioRad (München), Biomol (Hamburg), Roth (Karlsruhe), Serva (Heidelberg), Sigma (Deisenhofen), Qiagen (Hilden), Lancaster (Mülheim am Main), Perbio Science Deutschland (Bonn), and Merck (Darmstadt). Enzymes used in this study were purchased from Amersham-Pharmacia Biotech (Freiburg), Roche (Mannheim), New England Biolabs (Schwalbach), and Stratagene (Heidelberg).

Tab. 2. Antibiotics used in this study.

Antibiotic	Stock solution concentration	End concentration in medium
Ampicillin (Ap^r)	50 mg/ml	50 mg/L
Chloramphenicol (Cm^r)	25 mg/ml	25 mg/L
Gentamycin (Gm^r)	2.5 mg/ml	2.5 mg/L
Kanamycin (Km^r)	25 mg/ml	25 mg/L
Rifampicin (Rif^r)	50 mg/ml	50 mg/L
Spectinomycin (Sp^r)	25 mg/ml	25 mg/L
Streptomycin (Sm^r)	25 mg/ml	25 mg/L
Tetracycline (Tc^r)	25 mg/ml	25 mg/L

3.3 Kits

Tab. 3. Kits used in this study.

Kit	Company
Taq PCR Core	Qiagen (Hilden)
Plasmid Mini/Midi/Maxi Kit	Qiagen (Hilden)
QIAquick PCR purification kit	Qiagen (Hilden)
QIAEX II Gel Extraction Kit	Qiagen (Hilden)
Strep-tag Starter Kit	IBA (Göttingen)
Expand High Fidelity PCR System	Roche (Mannheim)
Immobiline DryStrip Kit for 2-D electrophoresis	Amersham-Pharmacia Biotech (Freiburg)
BM Chemiluminescence Blotting Substrate (POD)	Roche (Mannheim)
Rapid DNA Ligation Kit	Roche (Mannheim)

3.4 Antibodies

Tab. 4. Antibodies used in this study.

Antibody	Source
Mouse Anti-CmaB IgG	Oklahoma State University Hybridoma Center for Monoclonal Antibody Research
Anti-Rabbit IgG (whole molecule) Alkaline Phosphatase Conjugate	Sigma (Deisenhofen)
Anti-Mouse IgG (whole molecule) Alkaline Phosphatase Conjuagate	Sigma (Deisenhofen)
Streptavidin Alkaline Phosphatase Conjugate	Amersham-Pharmacia Biotech (Freiburg)
Rabbit Anti-CorS peptides IgG	Eurogentec (Hestal, Belgium)
Rabbit Anti-Alkaline Phosphatase (*E. coli*) IgG	donated by Ralf Schülein (Pharmacological Institute, Free University Berlin)
Mouse Monoclonal Anti-ß-galactosidase (*E. coli*) $IgG_{2b/\kappa}$	Roche (Mannheim)
Sheep Anti-Mouse IgG-POD	Chemicon International (Hofheim)
Mouse Monoclonal Anti-ß-galactosidase (*E. coli*) $IgG_{2a/\kappa}$	Promega (Mannheim)

3.5 Additional materials

Tab. 5. Additional materials used in this study.

Materials	Company
Chemiluminescence film (Hyperfilm ECL)	Amersham-Pharmacia Biotech (Freiburg)
Nitrocellulose membrane (Hybond-C)	Amersham-Pharmacia Biotech (Freiburg)
Molecular weight standards	GibcoBRL (Karlsruhe)
Filter paper 3MM	Schleicher & Schuell (Dassel)
Sterile filter (0.2 µm pore size)	Schleicher & Schuell (Dassel)

3.6 Media

All media were sterilized in an autoclave (30 min, 121°C, 1.3 bar). Some components of the media were sterilized by filtration through a sterile filter of 0.2 µm pore size. 1.5 % agar was added to a medium used for bacterial growth on a plate.

3.6.1 Complex medium for *Escherichia coli*

LB-medium

Lurea-**B**ertani-medium (Sambrook *et al*., 1989), pH 7.0

10	g	Bacto-trypton
10	g	NaCl
5	g	Yeast extract

Adjust to 1 L with H_2O

3.6.2 Complex medium for *Pseudomonas syringae*

KB-medium

King'**B** medium (King *et al*., 1954), pH 7.2

20	g	Peptone
1.5	g	K_2HPO_4
1.5	g	$MgSO_4 \times 7\ H_2O$
10	ml	glycerol

Adjust to 1 L with H_2O

3.6.3 Minimal media for *Pseudomonas syringae*

HSC-medium

Hoitink-**S**inden medium optimized for **C**OR biosynthesis (Palmer & Bender, 1993)

pH 6.0

Solution A:

1	g	NH_4Cl
0.2	g	$MgSO_4 \times 7\ H_2O$
4.1	g	KH_2PO_4
3.6	g	K_2HPO_4
0.3	g	KNO_3
5.4	mg	$FeCl_3$

Adjust to 0.9 L with H_2O

Solution B:

20	g	Glucose

Adjust to 0.1 L with H_2O

Solution A was autoclaved whereas solution B was sterile filtered. Both solutions were mixed 9:1 before use.

MG-medium

Mannitol-**G**lutamate medium (Keane *et al*., 1970), pH 7.0

10	g	Mannitol
2	g	L-Glutamic acid
0.5	g	KH_2PO_4
0.2	g	NaCl
0.2	g	$MgSO_4 \times 7\ H_2O$

Adjust to 1 L with H_2O

IM-medium

hrp-**I**nducible **m**inimal medium (Huynh *et al*., 1989), pH 5.7

Solution A:

0.74	g	K_2HPO_4
6.36	g	KH_2PO_4
1.0	g	(NH4)2SO4
0.35	g	$MgCl2 \times 6\ H_2O$
0.1	g	NaCl

Adjust to 0.9 L with H_2O

Solution B:

1.8	g	Fructose

Adjust to 0.1 L with H_2O

Solution A was autoclaved whereas solution B was sterile filtered. Both solutions were mixed 9:1 before use.

3.7 Oligonucleotides

Oligonucleotides were synthesized by MWG Biotech (Ebersberg).

Tab. 6. Oligonucleotides used in this study.

Name	Strand*	Nucleotide sequence**	Recognition site
fcsB	s	5'-GAC GGA TCC GTG ACT CAT TCT TAC GAA CTC-3'	*Bam*HI
rcsB	as	5'-GAC GGA TCC GCT CTC ACC GGC CTG ACC AGG-3'	*Bam*HI
corstrunc	s	5'-ATC GGA TCC GCC ATG CTG CTT TAC GG-3'	*Bam*HI
corSoutF	s	5'-ACT CCG CGG TGG TTA TCT GGG CGA CCG-3'	*Sac*II
corSoutR	as	5'-ACT GGT ACC CAC GCC GAA AGC CAT CTG-3'	*Kpn*I
corSinR	as	5'-ACT GAA TTC AGT CAC TGG CTG CAC TCG-3'	*Eco*RI
corSinF	s	5'-ACT GAA TTC TCG GGT CGG CAG CGC CTA-3'	*Eco*RI
LeuperphoA	as	5'-ACT GGT ACC TGG AGG GCA ATT TCG CAC-3'	*Kpn*I
LeucytphoA	as	5'-ACT GGT ACC TTC AGC GAC ACC TTG ACA-3'	*Kpn*I
ValperphoA	as	5'-ACT GGT ACC CCA ACG CGC AGA AAC CAC-3'	*Kpn*I
ArgcytphoA	as	5'-ACT GGT ACC TGC CGA CCC GAG TGC GCC-3'	*Kpn*I
Ala51phoA	as	5'-ACT GGT ACC TGG GCT GAC CAA GAC ACG-3'	*Kpn*I
Tyr85phoA	as	5'-ACT GGT ACC TGA TAG ATG ACT TGG CCC-3'	*Kpn*I
Thr27	as	5'-ACT GGT ACC TGG GTA GTC TTG ACC AGC-3'	*Kpn*I
Asp227	as	5'-ACT GGT ACC AGG TCA CGG CGT GCC CGC-3'	*Kpn*I
Leu249	as	5'-ACT GGT ACC GCC AGC AAC TGA CAG CGC-3'	*Kpn*I
Gln281	as	5'-ACT GGT ACC AAT TGC CGC TGT TGG GAA	*Kpn*I
InRSer22	as	5'-ACT GAA TTC CGA CTG GGT GAG TTC GAC-3'	*Eco*RI
pBlueMA1	s	5'-GCT GGA TCC AGT CCA AAT GGC CAT TAC GCA AGA CGT CCC AGT CAA GGA TCC CAG-3'	*Bam*HI, *Msc*I, *Aat*II
pBlueMA2	as	5'-CTG GGA TCC TTG ACT GGG ACG TCT TGC GTA ATG GCC ATT TGG ACT GGA TCC AGC-3'	*Bam*HI, *Aat*II, *Msc*I
phoA354rev	as	5'-ATT CTG AAT CAC GCA GAG-3'	
lacZF	s	5'-AGT GGT ACC CGT CGT TTT ACA ACG TC-3'	*Kpn*I
lacZR	as	5'-AGT GGT ACC TAT TAT TTT TGA CAC CA-3'	*Kpn*I
T3H	s	5'-GGC AAG CTT ATT AAC CCT CAC TAA AG-3'	*Hin*dIII
T7H	as	5'-GAC AAG CTT AAT ACG ACT CAC TAT AG-3'	*Hin*dIII
lacZfusTrev	as	5'-CTT CTG GTG CCG GAA ACC AGG CAA AGC-3'	
phoAfusTrev	as	5'-CAG GTT TAT CGC TAA GAG AAT CAC GCA-3'	

*s: *sense*-strand; as: *antisense*-strand.

**Endonuclease recognition sites are underlined.

3.8 Software

Tab. 7. Software used in this study.

Name	Company/Reference
DNA-STAR	Lasergene, USA
BLASTN, BLASTP, BLASTX, FASTEMBL	University of Wisconsin, Genetic Computer Group http://blast.genome.ad.jp/
Vector NTI 5	Informax Inc., USA
Pfam protein family database Pfam TMHMM (transmembrane hidden Markov model)	The Sanger Centre, UK http://www.sanger.ac.uk/Sofware/Pfam) http://www.cbs.dtu.dk/cgi-bin/nph-webface?jobid=TMHMM2
TopPred 2 (Topology prediction of membrane proteins)	Stockholm University, Theoretical Chemistry, Protein prediction Servers http://www.biochemi.su.se/~server/toppred2
MS Office	Microsoft, USA

3.9 Microorganisms

Tab. 8. Bacterial strains used in this study.

Microorganism	Relevant characteristics	Reference/Source
Escherichia coli DH5α	*F´/endA1 hsdR17($r_k^-m_k^+$) relA1 supE44 thi-1 recA1 gyrA (Nal^r) Δ(lacIZYA-argF)U169 deoR (ϕ80dlacΔ(lacZ)M15*	Raleigh *et al*., 1989
Escherichia coli MC1061	*F$^-$ araD139 Δ(ara-leu)7696 galE15 galK16 Δ(lac)X74 rpsL (Str^r) hsdR2 ($r_k^-m_k^+$) mcrA mcrB1*	Raleigh *et al*., 1989
Pseudomonas syringae pv. glycinea PG4180	COR$^+$, CMA$^+$, CFA$^+$	Bender *et al*., 1993
P. syringae PG4180.N9	Km^r; COR$^+$, CMA$^+$, CFA$^+$, overproduced CFA	Ullrich *et al*., 1994
P. syringae PG4180.D4	Km^r; COR$^-$, CMA$^-$, CFA$^-$	Bender *et al*., 1993
P. syringae PG4180.F7	Km^r; COR$^-$, CMA$^-$, CFA$^-$	Bender *et al*., 1993
P. syringae PG4180.P1	Gm^r; COR$^-$, CMA$^-$, CFA$^-$	Ullrich *et al*., 1995
P. syringae PG4180.AG28	Km^r; COR$^-$, CMA$^+$, CFA$^-$	Palmer *et al*., 1997

3.11 Plasmids

Tab. 9. Plasmids used in this study.

Plasmid	Relevant characteristics	Reference/Source
pBluescript II SK	Ap^r; high-copy number cloning vector	Stratagene (Heidelberg)
pBBR1MCS	Cm^r; *mob*$^+$; broad-host-range cloning vector, medium copy	Kovach *et al*., 1994
pRK415	Tc^r; *mob*$^+$; low-copy cloning vector, RK2-derivative	Keen *et al*., 1988
pRK2013	Km^r; *mob*$^+$, *tra*$^+$; helper plasmid for conjugation	Figurski & Helsinki, 1979
pRGMU1	Sm^r/Sp^r; contains a 2.9-kb *Pst*I fragment of *cmaABT* promoter region in pRG960sd	Ullrich & Bender, 1994
pMUH34	Tc^r; contains a 3.4-kb *Hin*dIII fragment with *corR*, *corS*, and *corP* genes in pRK415	Ullrich *et al*., 1995
pH34	Ap^r; contains a 3.4-kb *Hin*dIII fragment with *corRSP* genes derived from pMUH34 in pBluscript II SK	Ullrich *et al*., 1995
pBBRH34L	Cm^r; contains a 3.4-kb *Hin*dIII fragment with *corRSP* genes derived from pH34in pBBR1MCS	This study
pBBRH34R	Cm^r; contains a 3.4-kb *Hin*dIII fragment with *corRSP* genes derived from pH34 in pBBR1MCS oriented in opposite to pBBRH34L	This study
pRKE70L	Tc^r; contains a 7.0-kb *Eco*RI fragment from the COR biosynthetic region in pRK415	Ullrich *et al*., 1995
pRKE70R	Tc^r; contains a 7.0-kb *Eco*RI fragment from the COR biosynthetic region in pRK415 oriented in opposite to pRKE70L	Ullrich *et al*., 1995
pASK-IBA3	Ap^r; overexpression vector for recombinant proteins with C-terminal *Strep*-tag II and without signal peptide	IBA (Göttingen)
pASK-IBA7	Ap^r; overexpression vector for recombinant proteins with N-terminal *Strep*-tag II and without signal peptide	IBA (Göttingen)
pASK-IBA3corS	Ap^r; contains a 1.4-kb *Bam*HI PCR product of *corS* amplified from pH34 in pASK-IBA3	This study
pASK-IBA7corS	Ap^r; contains a 1.4-kb *Bam*HI PCR product of *corS* amplified from pH34 in pASK-IBA7	This study
pBSB24	Ap^r; contains a 2.3-kb *Bam*HI fragment derived from pMUH34 in pBluescript II SK; contains *corS*	Ullrich *et al*., 1995
pBlueMA	Ap^r; contains a 60-bp *Bam*HI *(Msc*I-*Aat*II*)* synthetic insert in pBluescript II SK, lacks *Not*I site of the vector	This study
pMA8	Ap^r; contains a 0.8-kb *Aat*II-*Msc*I insert derived from pBSB24 in pBlueMA	This study
pA51	Ap^r; contains a 1.6-kb *Sac*II-*Kpn*I PCR product amplified from pH34 in pBluescript II SK	This study
pY85	Ap^r; contains a 1.65-kb *Sac*II-*Kpn*I PCR product amplified from pH34 in pBluescript II SK	This study
pL125	Ap^r; contains a 1.7-kb *Sac*II-*Kpn*I PCR product amplified from pH34 in pBluescript II SK	This study

Plasmid	Relevant characteristics	Reference/Source
pL151	Ap^r; contains a 1.8-kb *Sac*II-*Kpn*I PCR product amplified from pH34 in pBluescript II SK	This study
pV177	Ap^r; contains a 1.87-kb *Sac*II-*Kpn*I PCR product amplified from pH34 in pBluescript II SK	This study
pR204	Ap^r; contains a 1.94-kb *Sac*II-*Kpn*I PCR product amplified from pH34 in pBluescript II SK	This study
pPHO7	Ap^r; contains promoterless *phoA* without signal peptide and a ribosome-binding site	Gutierrez & Devedjian, 1989
pA51phoA	Ap^r; contains *corS(Ala51)::phoA* translational fusion in pBluescript II SK	This study
pY85phoA	Ap^r; contains *corS(Tyr85)::phoA* translational fusion in pBluescript II SK	This study
pL125phoA	Ap^r; contains *corS(Leu125)::phoA* translational fusion in pBluescript II SK	This study
pL151phoA	Ap^r; contains *corS(Leu151)::phoA* translational fusion in pBluescript II SK	This study
pV177phoA	Ap^r; contains *corS(Val177)::phoA* translational fusion in pBluescript II SK	This study
pR204phoA	Ap^r; contains *corS(Arg204)::phoA* translational fusion in pBluescript II SK	This study
pBBRA51phoA	Cm^r; contains *corS(Ala51)::phoA* translational fusion derived from pA51phoA in pBBR1MCS	This study
pBBRY85phoA	Cm^r; contains *corS(Tyr85)::phoA* translational fusion derived from pY85phoA in pBBR1MCS	This study
pBBRL125phoA	Cm^r; contains *corS(Leu125)::phoA* translational fusion derived from pL125phoA in pBBR1MCS	This study
pBBRL151phoA	Cm^r; contains *corS(Leu151)::phoA* translational fusion derived from pL151phoA in pBBR1MCS	This study
pBBRV177phoA	Cm^r; contains *corS(Val177)::phoA* translational fusion derived from pV177phoA in pBBR1MCS	This study
pBBRR204phoA	Cm^r; contains *corS(Arg204)::phoA* translational fusion derived from pR204phoA in pBBR1MCS	This study
pBBRT27	Cm^r; contains a 1.5-kb *Sac*II-*Kpn*I PCR product amplified from pH34 in pBBR1MCS	This study
pBBRD227	Cm^r; contains a 2.0-kb *Sac*II-*Kpn*I PCR product amplified from pMUH34 in pBBR1MCS	This study
pBBRL249	Cm^r; contains a 2.1-kb *Sac*II-*Kpn*I PCR product amplified from pMUH34 in pBBR1MCS	This study
pBBRQ281	Cm^r; contains a 2.2-kb *Sac*II-*Kpn*I PCR product amplified from pMUH34 in pBBR1MCS	This study
pBBRT27phoA	Cm^r; contains *corS(Thr27)::phoA* translational fusion in pBBR1MCS	This study
pBBRD227phoA	Cm^r; contains *corS(Asp227)::phoA* translational fusion in pBBR1MCS	This study
pBBRL249phoA	Cm^r; contains *corS(Leu249)::phoA* translational fusion in pBBR1MCS	This study
pBBRQ281phoA	Cm^r; contains *corS(Gln281)::phoA* translational fusion in pBBR1MCS	This study

Plasmid	Relevant characteristics	Reference/Source
pBKE14	Ap^r; contains a 1.3-kb *Eco*RI-*Kpn*I PCR product amplified from pH34 in pBluescript II SK	This study
pSEEKS22	Ap^r; contains a 1.5-kb *Sac*II-*Eco*RI PCR product amplified from pH34 in pBKE14; contains 0.54-kb deletion of *corS*	This study
pSEEKT103	Ap^r; contains a 1.7-kb *Sac*II-*Eco*RI PCR product amplified from pH34 in pBKE14; contains 0.3-kb deletion of *corS*	This study
pRK415-E-B	Tc^r; vector pRK415 contains deletion of *Eco*RI and *Bam*HI restriction sites	This study
pRKΔT103L	Tc^r; contains a blunt-ended 3.0-kb *Sac*II-*Kpn*I fragment derived from pSEEKT103 and cloned into the blunt-ended *Hin*dIII site of pRK415-E-B	This study
pRKΔT103R	Tc^r; contains a blunt-ended 3.0-kb *Sac*II-*Kpn*I fragment derived from pSEEKT103 and cloned into the blunt-ended *Hin*dIII site of pRK415-E-B; insert oriented in opposite to pRKΔT103L	This study
pRKΔS22L	Tc^r; contains a 2.8-kb *Hin*dIII PCR product amplified from pSEEKS22 and cloned into pRK415-E-B	This study
pRKΔS22R	Tc^r; contains a 2.8-kb *Hin*dIII PCR product amplified from pSEEKS22 and cloned into pRK415-E-B; insert oriented in opposite to pRKΔS22L	This study
pMC-1871	Tc^r; contains promoterless *lacZ* without a ribosome-binding site and the first eight non-essential N-terminal part amino-acid codons	Amersham-Pharmacia Biotech (Freiburg)
pBBRT27lacZ	Cm^r; contains *corS(Thr27)::lacZ* translational fusion in pBBR1MCS; contains PCR amplified 3.0-kb *lacZ* from pMC-1871	This study
pBBRA51lacZ	Cm^r; contains *corS(Ala51)::lacZ* translational fusion obtained from pBBRA51phoA by substitution of *phoA* with the PCR amplified 3.0-kb *lacZ* from pMC-1871	This study
pBBRY85lacZ	Cm^r; contains *corS(Tyr85)::lacZ* translational fusion obtained from pBBRY85phoA by substitution of *phoA* with the PCR amplified 3.0-kb *lacZ* from pMC-1871	This study
pBBRL125lacZ	Cm^r; contains *corS(Leu125)::lacZ* translational fusion obtained from pBBRL125phoA by substitution of *phoA* with the PCR amplified 3.0-kb *lacZ* from pMC-1871	This study
pBBRL151lacZ	Cm^r; contains *corS(Leu151)::lacZ* translational fusion obtained from pBBRL151phoA by substitution of *phoA* with the PCR amplified 3.0-kb *lacZ* from pMC-1871	This study
pBBRV177lacZ	Cm^r; contains *corS(Val177)::lacZ* translational fusion obtained from pBBRV177phoA by substitution of *phoA* with the PCR amplified 3.0-kb *lacZ* from pMC-1871	This study
pBBRR204lacZ	Cm^r; contains *corS(Arg204)::lacZ* translational fusion obtained from pBBRR204phoA by substitution of *phoA* with the PCR amplified 3.0-kb *lacZ* from pMC-1871	This study
pRKBE11	Tc^r; contains a 1.1-kb *Eco*RI-*Bam*HI fragment derived from pMUH34 in pRK415	This study

4 METHODS

4.1 Bacterial growth

4.1.1 *Escherichia coli*

E. coli cells were grown overnight at 37°C on LB agar plates containing the appropriate antibiotics. Subsequently, *E. coli* cells were cultured overnight at 37°C by shaking at 250 rpm in LB medium containing the appropriate antibiotics. Microfuge and test tubes were used for growth of small volumes of *E. coli* cultures (1-5 ml), and Erlenmeyer flasks were used for growth of big volumes of *E. coli* cultures (50-500 ml).

4.1.2 *Pseudomonas syringae*

P. syringae cells were grown for 2-5 days at 28°C on MG agar plates containing appropriate antibiotics. Subsequently, *P. syringae* cells were inoculated in liquid media (HSC, KB, or IM) and grown to a certain optical density at 18°C and 28°C by shaking at 280 rpm.

4.1.3 Storage of bacterial strains

Fresh grow bacterial colonies or lawns from agar plates were resuspended in 15% sterile glycerol solution and stored at -80°C.

4.2 Molecular biology methods

4.2.1 Plasmid DNA isolation

4.2.1.1 1-2-3 Isolation of plasmid DNA

The method of plasmid DNA isolation from small amounts of cells was based on a Qiagen protocol. 1-1.5 ml of *E. coli* overnight cultures was harvested by centrifugation at 13,000 rpm for 2-5 min. The pellet was resuspended in 150 µl of precooled buffer P1 (100 µg/ml RNase A, 50 mM Tris/HCl, 10 mM EDTA-Na (pH 8.0)). Cells were lysed upon addition of 150 µl of buffer P2 (200 mM NaOH, 1% SDS) for 5 min, and the lysate was neutralized by addition of 150 µl of precooled 3 M potassium acetate solution (pH 5.5). This led to the precipitation of SDS. The denatured proteins, chromosomal DNA, and cellular debris trapped in salt-detergent complexes, whereas small plasmid DNA renatures correctly and remains in

the solution. Following incubation on ice for 10 min and subsequent centrifugation at 13,000 rpm for 15 min, the supernatant containing plasmid DNA was transferred into another microfuge tube. DNA was precipitated by addition of 0.7 volume (300 µl) of 2-propanol and subsequent centrifugation for 30 min. Then the DNA pellet was washed by 400-500 µl of 70% ethanol solution. After centrifugation for 15 min, the DNA pellet was dried in a speed-vacuum centrifuge for 5 min, and dissolved in 20 µl of TE buffer (10 mM Tris/HCl, 1 mM EDTA (pH 8.0)).

For the isolation of native plasmids from *P. syringae*, cells were grown on a MG agar plate for 3-4 days. Cells (2 full loops) scraped from a fresh growing area of the plate were resuspended in 150 µl of buffer P1. Subsequent steps were done as described above.

4.2.1.2 Midi and Maxi Qiagen plasmid DNA isolation

E. coli overnight cultures were harvested by centrifugation at 7,000 rpm for 10 min at 4°C. The volume of the harvested culture depended on the procedure (Midi or Maxi) and on the plasmid copy number in the cells (high/medium/low copy). Usually, for the DNA Midi-isolation 25-50 ml of the culture for a high-copy number plasmid and 100 ml of culture for medium- or low-copy plasmids were required. For the DNA Maxi-isolation 100 ml of the culture for a high-copy number plasmid and 250-500 ml of the culture for medium- or low-copy plasmids were required. The pellet was resuspended in 4 ml (10 ml for Maxi) of precooled buffer P1. Cells were lysed by addition of 4 ml (10 ml) of buffer P2 for 5 min, and the lysate was neutralized by addition of 4 ml (10 ml) of precooled 3 M potassium acetate solution (pH 5.5). Following an incubation on ice for 15-20 min and subsequent centrifugation at 13,000 rpm for 30 min at 4°C, the supernatant containing plasmid DNA was transferred into another tube, centrifuged again for 15 min, and then applied to a Qiagen column (Qiagen-tip 100 for Midi or -tip 500 for Maxi) pre-equilibrated with 4 ml (10 ml) of QBT buffer (750 mM NaCl, 50 mM MOPS, 15% ethanol (pH 7.0), 0.15% TritonX-100). The column was washed with 10 ml (30 ml) of QC buffer (1 M NaCl, 50 mM MOPS, 15% ethanol (pH 7.0)). DNA was eluted with 5 ml (15 ml) of QF buffer (1.25 M NaCl, 50 mM Tris/HCl, 15% ethanol (pH 8.5)). DNA was then precipitated by addition of 0.7 volume of 2-propanol and subsequent centrifugation at 11,000 rpm for 30 min at 4°C. Subsequently, the DNA was washed with 2 ml (5 ml) of 70% ethanol solution. After centrifugation at 11,000 rpm for 15 min, the DNA was air-dried for 10 min, and dissolved in 100-300 µl of TE buffer or sterile water.

For the isolation of native plasmids from *P. syringae*, cells were grown in 100 ml of HSC medium. The other steps were done as described above.

4.2.1.3 *Pseudomonas* plasmid isolation according to Kado and Liu (1981)

For the isolation of native plasmids from *P. syringae*, cells were grown on MG agar plates for 3-4 days. Cells (2 full loops) scraped from a fresh growing area of the plate were thoroughly resuspended in 166 µl of E-buffer (40 mM Tris-acetate, 2 mM EDTA-Na (pH 7.9)). The cell suspension was mixed gently with 333 µl of lysis buffer (50 mM Tris, 3% SDS (pH 12.6)). Alkaline lysis was followed by heat denaturation at 65°C for 1 hour. Heat treatment led to denaturation of fragmented (chromosomal) DNA, whereas plasmid DNA remains resistant to denaturation. Plasmids can be subsequently extracted by phenol and chloroform. For this, 500 µl of phenol and 500 µl of chloroform were added to the cell lysate and the suspension was mixed by gentle inversion for 1 min. Phenol-chloroform extraction traps protein in the organic phase and linear DNA/RNA in the interphase, whereas the aqueous phase contains pure plasmid DNA. To separate phases, the suspension was centrifuged for 30 min at 13,000 rpm. 250-300 µl of the upper (aqueous) phase was carefully transferred to fresh tube. 20 µl of this phase was loaded to 0.6-0.7% agarose gels for plasmid screening. The electrophoresis was performed at 55 V for 5 hours in a small BioRad™ chamber.

4.2.2 DNA separation by gel electrophoresis

Linear double-stranded DNA-fragments can be separated in an electric field due to the fact that the migration of DNA varies as the reciprocal of the logarithm of the base-pairs number (Meyers *et al*., 1976). Upon addition of ethidium bromide which is intercalated into GC-pairs, DNA becomes fluorescent and can be visualized under UV-light.

Agarose gels (0.6% to 3%) (Sambrook *et al*., 1989), depending on the size of the DNA fragments to be separated, were prepared in TAE buffer (1×: 40 mM Tris-acetate, 1.3 mM EDTA-Na, 0.47 mM acetic acid). DNA samples were mixed with 1/6 volume of loading buffer (6×: 0.25% bromphenol blue, 0.25 % xylene cyanol, 40% sucrose) and separated at 25 to 80 V in TAE buffer. The size of DNA fragments was determined by parallel loading to the gel of a 1-kb DNA ladder (GibcoBRL) (500 ng per lane). This molecular marker is suitable to estimate the size of DNA fragments in a range from 500 bp to 12 kb. After electrophoresis, the gel was stained in ethidium bromide solution (10 µg/ml in TAE buffer) for 5-15 min.

4.2.3 Polymerase chain reaction

Polymerase chain reaction (PCR) is a method used to amplify a specific DNA sequence *in vitro* by repeated cycles of synthesis with specific primers and thermostable DNA polymerase (Saiki *et al*., 1988). Specific primers are complementary to sequences that lie on opposite strands of the template DNA and flank the segment of DNA that is to be amplified. The template DNA was first denatured by heating in the presence of a large molar excess of each of the two primers and dNTPs. The reaction mixture was then cooled to a temperature that allows the primers to anneal to their target sequences, and subsequently the annealed primers were extended with DNA polymerase. Cycles of denaturation, annealing, and DNA synthesis were repeated several times.

The PCR with *Taq* polymerase was used for *E. coli* colonies and insert screening after cloning procedures where the presence of inserted DNA was checked with specific primers. Additionally, PCR was used to screen for positive transconjugants after conjugation of plasmids into *P. syringae*. As template DNA, either isolated plasmid DNA or bacterial cells were used. In the latter case, a single colony was resuspended in 200 µl of sterile water, and 1 µl of this suspension was used for a PCR mix. The following master mix and program were used for DNA amplification with *Taq* DNA polymerase:

Master mix and program for the PCR with *Taq* polymerase (25 µl)

2.5	µl	10×PCR buffer	Initial denaturation	94°C	5 min
4.0	µl	25 mM $MgCl_2$	Denaturation	94°C	1 min
1.0	µl	dNTPs mix (25 mM each)	Annealing	45-65°C	1 min
1.0	µl	forward primer (50 pmol/µl)	Extension	72°C	2-3 min
1.0	µl	reverse primer (50 pmol/µl)	Final extension	72°C	10 min
1.0	µl	template DNA (100 ng)	End	4°C	
14.1	µl	sterile H_2O			
0.4	µl	*Taq* DNA polymerase (5 U/µl)			

Taking into account (G+C) and (A+T) contents of primers, the melting temperature of primers (T_m) was calculated according to the formula: $T_m[°C] = 4°C \times (G+C) + 2°C \times (A+T)$. The annealing temperature used for DNA amplification was 4-5°C below T_m.

For cloning of PCR products, it is important to avoid errors in DNA amplification. In this case, DNA polymerases with proofreading function were used. The Expand High Fidelity PCR System (Roche, Mannheim) containing thermostable *Taq* and proofreading *Pwo* DNA polymerases as well as *PfuTurbo* DNA polymerase (Stratagene, Heidelberg) were used for high-fidelity PCR.

Master mix and program for the PCR with *PfuTurbo* polymerase (100 µl)

10	µl	10×PCR buffer	Initial denaturation	94°C	1 min
0.8	µl	dNTPs mix (25 mM each)	Denaturation	94°C	1 min
1.0	µl	forward primer (50 pmol/µl)	Annealing	45-65°C	1 min
1.0	µl	reverse primer (50 pmol/µl)	Extension	72°C	1 min/ 1 kb of PCR target
0.5	µl	template DNA (50 ng)			
85.7	µl	sterile H_2O	Final extension	72°C	10 min
1.0	µl	*PfuTurbo* DNA polymerase (2.5 U/µl)	End	4°C	∞

Master mixs for the PCR with Expand High Fidelity PCR System (100 µl)

Mater mix I			Mater mix II		
0.8	µl	dNTPs mix (25 mM each)	10	µl	10×PCR buffer
1.0	µl	forward primer (50 pmol/µl)	39.25	µl	sterile H_2O
1.0	µl	reverse primer (50 pmol/µl)	0.75	µl	enzyme mix (3.5 U/µl)
0.5	µl	template DNA (50 ng)			
47.7	µl	sterile H_2O			

Master mix I and II were mixed before the start of the PCR.

Program for the PCR with Expand High Fidelity PCR System (100 µl)

Initial denaturation	94°C	2 min
Denaturation	94°C	15 s
Annealing	50-65°C	30 s
Extension	72°C	1 min/ 1 kb of PCR target
Final extension	68°C	7 min
End	4°C	∞

4.2.4 Cloning techniques

4.2.4.1 Digestion of plasmid DNA with endonucleases.

Type II restriction endonucleases recognize a DNA region with a specific palindromic sequence of 4-8 bp and cut it. Cleavage of DNA linearizes it generating either blunt or 3'- or 5'-overhanging sticky ends. The DNA was incubated in an appropriate restriction buffer with enzyme(s) for 2-16 hours either at 30°C or 37°C. The amount of enzyme added to a reaction mixture and the duration of digestion were determined according to the assumption that 1 U of enzyme cleaves 1 µg of DNA for 1 h in 50 µl. For subsequent cloning procedures, an enzyme was inactivated by heating, and the digested DNA was purified.

4.2.4.2 Dephosphorylation of digested DNA

Following a restriction digestion the vector DNA was treated with shrimp alkaline phosphatase (SAP) to remove the phosphate groups from the 5'-ends and to facilitate more efficient cloning of insert DNAs. This prevents self-ligation of the vector DNA. SAP can be added directly to a digestion mix because the SAP buffer is usually compatible with the buffers for restriction endonucleases. 1/10 volume of the SAP buffer and 0.1 units/pmole 5'-ends (final concentration) of SAP were added to a sample. This mix was incubated for 30 min at 37°C to accomplish desphosphorylation. Afterwards, SAP and restriction enzymes were inactivated by heating at 65°C for 15 min. For subsequent cloning steps the DNA was purified. To determine the picomoles of ends of linear double-stranded DNA the following formula was used: (µg DNA / kb size of DNA) × 3.04 = pmole of ends.

4.2.4.3 Converting 5'-overhanging sticky ends to blunt ends

Some restriction enzymes, for instance *Hin*dIII or *Bam*HI, generate 5'-overhanging sticky ends following the DNA cleavage. If a digested vector possesses the 5'-overhanging ends, whereas an insert is blunt-ended, for cloning of the insert into the vector, it is necessary to convert the 5'-overhanging ends to blunt-ends. An enzyme suitable for the filling-in of gaps and for the repair of the termini of double-stranded DNA, is Klenow (DNA Polymerase I Large Fragment) polymerase which lacks 5'-3'-endonuclease activity.
Following the digestion with a restriction enzyme, the enzyme was inactivated by heating. 1/20 volume of 0.5 mM dNTPs, 1/10 volume of 10×buffer and 1 to 5 U units of Klenow

polymerase were added to a sample which was then incubated at 30°C for 20 min. The reaction was stopped by heating at 75°C for 10 min. For subsequent cloning steps the DNA was purified.

4.2.4.4 Converting 3'-overhanging sticky ends to blunt ends

Some other enzymes, for instance *Kpn*I or *Sac*II, generate 3'-overhanging sticky ends. Although the Klenow fragment has a 3'-5' exonuclease activity, T4 DNA polymerase is preferred over Klenow for converting 3'-overhanging ends to blunt ends, because this enzyme exhibits a 250-fold stronger 3'-5' exonuclease activity than Klenow fragment. T4 DNA polymerase catalyses the synthesis of DNA in the 5'-3' direction and lacks 5'-3' exonuclease activity.
Following the digestion with a restriction enzyme, the enzyme was inactivated by heating. 1/20 volume of 0.5 mM dNTPs, 1/10 volume of 10×buffer, 1/10 volume of 0.1% BSA and 3 to 5 U units of T4 DNA polymerase were added to a sample which was then incubated at 12°C in a water bath for 30 min. The reaction was stopped by heating at 75°C for 10 min. For subsequent cloning steps the DNA was purified.

4.2.4.5 Precipitation of DNA by ethanol

For subsequent ligation reactions it is necessary to purify DNA to get rid of enzymes used before and components of buffer which are incompatible with ligation buffer or which can inhibit the ligation reaction. One possible method is ethanol precipitation of the DNA. Upon addition of ethanol, DNA is precipitated as sodium salt from the aqueous phase.
1/9 Volume of 3 M sodium acetate (pH 5.8) and 2 volumes of cold absolute ethanol were added to the DNA solution. The sample was incubated for an hour at –20°C and then centrifuged at 13,000 rpm for 30 min at 4°C. The supernatant was discarded, and the DNA precipitate was washed in 70% ethanol solution with subsequent centrifugation at 13,000 rpm for 15 min at 4°C. The DNA was dried in a speed-vacuum centrifuge and dissolved in 10 µl of sterile water. DNA samples were stored at –20°C.

4.2.4.6 QIAEX II agarose gel extraction procedure

The QIAEXII-kit (Qiagen, Hilden) was used for purification of DNA fragments from preparative agarose gels. After DNA separation by electrophoresis, the band of interest was cut out of the gel, and agarose was solubilized in 3 volumes (w/v) of buffer QX1. Subsequently, for isolation of 2-10 µg DNA, 20-30 µl of QIAEX suspension was added, and the sample was incubated at 50°C for 10 min. The QIAEX suspension with bound DNA was shortly centrifuged (30 s at 13,000 rpm) and washed with 500 µl of buffer QX1 and 500 µl of buffer PE with subsequent centrifugation steps. Finally, the pellet was dried in a speed-vacuum centrifuge for 2 min. Then the DNA was eluted with 20 µl of sterile water. DNA samples were stored at –20°C.

4.2.4.7 QIAquick PCR purification kit

The QIAquick-kit (Qiagen, Hilden) was used to separate PCR products from primers, nucleotides, polymerases, and salts. 5 volumes of buffer PB were added to 1 volume of the PCR reaction and mixed. The sample was applied to a QIAquick spin column in a 2-ml collection tube, and shortly centrifuged to accomplish binding of PCR products to the column. Then the column was washed with 0.75 ml of buffer PE and placed into a 1.5 ml microfuge tube. To elute, 30 µl of sterile water was added to the center of the column, and after 1-3 min the sample was shortly centrifuged (1 min, 13,000 rpm). DNA samples were stored at –20°C.

4.2.4.8 Estimation of DNA concentration

To estimate DNA concentrations, 1 to 5 µl of a DNA sample and 5 µl (500 ng) of 1 kb DNA ladder were loaded to a 0.9% agarose gel. After electrophoresis and staining with ethidium bromide solution, DNA concentration was estimated visually comparing it to the amount of DNA ladder applied to the gel.

4.2.4.9 Ligation of DNA

T4 DNA ligase catalyzes the formation of phosphodiester bonds at juxtaposed 5'-phosphate and 3'-hydroxyl termini in duplex DNA. For each 10 µl of ligation reaction, a combination of 20-100 ng of vector DNA and three to eight-fold excess of insert as well as 1 µl of 10×buffer

and 1 µl of T4 DNA ligase was used. Low concentrated T4 DNA ligase (1 U/µl) was used for ligation of sticky-ended restriction fragments, and high concentrated T4 DNA ligase (10 U/µl) was used for blunt-ended restriction fragments. The ligation mix was incubated at 16°C for 20 hours. 1 or 3 µl of ligation mix was loaded to a agarose gel to check the efficiency of ligation reaction. Shifted and smearing bands of both vector and insert indicated that ligation was successful. In the case of cloning into a high-copy number vector (pBluescript II SK), the ligation mix was transformed into calcium-competent *E. coli* DH5α cells (4.2.4.11). However, for cloning into medium- (pBBR1MCS) and low-copy number vectors (pRK415) as well as for the ligation of blunt-ended restriction fragments, 10-20 µl of 10×ligation buffer, 2-3 µl of low (1 U/µl) or high concentrated T4 DNA ligase (10 U/µl), and 50-100 µl of sterile water were added to 10 µl of the overnight ligation mix. Following an additional incubation for 20 hours, the ligation mix was transformed into calcium-competent *E. coli* DH5α cells (4.2.4.11).

Alternatively, the Rapid DNA Ligation kit (Roche, Mannheim) was used for sticky-end cloning into the vector pBBR1MCS. 10 µl of DNA (100 ng of dephosphorylated vector and 600 ng of insert) in 1×DNA dilution buffer, 10 µl of 2× T4 DNA ligation buffer and 1 µl of T4 DNA ligase were mixed and incubated for 10 min at room temperature. Subsequently, the ligation mixture was transformed into calcium-competent *E. coli* DH5α cells (4.2.4.11).

4.2.4.10 Preparation of competent *E. coli* cells using calcium chloride

Competent cells are able to take up foreign DNA. This temporary state of *E. coli* cells can be induced by the treatment with either $CaCl_2$ or $RbCl_2$ (Dagert & Ehrlich, 1979; Mandel & Higa, 1970).

A single colony of fresh *E. coli* DH5α cells was inoculated in 5 ml of LB-medium and cultured overnight at 37°C. The overnight preculture was added to 500 ml of LB medium and cultured at 37°C until bacteria reached the early exponential phase (OD_{600nm} 0.4-0.5) at which competence of the cells can be efficiently induced. Following incubation on ice for 10 min, 300 ml of the cells were harvested at 5,500 rpm for 5 min at 4°C and resuspended in 240 ml of cold sterile 0.1 M $MgCl_2$ solution. After subsequent centrifugation at 5,000 rpm for 1 min, the cells were resuspended in 240 ml of cold sterile 0.1 M $CaCl_2$ solution and the centrifugation step was repeated. Finally, cells were resuspended in 15 ml of cold sterile 0.1 M $CaCl_2$ solution containing 15% glycerol. Aliquots of 200 µl cells were frozen in liquid nitrogen and stored at –80°C.

4.2.4.11 Transformation of DNA into *E. coli* cells by heat shock

Ca^{2+}-competent cells exposed to high temperature (37°C) rapidly take up free DNA. An aliquot of 200 µl of Ca^{2+}-competent cells was mixed with 10 to 100 µl of ligation mix and incubated on ice for 30 min. Uptake of DNA was induced by heat shock (5 min at 37°C). After the heat shock, the cells were diluted in 600 µl of prewarmed LB medium (37°C), and incubated at 37°C for 40-60 min by shaking at 250 rpm. 200 and 400 µl of the cell suspensions were plated onto LB agar plates containing the appropriate antibiotic(s). Plates were incubated overnight at 37°C until single *E. coli* colonies were visible.

4.2.5 Introduction of recombinant DNA into *Pseudomonas syringae*

4.2.5.1 Preparation of *P. syringae* electrocompetent cells

A single colony of fresh *P. syringae* cells was inoculated in 5 ml of KB medium and cultured at 28°C until cells reached the early exponential phase (OD_{600nm} 0.5-0.7). After a short incubation on ice bacteria were harvested at 7,000 rpm for 5 min. The pellet was resuspended in 5 ml of cold sterile 0.5 M sucrose solution and centrifuged again at 5,000 rpm for 3 min. The washing step with sucrose was repeated twice. Finally, the cells were resuspended in 0.5 ml of 0.5 M sucrose solution and directly used for electroporation.

4.2.5.2 Electroporation of *P. syringae* cells

100 µl of electrocompetent cells were mixed with 0.1-1 µg of plasmid DNA, and exposed to electric shock in a prechilled cuvette with a GenePulser-Apparatus (BioRad, München) set to 2.5 kV and 200 Ω. 1 ml of KB medium was added to the cuvette immediately after the pulse. The cells were then incubated at 28°C for 60 min by shaking at 280 rpm, and plated onto MG agar plates containing the appropriate antibiotic(s). Subsequently, plates were incubated at 28°C for 3-5 days until single *P. syringae* colonies were visible.

4.2.5.3 Conjugation by triparental mating

The native mechanism of plasmid conjugation via 'triparental mating' was used to transfer broad-host range plasmids into *P. syringae*. Donor plasmids with the *mob* function are mobilized and transferred into recipient *P. syringae* strain by the use of the helper strain *E. coli* HB101 (pRK2013) carrying the transfer function (*tra*). Recipient *P. syringae* strains

were grown for 2-3 days on MG agar plates prior to the conjugation. Approximately one full loop of recipient bacteria was resuspended in 1 ml of HSC medium. Subsequently, single colonies of overnight grown donor and helper *E. coli* strains were resuspended in the same suspension. The suspension was mixed well and spotted (2 µl) on a KB agar plate without antibiotics. The conjugation plate was then incubated for 12-16 hours at 28°C. Mating spots were scraped off the plate and resuspended in 1 ml HSC medium. This cell suspension was diluted from 10^{-1} to 10^{-5} in HSC medium. 200-300 µl of this dilution series were plated onto MG plates with the appropriate antibiotic(s) to select for transconjugants. Subsequently, plates were incubated at 28° for 3-5 days until single *P. syringae* colonies were visible. The single colonies were restreaked twice on MG plates containing the appropriate antibiotic(s) and the presence of plasmids was determined by DNA plasmid isolation and agarose electrophoresis.

4.2.6 Pentapeptide scanning mutagenesis

A 0.8-kb *Msc*I-*Aat*II fragment encoding the N-terminus of CorS was subjected to *in vitro* mutagenesis. *In vitro* transposition was performed with a modified mini-Mu transposon as the donor DNA, plasmid pMA8 containing 0.8-kb *Msc*I-*Aat*II fragment as the target DNA and purified MuA protein (Finnzymes) according to Taira *et al*. (1999). A standard reaction (25 µl) contained 10 nM donor DNA, 250 ng target DNA, 224 nM (0.4 µg) MuA, 25 mM Tris-HCl (pH 8.0), 100 µg/ml BSA, 15% (w/v) glycerol, 0.05% (w/v) TritonX-100, 126 mM NaCl and 10 mM $MgCl_2$. The reaction was carried out at 30°C. The transposon-containing plasmid pool was introduced to *E. coli* MC1061 by electroporation and selected for ampicilin (150 µg/ml) and chloramphenicol (5 µg/ml) resistance. The plasmid DNA pool was isolated. The resulting plasmid pool was subjected to a series of manipulation steps. First, the mutants containing a transposon insertion in the 0.8-kb *Msc*I-*Aat*II fragment were excluded from the mutants containing an insertion in the vector. To do so, after treatment of the plasmid pool with *Kpn*I and *Sac*I, bands of non-affected vector and of the insert containing a transposon insertion were eluted from the agarose gel, ligated to each other and subsequently electroporated into *E. coli* MC1061 and selected for ampicilin (150 µg/ml) and chloramphenicol (5 µg/ml) resistance. *Not*I digestion of the plasmid DNA pool removed the inserted chloramphenicol resistance-mediating transposon from the mutant clones leaving a unique *Not*I site within a 15 nucleotide insertion in each mutant. After digestion with *Not*I, DNAs were ligated together, electroporated into *E. coli* MC1061 and selected for ampicilin

(150 µg/ml) resistance and chloramphenicol (5 µg/ml) sensitivity. Colonies were pooled together again and plasmid DNA was isolated from this mutant pool. The plasmid pool was digested with *Msc*I and *Aat*II. The band of the mutagenized 0.8-kb *Msc*I-*Aat*II fragments was eluted from the agarose gel and then ligated to pBSB24. Ligations were transformed into *E. coli* DH5α, transformants were selected for ampicilin resistance, and then all colonies were pooled. The plasmid DNA pool was isolated and digested with *Bam*HI and *Hin*dIII. The band of the 2.3-kb *Bam*HI-*Hin*dIII fragments was eluted from the agarose gel and subsequently ligated to pRKBE11. Ligations were transformed into *E. coli* DH5α, transformants were selected for tetracycline resistance, and single colonies were kept for subsequent steps. Mutants were introduced separately to PG4180.D4 (pRGMU1) by conjugation.

4.3 Biochemical and analytical methods

4.3.1 Estimation of enzymatic activities

4.3.1.1 Quantitative estimation of specific ß-glucuronidase activity

The *E. coli* ß-glucuronidase gene (*uidA* or *gus*) (Jefferson *et al*., 1986) is commonly used in plant pathogenic bacteria as a reporter gene to demonstrate environmental-dependent gene expression. ß-glucuronidase activity (GUS) can be quantified by spectrophotometric or fluorescence assays. Plasmid pRGMU1 contains the promoterless *gus* gene fused to a 2.9-kb *Pst*I-fragment containing the *cmaABT* promoter region from the COR gene cluster of PG4180.

Samples of 1.5 ml were taken from *P. syringae* cultures carrying pRGMU1 grown at 18 and 28°C when the OD_{600nm} reached values of 1.5-2.0. After discarding supernatants, cells were resuspended in 500 µl GUS-extraction buffer (50 mM Na_2HPO_4, pH 7.0; 10 mM EDTA disodium salt; 0.1% N-laurolylsarcosyl sodium salt; 0.1% Triton X-100; 0.07% ß-mercaptoethanol), and kept on ice for 30 min. Subsequently, cells were disrupted by 3×15 sec ultrasonic treatment and transferred to precooled 96-wells microtiter plates. The wells of rows C, D, E, F, G, H from 1 to 12 were filled with 180 µl carbonate stop-buffer (0.2 M Na_2CO_3). Additionally, the well B12 was filled with 180 µl carbonate stop-buffer. 200 µl of cell extract were filled into wells A1-10, whereas A11 was filled with 200 µl of water, and A12 was filled with 200 µl of MU-standard (1 mM 7-hydroxy-4-methylcoumarin, sodium salt). Finally, wells B1-11 were filled with 180 µl of substrate buffer (2 mM 4-methylumbelliferyl-ß-D-glucuronide in GUS-extraction buffer). The reaction was initiated

by transferring 20 µl of cell extract to the substrate buffer wells from row A to row B (1:10 dilution) by use of a multi-channel pipetman. Immediate transfer of 20 µl from row B to rows C and D stopped the reaction. Therefore, the fluorescence values in wells C1-10 represented the $F(t_0)$ values. The microtiter plate was immediately placed into a water bath at 37°C. After 10 min the reaction was stopped by transfer of 20 µl from row B to row E, and subsequently to rows F, G and H. The plate was immediately read in a Fluorolite fluorometer (Dynatech Laboratories, Denkendorf) with the following set-up: extinction filter at 390 nm, emission filter at 450 nm, and lamp voltage at 3.0 V. The fluorescence values in wells E1-10 represented the $F(t_{10})$values. The fluorescence in the well B12 represented the standard fluorescence (F_{st}) of 100 µM MU-solutions. The GUS activity was calculated according to the equations:

$\Delta F_{450} = F(t_{10}) - F(t_0)$

GUS activity (U) = $\Delta F_{450} \times 100 / F_{st}$

Specific activity (U/mg protein) = UGUS / mg protein

4.3.1.2 Quantitative estimation of specific alkaline phosphatase (PhoA) activity

Quantitative estimation of specific alkaline phosphatase (PhoA) activity was performed following the method described by Rutz *et al*. (1999). Bacteria were harvested from 1.5 ml of cell culture (5 min, 13,000 rpm), and the supernatant was discarded. The pellet was resuspended in 300 µl of 1 M Tris/HCl (pH 8.0), and cells were permeabilized by addition of 25 µl of 0.1 % SDS and 2 drops of chloroform. Samples were stirred for 40 min at 28°C. 200 µl of cell extract were transferred to wells A1-10 of a microtiter plate. Well A11 was filled with 200 µl of water, and A12 was filled with 200 µl of a standard, 0.4 mM solution of *p*-nitrophenol. Wells B1-11 were filled with 200 µl of a substrate solution (5 mg/ml *p*-nitrophenyl phosphate in 1 M Tris/HCl (pH 8.0) buffer containing 5 mM $MgCl_2$). Well B12, and wells C1-12, D1-12 were filled with 200 µl of a 1 M NaOH solution (stop-buffer). Reactions were initiated by transfer of 50 µl of cell extract from wells A1-12 to wells B1-12 by use of a multi-channel pipetman. Plates were incubated for 180 min at 28°C, and the A_{405nm} was measured in a MRX Microplate Reader (Dynatech laboratories, Denkendorf). Specific alkaline phosphatase activity was defined as units per mg of cellular protein. One unit of PhoA activity corresponded to 1 µmole of *p*-nitrophenol released per minute at room

temperature. The concentration of *p*-nitrophenol for the calibration curve was ranged from 2-120 µmole.

4.3.1.3 Quantitative estimation of specific ß-galactosidase (LacZ) activity

Quantitative estimation of specific ß-galactosidase (LacZ) activity was performed following the method described by Rutz *et al*. (1999). Bacteria were harvested from 1.5 ml of cell culture (5 min, 13,000 rpm), and the supernatant was discarded. The pellet was resuspended in 300 µl of buffer Z (60 mM Na_2HPO_4, 40 mM NaH_2PO_4, 10 mM KCl, 1 mM $MgSO_4$, 50 mM ß-mercaptoethanol (pH 7.0)), and cells were permeabilized by addition of 25 µl of 0.1 % SDS and 2 drops of chloroform. Samples were stirred for 40 min at 28°C. 200 µl of cell extract were transferred to wells A1-10 of a microtiter plate. Well A11 was filled with 200 µl of water, and A12 was filled with 200 µl of a standard, 2 mM solution of *o*-nitrophenol. Wells B1-11 were filled with 200 µl of a substrate solution (4 mg/ml *o*-nitrophenyl ß-D-galactopyranoside (ONPG) in buffer Z (pH 7.0)). Well B12 and wells C1-12, D1-12 were filled with 200 µl of 1 M Na_2CO_3 solution (stop-buffer). Reactions were initiated by transfer of 50 µl of cell extract from wells A1-12 to wells B1-12 by use of a multi-channel pipetman. Plates were incubated for 90 min at 28°C, and the A_{405nm} was measured in a MRX Microplate Reader (Dynatech laboratories, Denkendorf). Specific ß-galactosidase activity was defined as units per mg of cellular protein. One unit of LacZ activity corresponded to 1 µmole of *o*-nitrophenol released per minute at room temperature. The concentration of *o*-nitrophenol for the calibration curve ranged from 10-1,000 µmole.

4.3.1.4 Qualitative determination of GUS, PhoA and LacZ activities

5-bromo-4-chloro-3-indolyl-ß-glucuronic acid (X-Gluc) was used as substrate for the qualitative determination of GUS expression on agar plates. 5 mg of X-Gluc was dissolved in 1 ml of dimethylformamide and added to 250 ml of agar medium. Blue color formation of colonies was an indicator of enzymatic activity.

Alkaline phosphatase activity in bacteria was detected qualitatively by blue color formation of colonies on agar plates containing 5-bromo-4-chloro-3-indolyl-phosphate-p-toluidine salt (X-Phos) at a concentration of 160 µg per ml of agar medium. 40 mg of the X-Phos was dissolved in 1 ml of dimethylformamide and added to 250 ml of agar medium.

ß-Galactosidase activity was detected qualitatively by blue color formation of colonies on agar plates containing 5-bromo-4-chloro-3-indolyl-ß-galactoside (X-Gal) at a concentration of 100 µg per ml of agar medium. 25 mg of the X-Gal was dissolved in 1 ml of dimethylformamide and added to 250 ml of agar medium.
For visual estimation of enzymatic activities in *P. syringae*, bacteria were resuspended in 1 ml of HSC medium and spotted (2 µl) on substrate-containing agar plates. To observe intensive and distinguishable color formation of colonies, plates with spotted bacteria were incubated for 3-6 days at 18°C and 28°C, respectively.

4.3.2 Protein techniques

4.3.2.1 Determination of protein concentration

Protein concentrations were determined using the Coomassie Brilliant Blue G 250 (Bradford, 1976). When this dye reagent binds to a protein, a shift of its absorbance maximum from 465 nm to 595 nm occurs under acidic conditions. The determination of protein concentration for cell extracts was carried out in microtiter plates. Usually, 180 µl of the cell extract was transferred to fresh microfuge tubes and precipitated with an equal volume of cold 10% trichloroacetic acid (TCA) solution. The amount of the cell extract varied and depended on either on the enzymatic assay used or on the total amount of cells. For instance, for alkaline phosphatase and ß-galactosidase assays, 50 µl of the cell extract was used for determination of protein concentration. After precipitation with TCA proteins were denatured by boiling for 5-10 min. After centrifugation for 5 min, the protein pellet and 1-2 mg of a protein standard (γ-globulin) were separately dissolved in 100 µl of 1 M NaOH and diluted to 1 ml with 900 µl deionised water (ddH_20). 150 µl of the protein solutions were transferred to wells A1-11 of a microtiter plate. Well A12 and all wells in rows B, C, D, E, F, G, and H were filled with 100 µl of ddH_20. Subsequently, 50 µl of the protein solutions were transferred from row A to rows B, C, D, E, G, and H resulting in a 1:3 dilution for each row. 200 µl of Bradford reagent (8.5% (v/v) H_3PO_4; 4.75% (v/v) C_2H_5OH; 0.01% (w/v) Coomassie Brilliant Blue G250) was added to the wells. The A_{600nm} was measured immediately in a MRX Microplate Reader (Dynatech laboratories, Denkendorf)

4.3.2.2 Whole cell extraction

Cells were harvested during late exponential or stationary phase by centrifugation at 7,000 rpm at 4°C. Subsequently, cells were resuspended in protein extraction buffer (PEB) and incubated in ice for 30 min. The amount of added PEB depended on the size of the pellet. Usually, 100-200 µl of this buffer was added to the pellet of 1.5 ml of cell culture, and 1-2 ml of the buffer were added to the pellet of a 100-ml cell culture.

Protein extraction buffer

50	mM	Tris/HCl (pH 7.4)
200	mM	NaCl
1	mM	EDTA
5	mM	DDT
1.5	mM	magnesium acetate
50	µg/ml	lysozyme
20	µg/ml	DNase I

For small protein amounts (in 200-500 µl PEB), cells were broken by 3×15 s ultrasonic treatment. Cells debris was spun down at 13,000 rpm at 4°C for 15 min. The supernatant was further used as the soluble protein fraction. The pellet was washed with 200-500 µl of 50 mM Tris/HCl (pH 8.0) buffer. After subsequent centrifugation, the pellet was resuspended in 100-500 µl of 50 mM Tris/HCl (pH 8.0) buffer and stored at –20°C.

For larger protein amounts, cells were broken under hydraulical pressure using a French Press apparatus (SLM Aminco, Rochester, USA). After subsequent centrifugation, the supernatant was used as the soluble protein fraction, and the pellet was washed with 50 mM Tris/HCl (pH 8.0) buffer. The pellet was resuspended in 50 mM Tris/HCl (pH 8.0) buffer, aliquoted and stored at –80°C.

4.3.2.3 Subcellular cell fractionation of *P. syringae*

Subcellular fractionation was done according to the method described by Boyd *et al*. (1987) with some modifications. 1.5 ml of an exponentially grown bacterial culture was spun down at 5,000 rpm at 4°C. The supernatant was used as the extracellular fraction. Cells were permeabilized by resuspending the pellet in 150 µl of cold SP buffer (0.1 M Tris/HCl (pH 7.5), 0.5 mM EDTA-Na, 0.5 M sucrose) and subsequent incubation on ice for 5 min. To

prevent membrane protein degradation by proteases, the protease inhibitors phenylmethylsulfonyl fluoride (PMSF) or 4-(2-aminoethyl)-benzensulfonyl fluoride hydrochloride (AEBSF) were added to give a final concentration of 1 mM. Permeabilized cells were spun down at 4°C and carefully resuspended in 100 µl of ddH_2O. Subsequently, the permeabilized cells were osmotically shocked by addition of 5 µl of 20 mM $MgCl_2$. After centrifugation of the cells for 15-20 min at 13,000 rpm at 4°C, the supernatant was further used as the periplasmic fraction. Spheroplasts were generated by incubating the cells resuspended in 300 µl of diluted SP-buffer (0.05M Tris/HCl (pH 7.5), 0.25 mM EDTA-Na, 0.25 M sucrose) with 1mg lysozyme/ml on ice for 5 min. After centrifugation for 30 min the pellet (spheroplasts) was resuspended in 500 µl of a 50 mM Tris/HCl (pH 8.0) buffer containing 0.2 mg/ml of RNase A and 0.2 mg/ml of DNase. Spheroplasts were broken by 5×10 s ultrasonic treatment. Subsequent centrifugation for 30 min at 13,000 rpm at 4°C separated the cytoplasmic fraction (supernatant) and the membrane fraction (pellet). Both fractions were stored at –80°C. For SDS-gels, the pellet was resuspended in 100 µl of 50 mM Tris/HCl (pH 8.0).

4.3.2.4 Trypsin treatment of spheroplasts

P. syringae was grown in 50 ml of HSC-medium at 18°C and at 28°C until the cultures reached an OD_{600nm} of 2.5-3.0. Cell fractionation to obtain spheroplasts was done according to 4.3.2.3. Subsequently, spheroplasts were lysed in 200 µl of lysis buffer (50 mM Tris/HCl (pH 8.0), 150 mM NaCl, 1 % TritonX-100, 0.1 % SDS). 200 µl of the lysate containing solubilized proteins was divided into two portions: 120 µl and 80 µl. 80 µl of the lysate was used directly for Western blotting. 120 µl of the lysate was treated with trypsin (1 µg/ml final concentration). Protease digestion was stopped by addition of 12 µl of a 10 mM solution of AEBSF protease inhibitor. Proteins were precipitated by cold 10% TCA, resuspended in 40 µl of Tris/HCl (pH 8.0), and used for Western blotting.

4.3.2.5 Membrane fraction preparation

Preparation of the membrane fraction was done following the method described by Osborn *et al*. (1972) and modified by Gramajo *et al*. (1991). Cells were harvested from late exponential or early stationary phase grown cultures by centrifugation at 7,000 rpm at 4°C. Pellets were resuspended in 10 ml of buffer (50 mM Tris/HCl (pH 8.0), 10% sucrose, 0.2 mM

dithiothreitol (DTT), 10 mg/ml of lysozyme, 0.2 mg/ml of RNase A, 0.2 mg/ml DNase) and incubated on ice for 1 h to generate spheroplasts. Spheroplasts were spun down at 7,000 rpm at 4°C and subsequently resuspended in 50 mM Tris/HCl (pH 8.0) containing 0.2 mM DTT and 0.1 mM PMSF or AEBSF. Spheroplasts were broken by use of the French Press apparatus (two times). Unbroken cells were removed by centrifugation for 10 min at 8,000 rpm at 4°C. The membrane fraction was harvested by ultracentrifugation for 2 h at 35,000 rpm at 4°C. The pellet (membrane fraction) was resuspended in 1 ml of 50 mM Tris/HCl (pH 8.0) containing 0.1 mM PMSF or AEBSF and stored at –80°C.

4.3.2.6 Solubilization of membrane proteins

a) Solubilization of membrane proteins for 2-D electrophoresis

To improve solubilization of membrane proteins used for 2-D electrophoresis, membrane fractions were resuspended in an extraction buffer containing chaotropes urea, thiourea and the surfactants 3-[(3-cholamidopropyl)-dimethylammonio]-1-propanesulfonate (CHAPS) and N-decyl-N,N-dimethyl-3-ammonio-1-propanesulfonate (SB 3-10).

Extraction buffer

8 M Urea
2 M Thiourea
2 % CHAPS
1 % SB 3-10

b) Solubilization of the CorS$_{Strep\text{-tag}}$ protein

The membrane fraction of *E. coli* cells overexpressing CorS$_{Strep\text{-tag}}$ was thawn on ice and centrifuged at 13,000 rpm at 4°C. The pellet was resuspended in 800 µl of solubilization buffer (62.5 mM Tris/HCl (pH 8.0), 12.5 % glycerol, 1.25 mM EDTA, 2.5 mM ß-mercaptoethanol). While stirring at 4°C, CorS$_{Strep\text{-tag}}$ was extracted with 200 µl of TritonX-100 (20 % solution) which was added stepwise (10×20 µl). After stirring on ice for 1 h, the solubilizate was centrifuged for 30 min at 30,000 rpm. The supernatant (1 ml) was transferred to a fresh tube. The pellet was resuspended again in 800 µl of solubilization buffer and the solubilization procedure was repeated once. Supernatants containing solubilized CorS$_{Strep\text{-tag}}$ were combined and CorS$_{Strep\text{-tag}}$ was further purified by StrepTactin affinity chromatography (IBA, Göttingen) (4.3.2.7).

4.3.2.7 Purification of solubilized CorS*Strep*-tag using Strep-tag affinity chromatography

The purification procedure for solubilized CorS*Strep*-tag was performed according to the method described by Rübenhagen *et al*. (2000). 2 ml of the supernatant fraction containing solubilized CorS*Strep*-tag was diluted to 4 ml with membrane buffer. The mix was applied to a StrepTactin affinity column, which had been pre-equilibrated with 4 ml of pre-equilibration buffer. After the sample had completely entered the column, the column was washed 5 times with 1 ml of membrane buffer. The column-bound protein was eluted six times with 0.5 ml of pre-equilibration buffer containing 5 mM desthiobiotin. Subsequently, 30 µl of each fraction was applied to an analytical SDS-10%-polyacrilamide gel. For regeneration of the column, the column was washed three times with 5 ml of washing buffer containing 1 mM 4-hydroxyazobenzene 2-carboxylic acid (HABA). A color change from yellow to red served as an indicator of the column activity status. To remove HABA, the column was washed twice with 4 ml of washing buffer containing 1 M NaCl. The column was stored at 4°C overlaid with 2 ml of washing buffer.

Membrane buffer

50	mM	Tris/HCl (pH 8.0)
10	%	glycerol
2	mM	mercaptoethanol
1	mM	EDTA

Pre-equilibration buffer

50	mM	Tris/HCl (pH 8.0)
10	%	glycerol
2	mM	mercaptoethanol
1	mM	EDTA
200	mM	NaCl
0.1	%	TritonX-100

Washing buffer

100	mM	Tris/HCl (pH 8.0)
1	mM	EDTA

4.3.2.8 Sodium dodecyl sulfate-polyacrylamide gel electrophoresis (SDS-PAGE)

Denaturing conditions (0.1 % SDS) are used to separate proteins according to their molecular weights using SDS-polyacrylamide electrophoresis (SDS-PAGE) (Laemmli, 1970). A discontinuous electrophoretic gel/buffer system was employed using the electrophoresis apparatus Mini Protean II cell (BioRad, München) for SDS-PAGE. The polyacrylamide gel of 8.2×7.3×0.075 cm^3 was cast stepwise. First, a separating gel (4-12.5 % of acrylamide/

bisacrylamide) for protein separation was cast then on top of it a stacking gel (4 % of acrylamide/bisacrylamide) was cast to concentrate proteins before entering the separating gel. Protein loading buffer containing tracking dye (bromphenol blue) was added to each sample which was then incubated at 70°C for 10 min. Subsequently, the protein samples were loaded to the gel. Either prestained protein marker, low range (BioRad) or 10 kDa Protein Ladder (GibcoBRL) were used as molecular weights standards in SDS-PAGE. The electrophoresis chamber was completely filled with SDS-electrophoresis buffer. The electrophoresis was started at 20 mA per gel until the tracking dye reached the top of the separating gel then performed at 40 mA per gel until the tracking dye reached the bottom of the separating gel.

	Stacking gel	**Separating gel**		
	4%	6%	10%	12.5%
Acrylamide/bisacrylamide (30% / 0.8%)	0.94 ml	2.4 ml	4 ml	5 ml
0.5 M Tris/HCl (pH 6.8)	1.76 ml			
1 M Tris/HCl (pH 8.8)		4.5 ml	4.5ml	4.5ml
H_2O	3.84 ml	4.46ml	2.86 ml	1.86 ml
10% (w/v) SDS	70 µl	120 µl	120µl	120µl
TEMED	10 µl	12 µl	12 µl	12 µl
1% (w/v) APS	0.4 ml	0.5 ml	0.5 ml	0.5 ml

Protein loading buffer

125	mM	Tris/HCl (pH 6.8)
4	% (w/v)	SDS
20	% (v/v)	glycerol
20	µg/ml	bromphenol blue
10	% (v/v)	2-mecraptoethanol

SDS-electrophoresis buffer

25	mM	Tris/HCl
192	mM	glycine
0.1	% (w/v)	SDS

4.3.2.9 Protein staining procedures

Following the electrophoresis, the gel cast was disassembled and proteins were usually visualized by staining the gel in 0.04 % Coomassie Brilliant Blue R-250 in a mixture of methanol/water/acetic acid (4:5:1). Destaining was carried out in a mixture of

methanol/water/acetic acid (4:5:1). After destaining and washing in water for several times, the gel was dried at 60°C for 1.5 h.

An alternative more sensitive staining procedure was performed using the GelCode Blue Stain Reagent (Pierce, USA). This procedure lacks a destaining step. The gel was washed three times with ddH_2O. Then the gel was stained for 30 min in the GelCode Blue to visualize proteins.

For detection of very small amounts of proteins, the silver staining procedure applied. After disassembling the gel cast, the gel was incubated overnight in fixation solution (50 % (v/v) methanol, 12 % (v/v) acetic acid, 0.05 % (v/v) formaldehyde). The gel was then washed 3×20 min by gentle shaking in 50 % ethanol solution. The first step of the staining reaction comprises the addition of 0.8 mM sodium thiosulfate ($Na_2S_2O_3$) solution. The excess of $Na_2S_2O_3$ was removed by washing three times for a few seconds in ddH_2O. A 12 mM silver nitrate ($AgNO_3$) solution containing 0.08 % (v/v) formaldehyde was then added. The excess of $AgNO_3$ was removed by washing three times for a few seconds in ddH_2O. Following the addition of 0.57 M sodium carbonate (Na_2CO_3) solution containing 0.05 % (v/v) formaldehyde and 16 µM of $Na_2S_2O_3$, the product of reaction was precipitated thereby visualizing proteins in form of yellow-brown bands. The reaction was stopped by addition of 10 % acetic acid.

4.3.2.10 Two-dimensional gel electrophoresis

Two-dimensional gel electrophoresis (2-DE) is a method combining isoelectric focusing (IEF) in the first dimension and SDS-PAGE in the second dimension (O'Farrell, 1975). IEF allows to separate proteins according to their isoelectric points (pI). The presence o f a pH gradient is critical for the IEF technique. In a pH gradient, under the influence of an electric field, a protein will move to the position in the gradient where its net charge is zero. The original method for the first-dimension (IEF) depended on carrier ampholyte-generated pH gradients in polyacrylamide tube gels. Because of the limitations of the carrier ampholytes method, an alternative technique for pH gradient formation was developed: immobilized pH gradients (IPG) (Bjellqvist *et al*., 1982; Görg *et al*., 1988). An immobilized pH gradient (IPG) is created by covalently incorporating a gradient of acidic and basic buffering groups into a polyacrylamide gel at the time it is cast.

a) 2-D electrophoresis of proteins using the IEF method

P. syringae cells grown at 18°C and 28°C were harvested during late exponential or stationary phase. Subsequently, cells were fractionated according to a modified method described by Boyd *et al*. (4.3.2.3). Cell fractions enriched in membrane proteins were used as samples for 2-DE analysis. A pellet of the fraction containing 100-400 µg of protein was resuspended in 30 µl of IEF sample buffer and used for the IEF electrophoresis immediately. Polyacrilamide tube gel containing carrier ampholytes with a pH range of 3-10 was filtered before addition of initiators of the polymerization reaction (TEMED and APS) to avoid mechanical distortion during electrophoresis. The gel was cast into glass tubes (145×5 mm) by use of a syringe. Gel surfaces were overlaid with 50 µl ddH_2O. After 45 min of polymerization the water was discarded and the gel surfaces were overlaid with 50 µl of IEF sample buffer. Tubes were placed vertically into the IEF-chamber (Model 175 Tube Cell, BioBad). After additional 30 min the IEF sample buffer was discarded and 30 µl of the protein sample was loaded to each tube gel. Subsequently, protein samples were overlaid with 50 µl of IEF sample overlaying buffer. The lower part of the IEF-chamber was filled with anode solution (0.01 M H_3PO_4 in ddH_2O) and its upper part was filled with catode solution (0.1 M NaOH in ddH_2O). The IEF-electrophoresis was performed overnight at room temperature according to the following program:

15 min	100 V
15 min	200 V
30 min	300 V
2 h	400 V
12 h	1000 V

Polyacrylamide tube gel for 12 tubes(145×5 mm)

13.75	g	Urea
2.63	ml	Acrylamide/bisacrylamide (38.8% / 2%)
5	ml	NP-40 or Igepal (10 %)
6.4	ml	ddH_2O
1	ml	Ampholyte 5-7
0.25	ml	Ampholyte 3-10
37.5	µl	APS (10 %)
25	µl	TEMED

IEF sample overlaying buffer

3	g	Urea
0.2	ml	NP-40 or Igepal (10 %)
0.25	ml	Ampholyte 3-10
0.77	g	DTT

Adjust volume to 100 ml with ddH_2O

IEF sample buffer

0.5	g	DTT
2	g	CHAPS
27	g	Urea
2.5	ml	Ampholyte 3-10
30	ml	ddH_2O

At the end of IEF-electrophoresis, gels were carefully squeezed out of the tubes and equilibrated by gentle shaking for 45 min in IEF equilibration buffer. Previously, the SDS-10%-polyacrylamide gels were cast stepwise. First, the bottom gel was cast, then the separating and the stacking gels. After equilibration tube-gels were placed on top of the gel in the PAGE chamber (Protean II xi, BioRad) between the glass plates, dipped into the SDS-electrophoresis buffer to lubricate them and fixed between glass plates by SDS-agarose. The electrophoresis was performed overnight at constant power (1W per gel) at 4°C with permanent stirring of SDS-electrophoresis buffer. Either Coomassie (400 µg of total protein) or silver staining (100 µg or less of total protein) was used to visualize proteins in the gel.

IEF equilibration buffer

25	ml	0.5 M Tris/HCl (pH 6.8)
20	ml	Glycerol (99 %)
4.6	g	SDS
1.54	g	DTT
50	µg/ml	bromphenol blue

Adjust volume to 200 ml with ddH_2O

Separating-gel solution
(for 8 SDS-10%-polyacrylamide gels)

83.3	ml	Acrylamide/bisacrylamide (30% / 0.8%)
50	ml	2 M Tris/HCl (pH 8.8)
114.2	ml	ddH_2O
2.5	ml	SDS (10 %)

SDS-agarose

12.5	ml	0.5 M Tris/HCl (pH 6.8)
2.3	g	SDS
1	g	Agarose

Adjust volume to 100 ml with ddH_2O.

Bottom-gel

1.5	ml	Separating gel solution
28	µl	APS (10 %)
5	µl	TEMED

Separating gels

250	ml	Separating-gel solution
840	µl	APS (10 %)
l24	µl	TEMED

Stacking gels (8 gels)

5.6	ml	Acrylamide/bisacrylamide (30% / 0.8%)
10.5	ml	0.5 M Tris/HCl (pH 6.8)
25.2	ml	ddH_2O
210	µl	APS (10 %)
42	µl	TEMED

b) 2-D electrophoresis of proteins using immobilized pH gradients

Either the pellets of cell fractions enriched in membrane proteins were resuspended in 150 µl of IPG rehydration buffer or the membrane fractions prepared following the Gramajo *et al*., 1991 method (4.3.2.5) was diluted in IPG rehydration buffer to 150 µl of total volume. After appropriate solubilization of the proteins, 150 µl of rehydration buffer containing bromphenol blue was added. 300 µl of this solution was equally distributed in the slot of the Immobiline DryStrip Reswelling Tray. Each IPG strip of 18-cm length was carefully dipped into the solution avoiding bubbles under the strip. The IPG strip was overlaid with 2 ml of IPG DryStrip Cover Fluid (Amersham-Pharmacia Biotech, Freiburg). The Reswelling Tray was covered by a lid. IPG strips were rehydrated overnight at room temperature. Then the IPG strips were removed from the Reswelling Tray and rinsed briefly with deionised water. The strips were slightly blotted between two moistened sheets of filter paper. Afterwards, the strips were immediately transferred to adjacent grooves of the aligner in the Immobiline DrySrtip tray of the Multiphor II unit. The strips were placed with the pointed (acidic) end at the top of the tray near the anode, and with the blunt end at the bottom of the tray near the catode. Moistened electrode strips were placed across the cathodic and anodic ends of the aligned IPG strips in such way that they contacted the gel surface of the IPG strips. An additional strip moistened with 15 mM DTT solution was placed next to the catode strip. Once the electrodes were placed over the electrode strips, the strips were overlaid with IPG DryStrip Cover Fluid. Finally, the lid was placed on the Multiphor II unit and the electrophoresis was started. The electrophoresis was performed according to the following program:

Phase	Voltage(V)	Current (mA)	Power (W)	V/h
1	500	1	5	1,000
2	500	1	5	2,000
3	3,500	1	5	10,000
4	3,500	1	5	35,000

After running the first dimension, the strips were equilibrated for 15 min in IPG equilibration buffer A containing DTT, which preserves the fully reduced state of denatured, unalkylated proteins, and then for 15 min in IPG equilibration buffer B containing iodoacetamide, which alkylates thiol groups on proteins preventing their reoxidation during electrophoresis. Addition of tracking dye (bromphenol blue) to the IPG equilibration buffer B allowed the monitoring of the electrophoresis in the SDS-gel. The strips were then placed into the SDS-PAGE chamber (Protean II xi, BioRad) between the glass plates, dipped into the SDS-electrophoresis buffer to lubricate them and fixed between the glass plates by SDS-agarose. Electrophoresis was performed overnight at constant power (1W per gel) at 4°C with permanent stirring of the SDS-electrophoresis buffer. Either Coomassie (400-500 µg of total protein) or silver staining (100 µg protein) was used to visualized proteins in the gel.

IPG rehydration solution (25 ml)

12	g	Urea
3.81	g	Thiourea
0.5	g	CHAPS
0.25	g	SB 3-10
109.4	mg	DTT
131.3	µl	Pharmalytes 3-10

IPG equilibration buffer (10 strips)

5	ml	0.5 M Tris/HCl (pH 6.8)
18	g	Urea
15	ml	Glycerol (99 %)
20	ml	SDS (10 %)

Adjust volume to 50 ml with ddH_2O.

Buffer A: add 87.5 mg of DTT to 25 ml of equilibration buffer.

Buffer B: add 1.125 g of iodoacetamide to 25 ml of equilibration buffer.

4.3.2.11 Protein immunodetection

a) Conventional Western blot analysis

Equal amounts of protein for Western blot analysis were separated by SDS-PAGE on two gels running in the same chamber. Subsequently, proteins from one of these gels were electrotransferred to Hybond-C nitrocellulose membrane (Amersham-Pharmacia Biotech, Freiburg). Electroblotting was performed in electrotransfer buffer overnight at 20 mA per gel using a Mini Trans-Blot Electrophoretic Transfer Cell (BioRad, München). The other gel was stained with either Coomassie Brilliant Blue R 250 or GelCode Blue Stain Reagent (Pierce, USA). Following the electrotransfer of proteins, the membrane was blocked with 10 ml of 5% blocking reagent solution (Roche, Mannheim) in blocking buffer at 37°C for an hour.

Subsequently, the membrane was incubated in a plastic bag with 5 ml of 1% blocking reagent solution in washing buffer I containing the specific primary antibody at the appropriate concentration (from 1:100 to 1:1,000 dilution) at 37°C for 1.5 h. The unbound primary antibody was then removed by washing the membrane 3×15 min with washing buffer I at 37°C. Then, in a plastic bag the membrane was incubated with 5 ml of 1% blocking reagent solution in washing buffer I containing the secondary antibody (anti-rabbit IgG alkaline phosphatase, anti-mouse IgG alkaline phosphatase or anti-mouse IgG horseradich peroxidase (POD) conjugates) at a dilution 1: 7,500 at 37°C for 1.5 h. Excess of conjugates was removed by washing the membrane with washing buffer I for 3×15 min at 37°C. To remove TritonX-100, the membrane was washed in washing buffer II for 2×5 min at room temperature. The membrane was placed in a plastic bag and the chromogenic reaction was initiated by adding 20 ml of color reaction buffer containing 45 µl of 7.5% (w/v) nitrotetrazolium blue dissolved in 70 % (v/v) dimethylformamide and 35 µl of 5% (w/v) 5-bromo-4-chloro-3-indolyl-phosphate-p-toluidine salt dissolved in dimethylformamide (Blake *et al*., 1984). The membrane was then kept at 4°C in the dark until the signals developed. The reaction was stopped by washing the membrane several times with tap water. The membrane was then air dried and stored in the dark.

Alternatively, a chemiluminescent detection method was used. The BM chemiluminescence blotting system was used to detect peroxidase-labeled secondary antibody according to a protocol provided by the manufacturer (Roche, Mannheim). For detection of alkaline phosphatase-labeled secondary antibody, the CSPD substrate was used (1:10 dilution). The membrane was incubated with 0.5 ml of CSPD substrate solution at 37°C for 15 min. Then the membrane was exposed to an X-ray film at room temperature for 15-60 min. The film was developed and signals were visually monitored.

Electrotransfer buffer (pH 8.3)

25	mM	Tris/HCl
192	mM	Glycine
10	%	methanol

Blocking buffer (pH 7.4)

20	mM	Na_2HPO_4
200	mM	NaCl

Washing buffer I (pH 7.4)

20	mM	Na_2HPO_4
200	mM	NaCl
1	mM	EDTA-Na
0.3	%	TritonX-100

Washing buffer II (pH 7.4)		
20	mM	Tris/HCl
200	mM	NaCl

Colour reaction buffer (pH 9.5)		
100	mM	NaCl
50	mM	$MgCl_2$
100	mM	Tris/HCl

b) Western blot analysis for *Strep*-tag II recombinant proteins

Equal amounts of protein were separated by SDS-PAGE and subsequently electrotransferred to Hybond-C nitrocellulose membrane (Amersham-Pharmacia Biotech, Freiburg) as described above (4.3.2.11 (a)). Since milk is a rich source of biotin, milk powder can not be used for blocking of the membrane when *Strep*-tag II recombinant protein needs to be detected. Therefore, the membrane was blocked with 20 ml 3% BSA, 0.5% Tween 20 in PBS buffer for 1 h at room temperature. Subsequently, the membrane was washed for 3×5 min in PBS-Tween buffer (PBS with 0.1% Tween 20). Before detection of the recombinant protein via *Strep*-tag II, the membrane was incubated for 10 min in 10 ml PBS-Tween buffer containing 6 µg/ml avidin to block the endogenous biotin carboxyl carrier protein (22 kDa) of *E. coli*. Then, 2.5 µl of streptavidin-alkaline phosphatase conjugate (Amersham) was added to 10 ml of PBS-Tween buffer for detection of the *Strep*-tag II fusion protein. The membrane was incubated with the conjugate solution for 1 h. Excess of conjugates was removed by washing the membrane 3×5 min with PBS-Tween and 2×5 min with PBS. The chromogenic reaction was carried out in 20 ml of color reaction buffer. When signals developed after 2-3 hours, the membrane was washed several times with tap water, then air dried, and stored in the dark.

PBS-buffer (pH 7.2)		
4	mM	KH_2PO_4
16	mM	Na_2HPO_4
115	mM	NaCl

Colour reaction buffer (pH 8.8)		
100	mM	NaCl
5	mM	$MgCl_2$
100	mM	Tris/HCl

4.3.3 Quantitative estimation of COR/CFA-production

4.3.3.1 Isolation of coronafacoyl compounds

The extraction of the organic acids, COR and CFA, from cell supernatants was done following the protocol developed by Mitchell (1982) and modified by Palmer and Bender (1993). This isolation is based on ethyl acetate extraction from cell supernatants adjusted to low pH values. 1.5 ml of supernatant was adjusted to a pH value of 1-2 by addition of 25 µl concentrated HCl and extracted three times with ethyl acetate. After addition of ethyl acetate, the water phase was mixed with organic phase by shaking the tubes for 5 min at 37°C. The organic phases were transferred to a fresh tube and combined. Ethyl acetate was then evaporated from the tubes using a thermomixer adjusted to 65-70°C. The pellet was resuspended in 200 or 300 µl of trifluoroacetic (TFA; 0.05% in H_2O)/acetonitrile (9:1). 50 µl was applied to quantitative High Pressure Liquid Chromatography (HPLC) analysis.

4.3.3.2 Reverse-phase High Pressure Liquid Chromatography (HPLC) analysis

Quantitative estimation of COR and CFA production was performed by use of a Sykam HPLC system, consisting of a pump, a degaser, a gradient mixer, an autosampler, a C_{18}-reverse-phase column (250 × 4 mm; 5 µm), and a variable wavelength UV-detector. Peak areas, retention times and response factors were automatically determined by the program PeakSimple (SR1 Instruments, Torrance, USA). Elution of metabolites was done at a flow rate of 1 ml/min followed a binary gradient flux of solution A (0.05% TFA in H_2O) and B (0.05% TFA in acetonitrile) beginning with the ratio 90% A to 10% B and subsequently reducing the flux ratio to 50% of the solution A. Isocratic conditions (50% A) were maintained for 2.5 min. Then the flux of A was set to 0% (100% of B) for 3 min. At the end of the run a gradient flux of 90% A and 10% B was re-established. The total run time was 23.5 min. COR and CFA were detected at a wavelength of 208 nm. Standards of COR and CFA for calibration of the column were obtained from C.L. Bender (Oklahoma State University).

4.3.4 Gas chromatographic (GC) analysis

4.3.4.1 Whole-cell fatty acid extraction of bacteria

P. syringae was maintained on MG plates with appropriate antibiotics at 28°C. Parallel cultures were incubated in 100 ml of HSC medium with antibiotics in 250 ml Erlenmeyer flasks on a rotary shaker at 280 rpm at 18°C and 28°C. 10 ml samples were taken when cells reached a certain optical density (OD_{600nm}) in the range of 1.5-4.0. Cells were spun down in glass vials with screwable lids at 5,000 rpm for 10 min, resuspended and then saponified in 1 ml of reagent (15% NAOH in CH_3OH/H_2O (50:50, v/v)) for 30 min at 95-100°C. After cooling, 2 ml of reagent (6 N HCl in CH_3OH/H_2O (50:50, v/v)) was added. Fatty acids were converted into methyl esters following the incubation at 80°C for 10 min. The extraction of the methylated fatty acids was performed in 1.5 ml of reagent (n-hexane/diethylether (50:50, v/v). After a subsequent centrifugation at 5,000 rpm for 20 min, the lower phase was discarded and upper phase was washed with 3 ml of reagent (1.2% NaOH in H_2O). 2/3 of the upper phase containing fatty acid methyl esters (FAME) was transferred to a GC-tube with 0.5 g of anhydrous Na_2SO_4 to dry the sample. 3 µl of each sample was injected into a GC-column (4.3.4.2).

4.3.4.2 Bacterial fatty acid analysis

FAME were analysed with a GC 6000 VEGA Series gas chromatograph (Carlo Erba Strumentazione, Italy, Milan) equipped with a flame ionisation detector and a fused silica capillary DB-5ms column (5% phenyl nonpolar) of 30 m length and of 0.25 mm inner diameter. Nitrogen was used as the carrier gas at a flow rate of 23 ml/min. The column was operated isothermally at 150°C for 4 min after injection of sample, then increased from 150°C to 250°C at a rate of 4°C/min, and finally kept isothermally at 250°C for 10 min. The injector and detector were heated to 275°C and 305°C, respectively. Peak areas, retention times and response factors were automatically determined by the SP4270 integrator, and the percentage of each fatty acid was calculated from the ratio of the respective area of its peak to the total area of all peaks. FAME peaks were identified by comparing them with peaks of similar retention times derived from methyl ester standards (Sigma, Deisenhofen).

4.3.4.3 Isolation of phospholipids

Bacterial phospholipids were extracted using the so-called Folch method (Folch *et al*., 1957). After harvesting 10 ml of bacterial culture, cells were resuspended in 8 ml of chloroform-methanol 2:1(v/v) in a glass tube. Following a stir at room temperature for 20 min and a centrifugation step at 5,000 rpm for 10 min, 1/5 of volume (1.6 ml) of a 0.05 M $CaCl_2$ solution was added and mixed well to form an emulsion. After phase separation by subsequent centrifugation for 20 min, the upper phase was discarded, and the lower (chloroform) phase containing phospholipids was washed twice with methanol-water 1:1 (v/v). Ultimately, the lower phase was dried under nitrogen stream. FAME of phospholipids were extracted following the procedure described above (4.3.4.1).

4.3.5 Methods of artificial modification of membrane fluidity

4.3.5.1 Feeding of bacterial cultures with fatty acids

Stock solutions of fatty acid sodium salts (1mg/ml) pH 7.0 were freshly prepared and sterile-filtered before use. The stock solutions were added to the bacterial cultures once they reached an OD_{600nm} of 0.5-1.5 to a final fatty acid concentration of 0.2-0.8 mg/ml. For subsequent GUS activity measurements samples of 1.5 ml were taken when the cultures had reached an OD_{600nm} of 1.5. The GUS activity was then quantified fluorometrically as described above (4.3.1.1). For GC analysis samples of 10 ml were taken when an OD_{600nm} reached 2.5.

4.3.5.2 Addition of benzyl alcohol

Bacterial cultures were incubated at 28°C until they reached an OD_{600nm} of 0.5 or 1.0. The cultures were then divided into several flasks. Two of them were used as 18°C- and 28°C-controls, respectively. Benzyl alcohol was added to the other parallels to give a final concentration of 3, 5, and 10 mM. Cultures of an OD_{600nm} of 1.0 were diluted to an OD_{600nm} of 0.5 with fresh HSC medium before addition of benzyl alcohol. Afterwards, all cultures excepting the 28°C control culture, were further grown at 18°C. 1.5 ml samples were taken every 2-3 hours within the following 29 hours of growth to measure GUS accumulation after the temperature shift. Simultaneously, bacterial growth was monitoring by measuring of the OD_{600nm}.

5 RESULTS

5.1 Fatty acid composition of the *P. syringae* inner membrane and artificial modification of the bacterial membrane composition

5.1.1 Fatty acid composition of the *P. syringae* inner membrane

One of our working hypotheses was that the HPK CorS might sense fluidity of the bacterial inner membrane, because temperature markedly affects the physical state or the fluidity of the membrane. The major way in which bacteria, which generally lack cholesterol, maintain a constant physical state of the membrane following changes in temperature is by changing membrane fatty acid composition. Possibly, *P. syringae* cells grown at the two respective temperatures, 18°C and 28°C, have significantly different lipid compositions of their bacterial membranes. For the investigation of fatty acid profiles of *P. syringae* PG4180 cells grown at 18° and 28°C, the methyl esters of fatty acids (FAME) were isolated either directly from the harvested cells or from prepared phospholipid fractions. The FAME fractions were analyzed by gas chromatography (GC) (**Fig. 11**). The main FAME detected in samples of PG4180 were

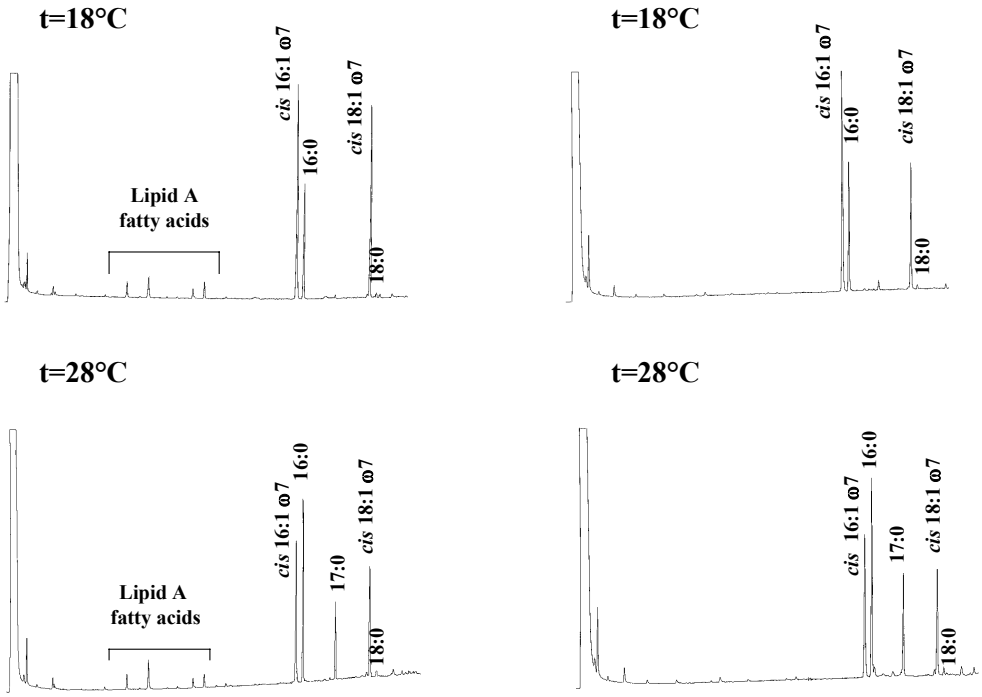

Fig. 11. Comparison of the fatty acid profiles of *P. syringae* PG4180 grown at 18 and 28°C. Fatty acids were extracted from whole cells (left) or from the phospholipid fractions (right) as methyl esters and separated by gas chromatography.

even-numbered saturated (SFA) and monounsaturated (MUFA) of the range C_{10}-C_{18} which are characteristic of many if not most bacteria (Wilkinson, 1988). According to the obtained spectra, the most abundant fatty acids were *cis*-9-hexadecenoic (palmitoleic) (16:1ω7), hexadecanoic (palmitic) (16:0), *cis*-11-octadecenoic (vaccenic) (18:1ω7), and cyclo heptadecanoic (17:0 cyclo) acids. Traces of octadecanoic (stearic) (18:0) acid were also identified. The other peaks might represent the fatty acids isolated from Lipid A. Lipid A usually contains 3-hydroxydecanoic acid (3-OH 10:0), dodecanoic acid (12:0), 3-hydroxydodecanoic (3-OH 12:0) and 2-hydroxydodecanoic acid (2-OH 12:0) (Kropinski *et al*., 1987). The content of Lipid A fatty acids was not affected by temperature. However, according to the spectra obtained from whole cell extracts and phospholipid fractions of PG4180, the content of the other fatty acids differed markedly at the two tested temperatures. As expected, the bacteria produced more of the MUFAs, 16:1ω7 and 18:1ω7, at 18°C at the expense of the SFA content. Interestingly, a significant amount of cyclo heptadecanoic (17:0 cyclo) acid was produced at 28°C, whereas the biosynthesis of this fatty acid was negligible at 18°C (**Fig. 12A**). Growth phase influenced the production of the 17:0 cyclo fatty acid. Its production increased in the transition to the stationary phase (**Fig. 12B**). Obviously, changes in the saturation degree of fatty acids and in the production of cyclo fatty acids are major methods of thermoadaptation in membranes of *P. syringae*.

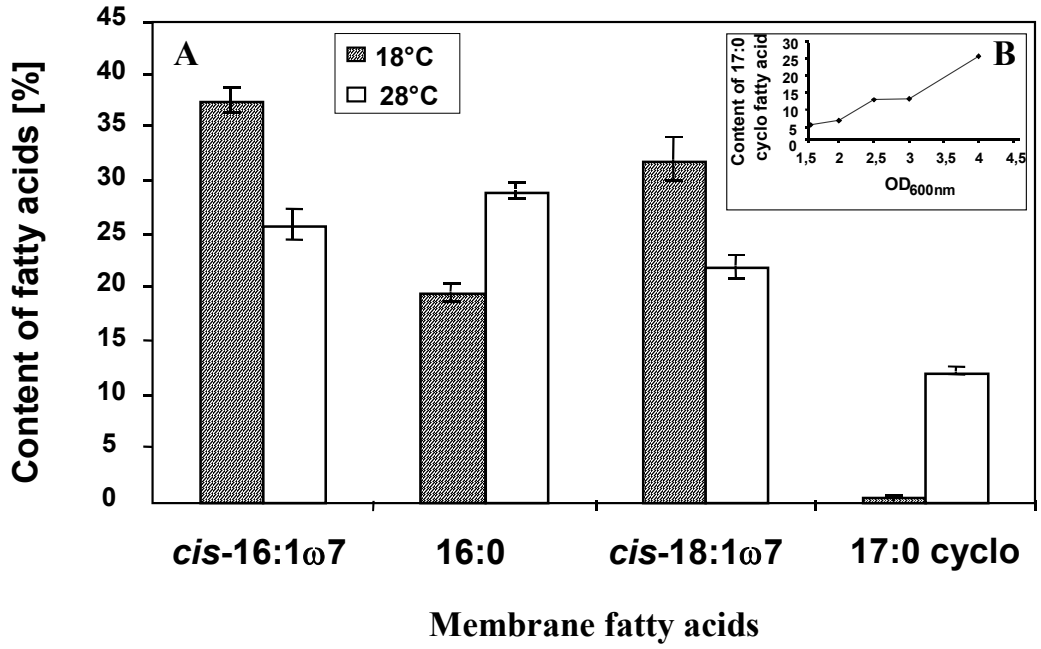

Fig. 12. Changes in the content of the most abundant membrane fatty acids of PG4180 in response to temperature change (A) and production of cyclo heptadecanoic fatty acid (C17:0 cyclo) in dependence of the growth phase (B).

5.1.2 Artificial modification of the composition of the bacterial membrane by addition of fatty acids

To detect a possible physiological impact of fatty acid composition on the transcriptional activation of COR biosynthetic promoters, attempts were made to artificially modify the membrane of PG4180 by addition of 0.1-0.8 mg/ml of *cis*-9-hexadecenoic (palmitoleic) (16:1ω7), *cis*-9-octadecenoic (oleic) (18:1ω9), hexadecanoic (palmitic) (16:0), and octadecanoic (stearic) (18:0) acids at both test temperatures. Plasmid pRGMU1 introduced into PG4180 contains a promoterless ß-glucuronidase reporter gene (*uidA*) fused to a 2.9-kb *Pst*I fragment of the *cmaABT* promoter region from the COR gene cluster of PG4180. The transconjugant allows quantification of promoter activity *in trans* by measuring the ß-glucuronidase (GUS) activity in a fluorescence assay. Transcriptional activation of the *cmaABT* promoter was previously shown to be temperature dependent (Ullrich & Bender, 1994).

According to subsequent GC analysis of FAME isolated from the cultures of PG4180 (pRGMU1) fed with 18:1ω9 at 28°C, this fatty acid was only partially incorporated into the membrane (**Fig. 13A**). The bacteria might have used a considerable portion of 18:1ω9 as a carbon source since the 18:1ω9-fed cultures grew faster than a control culture without added

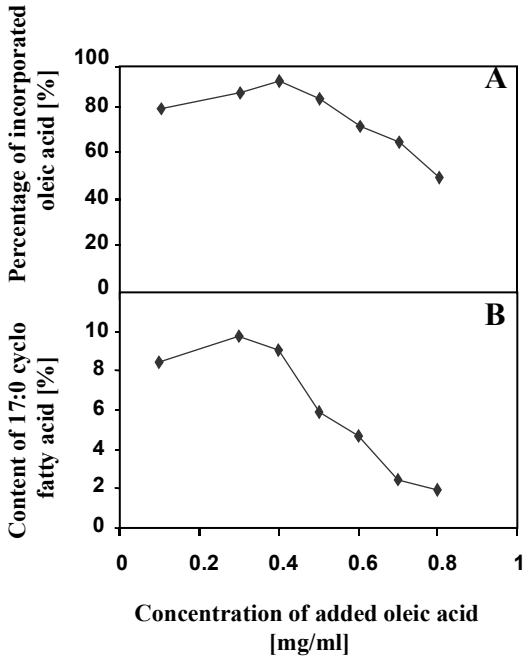

Fig. 13. Incorporation of externally added oleic acid (*cis*-18:1ω9) into the membrane of PG4180 (A) and the change of the content of cyclo heptadecanoic acid (17:0 cyclo) following the feeding of PG4180 cells with oleic acid at 28°C (B).

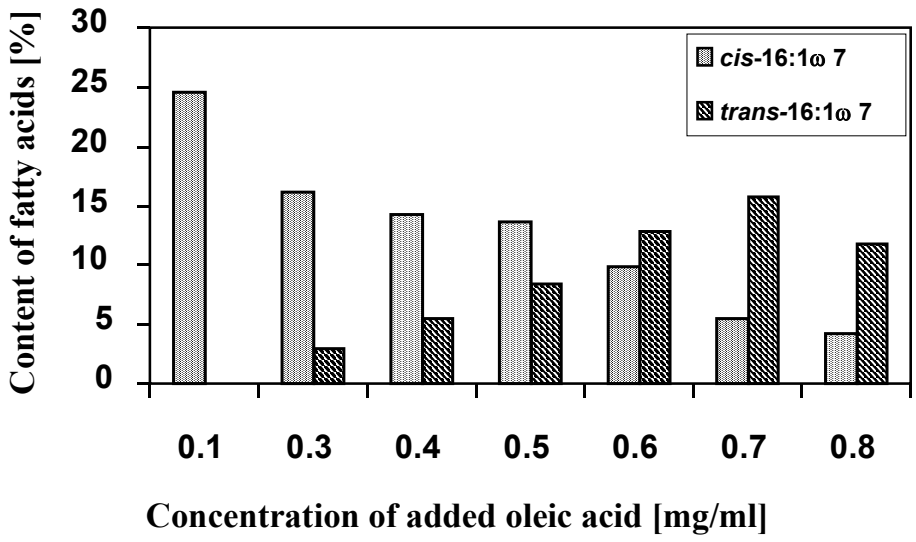

Fig. 14. Conversion of palmitoleic acid (*cis*-16:1ω7) to palmitelaidic acid (*trans*-16:1ω7) induced by addition of oleic acid (*cis*-18:1ω9) to PG4180 cultures at 28°C and subsequent measurement of the FAME for whole cell preparations.

fatty acids. Interestingly, the addition of 18:1ω9 resulted in a conversion of 16:1ω7 *cis* to its *trans* isomer (**Fig. 14**) and in a dramatic decrease of the content of 17:0 cyclo fatty acid (**Fig. 13B**). Similar effects were observed as a result of addition of *cis*-16:1ω7 to the cultures grown at 28°C. Feeding experiments with 16:0 and 18:0 SFA at 18°C gave rise to incorporation of these SFA into the membrane. However, the general fatty acid profile for 18°C did not change. There was no significant effect on GUS activity in the feeding experiments at either temperature, even though various conditions were tested. These conditions were the addition of fatty acids at different culture optical densities and variation of the added concentrations.

5.1.3 Modulation of membrane fluidity by addition of benzyl alcohol

Benzyl alcohol (BA) was efficiently used *in vivo* as a membrane fluidizer in *Bacillus subtilis* (Konopásek *et al*., 2000) and in *Synechocystis* (Horváth *et al*., 1998). It was suggested that BA could induce membrane perturbation in a manner analogous to that of heat shock (Vígh *et al*., 1998). The effect of BA addition to PG4180 (pRGMU1) cultures on the *cmaABT* promoter activity was tested following a temperature shift from 28° C to 18°C. Addition of 3 mM BA to the cultures of PG4180 (pRGMU1) affected neither growth nor GUS activity of these cultures as compared to control cultures. However, addition of 5 and 10 mM BA slowed cell growth (**Fig**. **15A**) and had a dramatic effect on GUS accumulation. Following the

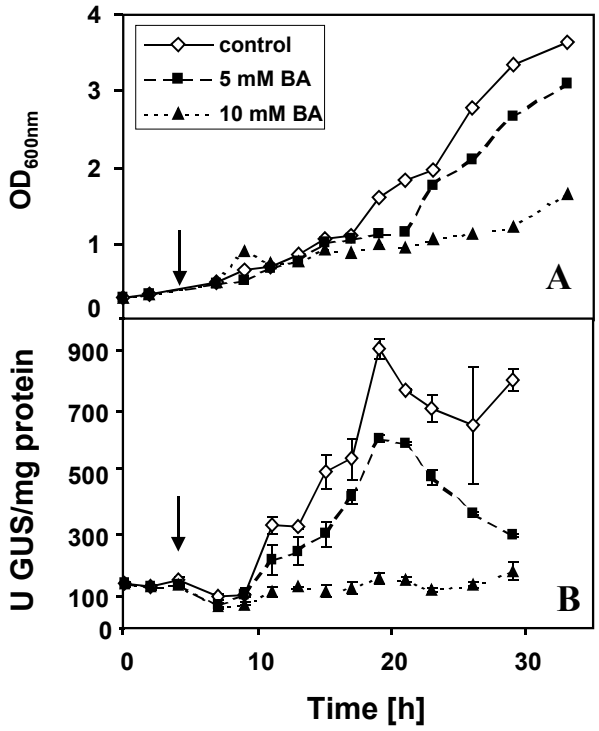

Fig. 15. Bacterial growth (A) and *cmaABT::uidA* expression (B) of PG4180 (pRGMU1) after addition of different concentrations of benzyl alcohol (BA) and upon a temperature shift from 28°C to 18°C. The arrow indicates the time-point of the temperature shift.

temperature down-shift, GUS activity decreased upon addition of 5 mM BA, and when 10 mM BA was added, GUS accumulation at 18°C was completely abolished (**Fig. 15B**). This result indicated that an artificial increase of membrane fluidity at 18°C led to growth inhibition and also to a decrease of *cmaABT* promoter activity.

5.2 Effect of growth rate on COR biosynthesis

Previously, the effects of various environmental factors such as temperature, osmolarity, different carbon and nitrogen sources on transcriptional activity within the COR gene cluster were tested and temperature was shown to have the most significant effect on transcription (Palmer *et al*., 1997). However, the effect of growth rate or oxygen availability has not been tested yet. Temperature might not be the only environmental factor sensed by the HPK CorS, which is thought to be responsible for the signal perception in this respect. Taking into account that oxygen is one of the most important environmental factors, the effects of oxygen availability on the transcriptional activity of the *cmaABT* promoter and on COR biosynthesis in PG4180 (pRGMU1) were tested by growing the bacterial cultures in flasks placed on magnetic stirrers with different rpm values at 18°C and 28°C. When bacterial cultures reached

OD_{600nm} values of 1.3-1.5, samples of 1.5 ml were centrifuged. The cell pellets were used for the GUS fluorescence assay. The supernatants were used to extract the coronafacoyl compounds, COR and CFA. The amounts of the extracted compounds were analyzed by HPLC. As expected, at 28°C there was no detectable COR and CFA production by PG4180 (pRGMU1). **Fig. 16A** shows the results of the COR/CFA extraction for cultures incubated at 18°C on a magnetic stirrer at 250, 500, 750, and 1,000 rpm values compared to the control cultures grown in the shaker at 280 rpm. The results suggest that cultures grown at 250 rpm on a magnetic stirrer were not supplied with sufficient amounts of oxygen since significantly less COR and CFA was produced (3.25 and 0.8 mg/L) as compared to the shaker cultures (6.05 and 2.16 mg/L). However, at 500 rpm bacteria produced more COR (8.8 mg /L) and half as much CFA (1.2 mg/L). The amount of COR produced decreased when the cells

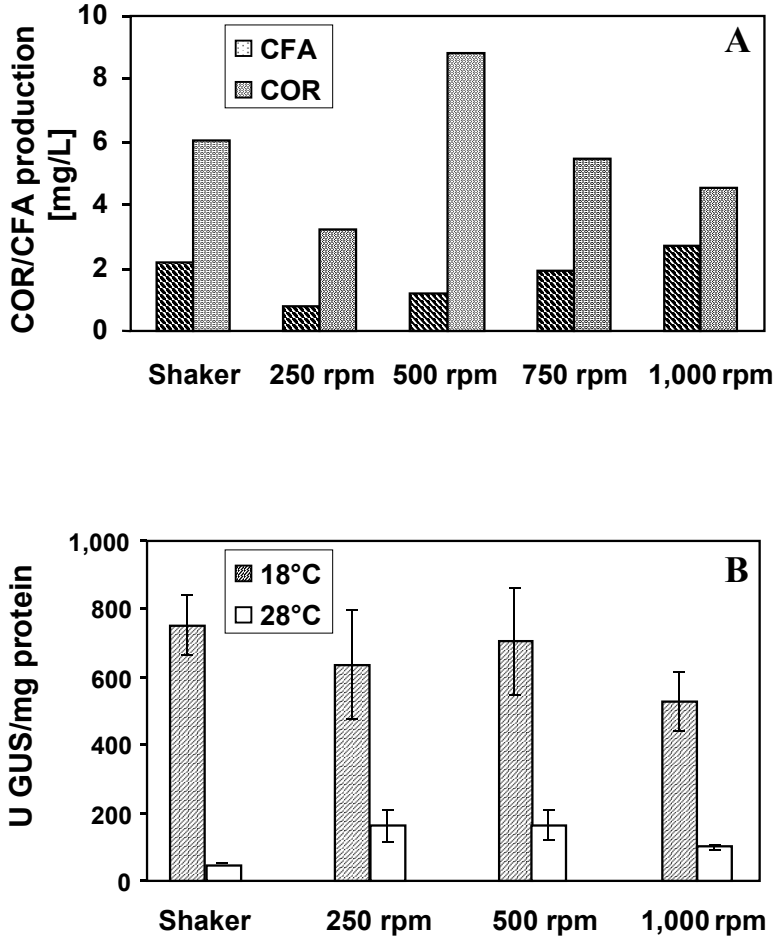

Fig.16. COR/CFA production at 18°C (A) and thermoresponsive *cmaABT::uidA* expression (B) in PG4180 (pRGMU1 grown on a shaker or on a magnetic stirrer with different rpm-values. Quantities of COR and CFA represent the results of three extractions and GUS-values represent the averages from 12 cultures with two replicates each.

were grown at 750 and 1,000 rpm (5.44 and 4.51 mg/L) respectively, and the amount of CFA produced increased (1.92 and 2.69 mg/L). Thus, COR production is optimal when bacteria were grown at 500 rpm on a magnetic stirrer. This result agrees with quantitative estimation of the *cmaABT* promoter activity. Average GUS expression from 12 cultures with two replicates grown at 1,000 rpm was 528 U GUS/mg protein, whereas the GUS expression of the control cultures grown in the shaker was 703 U GUS/mg protein (**Fig. 16B**). Approximately similar levels of GUS activity were measured for cultures grown in the shaker and for those incubated at 500 rpm. Cultures grown at 250 rpm on a magnetic stirrer showed a decrease in the average GUS activity (**Fig. 16B**).

5.3 Temperature shift experiments

Quantitation of *cmaABT* promoter activity demonstrated that growth of PG4180 (pRGMU1) at 18°C was optimal for transcriptional activation. However, it remained unclear how soon transcriptional activation is induced after the temperature is shifted from 28°C to 18°C. Shift experiments were carried out for bacterial cultures grown in minimal or complex medium. Bacterial cultures were subjected to temperature shifts after growth to different optical densities. PG4180 (pRGMU1) cultures were grown in HSC medium at 28°C to an OD_{600nm} of 0.7, 1.4, and 1.8 and then adjusted to an optical density of 0.5. Subsequently, cultures were shifted to 18°C and kept growing for additional 26 hours. Samples for measurement of GUS activity were taken after 0.5, 1, and 2 hours, and at 2-hour intervals thereafter. Simultaneously, bacterial growth was monitored by measurement of the OD_{600nm}. Upon temperature shift, there was a short lag phase, and then GUS expression increased steadily, reaching 18°C-values (≈500 U GUS/mg protein) within 10-12 hours (**Fig. 17A, B, C**). The lag phase for GUS accumulation depended on the age of the cultures before the temperature shift. The culture with an OD_{600nm} of 1.8 had an elongated lag phase of about 10 hours (**Fig. 17C**), whereas the OD_{600nm} 0.7-culture had a lag phase of about 5 hours (**Fig. 17A**). However, growth of cultures at all three OD_{600nm} values as well as GUS accumulation after the lag phase were not affected by the age of the culture.

In order to investigate whether the *cmaABT* promoter was cold-shock inducible, cultures were incubated on ice before the temperature shift. When a culture was kept on ice for 30 min and then shifted to 18°C, there was no significant difference in GUS expression compared with a non-treated control culture (**Fig. 18**). These results indicate that transcriptional activation of the *cmaABT* promoter was not a rapid process and was not cold shock-dependent.

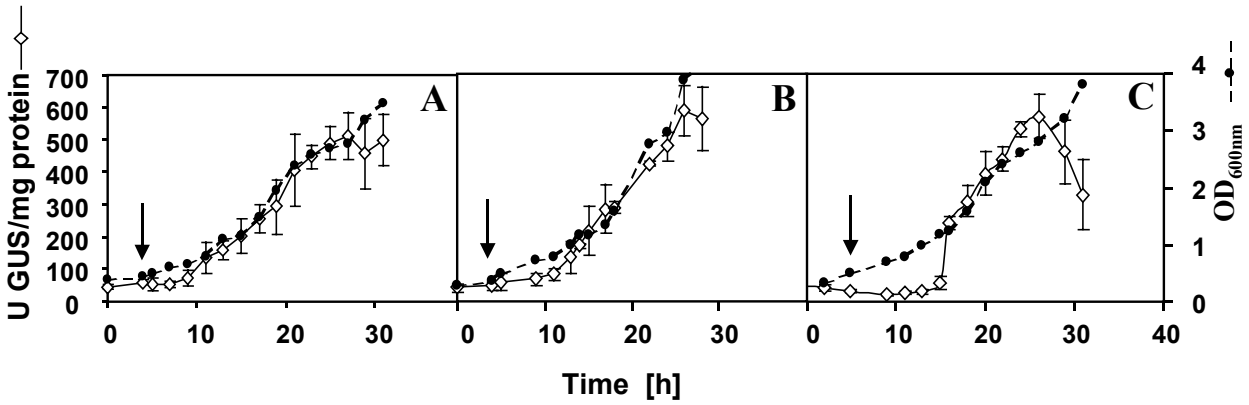

Fig. 17. Bacterial growth and *cmaABT::uidA* expression of PG4180 (pRGMU1) after a temperature shift from 28 to 18°C. (A) Cells which had reached an OD_{600nm} of 0.7 prior to the temperature shift. (B) Cells which had reached an OD_{600nm} of 1.4 prior to the temperature shift. (C) Cells which had reached an OD_{600nm} of 1.8 prior to the temperature shift. The arrow indicates the time-point of the temperature shift. Quantities are averages of two experiments with three replicates each.

In order to test whether *cmaABT* transcription is nutrient-dependent, the culture medium was exchanged at the time point of the temperature shift. Previously, it had been demonstrated that temperature-dependent COR production and *cmaABT* transcription occurred in minimal medium (HSC medium), whereas temperature dependence of both processes was negligible in complex media such as King's B. PG4180 (pRGMU1) cells were initially grown in HSC medium at 28°C, harvested by centrifugation, and resuspended in King's B medium. The cultures were subsequently incubated at 18°C. Control cultures were treated equally except that the cells were resuspended in HSC medium at the time of the temperature shift. As expected, subsequent growth of cells in HSC medium gave rise to increased GUS activity. In contrast, in King's B medium GUS expression remained at the basal level (**Fig. 19**).

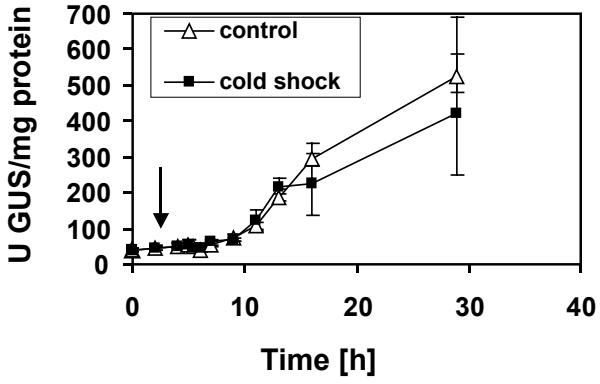

Fig. 18. *cmaABT::uidA* expression of PG4180 (pRGMU1) after a temperature shift from 28 to 18°C. Cells reached an OD_{600nm} of 0.7 and were incubated on ice prior to the temperature shift. Quantities are averages of two experiments with three replicates each.

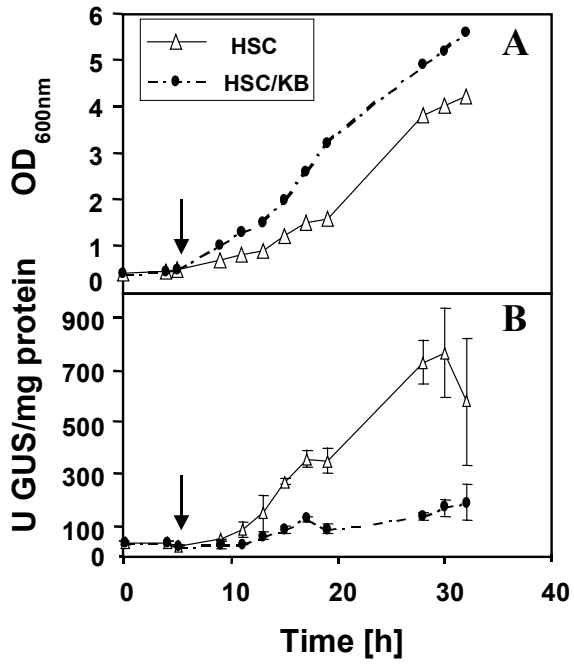

Fig. 19. Effect of medium change on bacterial growth (A) and *cmaABT::uidA* promoter activity in PG4180 (pRGMU1) (B) after a temperature shift from 28 to 18°C. The arrow indicates the time-point of the temperature shift. Quantities represent the averages of two experiments with three replicates each.

These results suggested that *cmaABT* transcription was only induced upon temperature-down shift when the cells were incubated in minimal medium. Furthermore, our results indicated that the regulatory machinery required for *cmaABT* expression was not present in cells grown in complex medium and had to be initialized in minimal medium at low temperature.

5.4 Protein profile of *P. syringae* at two test temperatures

5.4.1 Two-dimensional protein gel electrophoresis analysis of *P. syringae* cell fractions enriched in membrane proteins

The aim of the following set of experiments was to identify the CorS protein in the membrane fraction of *P. syringae*, taking into account that CorS is a membrane-associated protein. Membrane fractions *P. syringae* were isolated following the method described by Boyd *et al*. (1987). To check the purity of the isolated membrane fractions, Western blotting with antibodies against the cytoplasmic protein CmaB was performed with periplasmic, cytoplasmic, and membrane fractions of PG4180 cells grown to stationary phase in HSC medium at 18°C and 28°C, respectively. CmaB is a COR biosynthetic protein which accumulates in the late stationary phase of *P. syringae* cultures grown at 18°C and is more

stable at 18°C than at 28°C (Budde *et al*., 1998). Western blot analysis demonstrated that CmaB was an abundant protein in the cytoplasmic fraction at 18°C. Periplasmic and membrane fractions of 18°C-grown cultures were contaminated with only minor amounts of CmaB. This contamination may be explained by the presence in these fractions of some unbroken cells which lysed during heating of the samples prior to loading them on the gel. Our results allowed us to consider the membrane fractions isolated by this way to be cell fractions enriched in membrane proteins. These fractions were obtained from PG4180 wild-type cells and from the PG4180.D4 mutant defective in COR production, grown to stationary phase in HSC medium at 18°C and 28°C. The fractions (400 µg protein) were analyzed by 2-DE. Isoelectric focusing was the electrophoresis on the first dimension. It was performed with carrier ampholyte-generated pH gradients in polyacrylamide tube gels. Then proteins were then separated by SDS-10%-PAGE according to their molecular masses. In general, protein profiles of PG4180 grown at 18°C and 28°C showed identical patterns, except for a protein spot of ca. 35 kDa which was observed at 18°C and was clearly less pronounced at

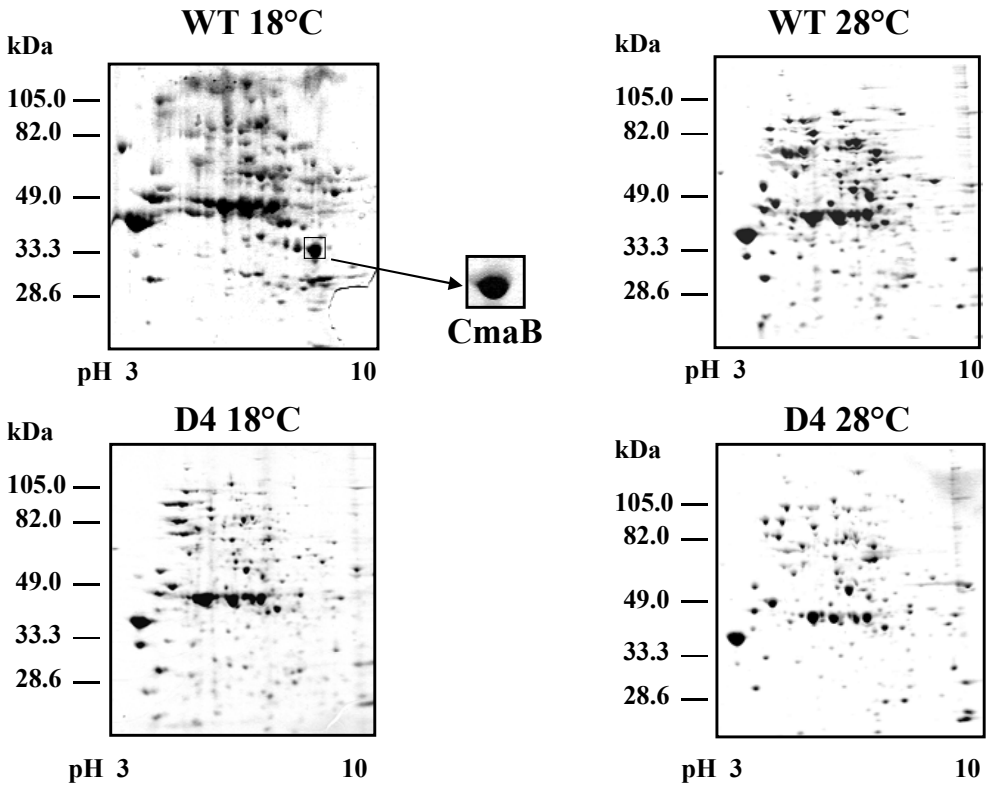

Fig. 20. Two-dimensional gel electrophoresis of proteins (400 µg) isolated from cells of PG4180 and its mutant PG4180.D4, grown in HSC medium at 18 and 28°C. Cells were harvested in the stationary phase (OD_{600nm} 4.0). A protein spot which was predominantly found in samples of 18°C-grown cells is shown in the insert box.

28°C (**Fig. 20**). This indicated that the expression of the 35-kDa protein might be temperature-dependent. The protein spot was hardly visible in the 2-D protein profile of PG4180.D4 regardless of temperature, indicating that expression of the 35-kDa protein depended on the CorSPR two-component regulatory system. Subsequently, the protein spot was excised from the gel and subjected to N-terminal sequencing (Dr. Roland Schmid, University of Osnabrück). The N-terminal sequencing demonstrated that the protein expressed in a temperature-dependent manner was CmaB, thus confirming earlier finding (Budde *at al*., 1998 and this work).

Furthermore, the membrane fraction preparation technique was improved by using the method of Osborn *et al*. (1972) as modified by Gramajo *et al*. (1991). To improve solubilization of membrane proteins, additional chaotropes such as thiourea and sulfobetaine surfactant, N-decyl-N,N-dimethyl-3-ammonio-1-propanesulfonate were used as suggested by Molloy *et al.* (1998). Additionally, for the isoelectric focusing immobilized pH gradients strips were used instead of carrier ampholytes. However, even these modifications did not allow the identification of the HPK CorS by 2-DE.

5.4.2 Temperature- and medium-dependent expression of polyketide synthases in *P. syringae*

Cell fractions enriched in membrane proteins of PG4180 cells grown in HSC medium at 18°C and 28°C, and prepared according to the method of Boyd *et al*. (1987), were tested by SDS-PAGE. An interesting feature that suggested a possible temperature-dependence of protein expression was that two protein bands of ca. 200 kDa were more pronounced at 18°C than at 28°C (**Fig. 21**). It was shown previously that these large protein bands might represent polyketide synthases involved in COR biosynhesis (Rangaswamy *et al*., 1998b). The finding was verified by testing protein samples from the CFA^- CMA^+ mutant PG4180.AG28, which carries Tn*5* insertion in the CFA biosynthetic region (Palmer *et al*., 1997) and from the CFA^- CMA^- mutant PG4180.D4 (*corR*$^-$ *corS*$^-$). Cell fractions enriched in membrane proteins of PG4180 cells grown in KB medium at 18°C and 28°C were tested in parallel (**Fig. 21**). The two protein bands of ca. 200 kDa could be detected in samples of PG4180 grown in HSC medium but were absent in samples of PG4180 grown in KB medium as well as in samples of PG4180.D4 and PG4180.AG28 at both temperatures. This showed that the two bands might indeed be related to polyketide synthases and that these proteins are expressed in PG4180 in a temperature-, CorSR-, and medium-dependent manner.

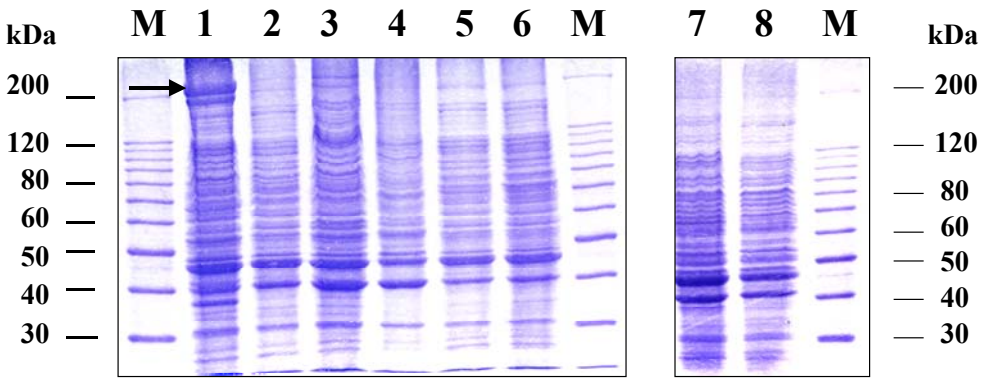

Fig. 21. Effects of temperature and medium composition on the expression of proteins related to polyketide synthases in *P. syringae*. Proteins of cell fractions enriched in membrane proteins were separated by SDS-10%-PAGE. Lanes: M, molecular weight standard; 1, PG4180, 18°C and HSC medium growth; 2, PG4180, 28°C and HSC medium growth; 3, PG4180, 18°C and KB medium growth; 4, PG4180, 28°C and KB medium growth; 5, PG4180.D4, 18°C and HSC medium growth; 6, PG4180.D4, 28°C and HSC medium growth; 7, PG4180.AG28, 18°C and HSC medium growth; 8, PG4180.AG28, 28°C and HSC medium growth. The arrow indicates two proteins which might be related to polyketide synthases.

5.5. Theoretical characterization of the structure of the histidine protein kinase CorS

5.5.1 Hydropathy profile and membrane topology prediction

The deduced amino acid sequence of CorS showed relatedness to histidine protein kinases of two-component regulatory systems. The identity was predominantly in the C-termini of HPKs (33 % to 47 %), with the highest identity to VsrB of *Rastonia solanacerum*, BvgS of *Bordetella pertusis*, GacS of *P. syringae*, DivJ of *Caulobacter crescentus*, and RpfA of *Erwinia carotovora* (**Tab. 10**). Much more sequence diversity was found for the N-termini of the respective amino acid sequences.

The sequence of CorS was also subjected to hydropathy profile analysis based on the Kyte-Doolittle method (Kyte & Doolittle, 1982) using the program PROTEAN (DNA-STAR Software). According to a hydrophilicity plot, the N-terminal region of CorS (approximately 200 amino acid residues) contained multiple hydrophobic zones (**Fig. 22A**). This indicated a potential membrane localization for this portion of the protein. The programs **TopPred 2** and **Vector NTI** were used to analyze and predict the membrane topology of CorS. According to the **TopPred 2** prediction, CorS might posses 5, 6 or even 7 membrane-spanning domains (TMDs) (**Tab. 11**). Interestingly, the 7th TMD was predicted to occur in the region of the

Tab. 10. Amino-acid sequence identity and similarity of CorS to other HPKs in their C-termini.

Organism	Protein	Identity score (%)	Similarity score %
Ralstonia solanacearum	VsrB	47	63
Caulobacter crescentus	DivJ	40	56
Erwinia carotovora	RpfA	37	55
Bordettella pertusis	BvgS	36	50
Pseudomonas syringae	GacS	33	50

conserved H-box, where the actual site of autophosphorylation, residue His^{254}, is located (**Fig. 22B**). This prediction is unlikely, because in order to be phosphorylated, the His residue must be located in the cytoplasm. Besides this, the 2^{nd}, 6^{th}, and 7^{th} TMDs were predicted to be putative. The 6^{th} TMD showed the lowest hydropathy index among all TMDs. The results were verified by the program **Vector NTI**. According to the topology prediction made by the latter program, CorS might possess six TMDs, and the 2^{nd} and 6^{th} TMDs showed lower hydrophobicity scores than the others (**Tab. 11**). Taking into account those prediction results, it is likely that CorS is a hydrophobic protein with six TMDs in its N-terminus.

Tab. 11. Membrane topology for CorS predicted by two programs.

Transmembrane domain	Amino acid residues of CorS	Toppred 2 hydropathy index	Vector NTI hydrophobicity score
1	21(23)-43	1.405	1131
2	61(63)-81(85)	0.729	957
3	104(105)-124	1.230	1408
4	127(129)-147	1.898	1559
5	155(158)-175	1.123	1312
6	181-201	0.682	1156
7	257-277	0.786	

5.5.2 Domain organization of CorS

The **Pfam** database of protein domain families is designed to identify the domain architecture of a given protein. This allows an assumption to be made about the possible mode of action of this protein.

Therefore, the amino acid sequence of CorS was analyzed using the **Pfam** domain search program. Analysis resulted in a graphic representation of the domain organization of CorS

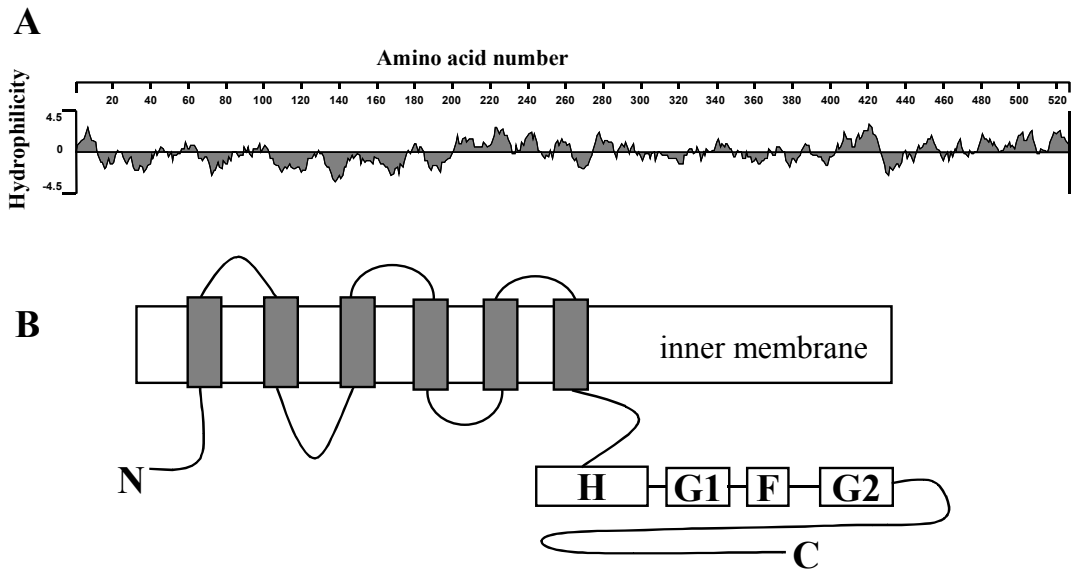

Fig. 22. Kyte-Doolittle hydrophilicity plot (A) and possible membrane topology of the HPK CorS (B). The H, G1, G2, and F boxes indicate the conserved sequence motifs identified in various HPKs.

where a conserved histidine kinase domain and a transmembrane region were identified (**Fig. 22B**). However, none of the other known domains or motifs of HPKs, such as PAS, DUF5, response regulator domains, Walker motif, and periplasmic substrate-binding motifs were found in CorS.

5.6 Biochemical characterization of CorS

5.6.1 Heterologous expression of CorS in *E. coli* and its solubilization

CorS was overproduced in *E. coli* as an N-terminal $CorS_{Strep\text{-tag}}$ fusion protein. The expression system used is based on vectors which take advantage of the tightly controlled *tetA*-promoter (Skerra, 1994). The purification procedure is based on a specific binding of the *Strep*-tag II peptide to immobilized StrepTactin (Voss & Skerra, 1997). Specific competition with desthiobiotin enables elution of the recombinant protein from the column.

A 1.4-kb *Bam*HI fragment comprising the entire *corS* gene was amplified by PCR using proofreading polymerase *PfuTurbo* (Stratagene) and the primers fcsB and rcsB (3.7). The PCR fragment was cloned into the *Bam*HI treated *Strep*-tag II expression vectors pASK-IBA3 and pASK-IBA7 (IBA, Göttingen). Cloning in pASK-IBA3 generated a translational fusion protein with CorS carrying a C-terminal *Strep*-tag II fusion. Cloning in pASK-IBA7 generated a translational fusion protein with CorS carring an N-terminal *Strep*-tag II fusion (**Fig. 23**). The ligation mixtures were transformed into *E. coli* DH5α. Insertion of the PCR

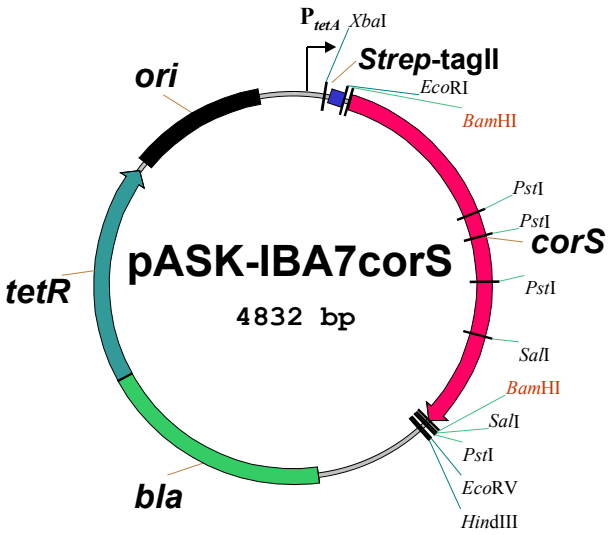

Fig. 23. Physical map of plasmid pASK-IBA7corS for the expression of the recombinant CorS protein with an N-terminal *Strep*-tag II fusion. The expression cassette is under control of the *tetA* promoter (P_{tetA}). The PCR fragment containing the *corS* gene and the *Strep*-tag II are indicated. The repressor *tetR* is transcriptionally fused to the constitutively expressed *bla* gene.

fragment into vectors was verified by restriction analysis of DNAs isolated from single transformants. Additionally, the DNA region of the *corS*/*Strep*-tag II fusion was sequenced in both cases. Sequence analysis indicated that *corS* was fused in-frame to *Strep*-tag II and did not contain any PCR-based mutations.

In order to establish a tight repression of the *tetA* promoter under non-induced conditions, the repressor gene *tetR* is located on pASK-IBA vectors (**Fig. 23**). Upon addition of the inductor anhydrotetracycline which binds to the TetR repressor, synthesis of recombinant proteins is induced. In order to establish conditions under which the recombinant CorS protein is optimally expressed, different concentrations of the inductor were tested in the range of 200-3,000 µg per liter. The inductor was added at growth stages corresponding to OD_{600nm} of either 0.5 or 1.0. Different temperatures for *E. coli* growth such as 18°C, 28°C, and 37°C were tested as well. Synthesis of the recombinant protein was induced in *E. coli* DH5α (pASK-IBA7:*corS*) grown at 28°C by addition of 3 mg of anhydrotetracycline per liter at an $OD_{600\ nm}$ of 0.5. Expression levels for $CorS_{Strep\text{-tag}}$ were low and could be detected by Western blot analysis with streptavidin alkaline phosphatase conjugates (Amersham) (**Fig. 24**). According to this analysis, $CorS_{Strep\text{-tag}}$ which has a size of about 48 kDa, was localized in the insoluble protein fraction (pellet). Membrane fraction preparation from *E. coli* cells indicated that expression of $CorS_{Strep\text{-tag}}$ led to membrane incorporation of this protein. To purify $CorS_{Strep\text{-tag}}$ with the StrepTactin affinity chromatography column, the proteins were

solubilized with TritonX-100. Subsequently, solubilized CorS$_{Strep\text{-tag}}$ was purified with the StrepTactin column following the method of Rübenhagen *et al.* (2000). According to the immunological detection, CorS$_{Strep\text{-tag}}$ was eluted from the column predominantly in the 3rd fraction (**Fig. 25**). However, additional protein bands in the elution fractions indicated that some other proteins were co-eluted with CorS$_{Strep\text{-tag}}$, suggesting that the purification procedure will have to be optimized in future experiments.

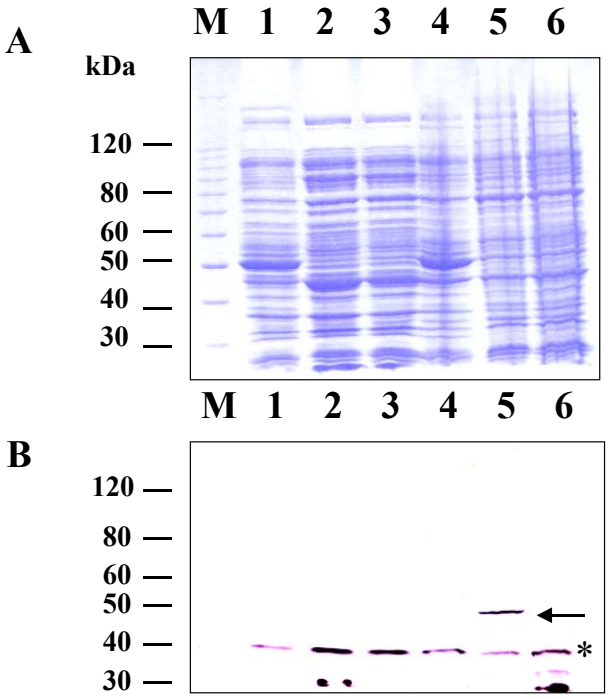

Fig. 24. SDS-PAGE (A) and Western blot analysis (B) of *E. coli* (pASK-IBA7corS) cell fractions. Cells were grown at 28°C before induction and at 18 or 28°C after induction with 3 mg/L of anhydrotetracycline. Induced and non-induced cells were spun down after 6 hours of growth. The supernatants and the pellets were used for Western blot analysis. Proteins were separated by SDS-10%-PAGE, transferred to a nitrocellulose membrane, and stained with streptavidin alkaline phosphatase conjugates. The arrow indicates the detected CorS$_{Strep\text{-tag}}$ recombinant protein. *Non-specific bands represent the endogenous biotin-rich proteins of *E. coli*. Lanes: M, molecular weight standard; 1, supernatant of non-induced sample, 28°C growth; 2, supernatant of induced sample, 28°C growth; 3, supernatant of induced sample, 18°C growth; 4, pellet of non-induced sample, 28°C growth; 5, pellet of induced sample, 28°C growth; 6, pellet of induced sample, 18°C growth.

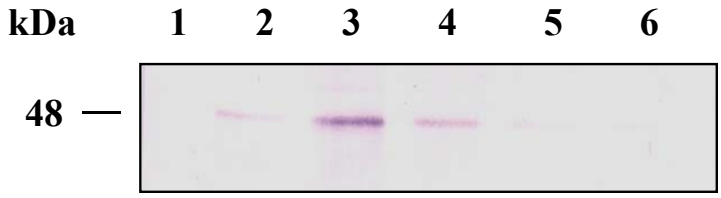

Fig. 25. Detection of the solubilized CorS$_{Strep\text{-tag}}$ recombinant protein by Western blot analysis in elution fractions from a StrepTactin column. Lanes represent the elution fractions 1-6.

5.6.2 Immunological detection of CorS with antibodies raised against synthetic peptides derived from CorS

Immunological detection is a sensitive method to identify proteins even if they are not abundant in cell extracts. Within the amino acid sequence of CorS there is a linker region (aa 200-250) between the 6th predicted TMD and the conserved histidine kinase domain (H-box). Two peptides within this linker region were chosen for production of antibodies. Selecting peptides from within the hydrophobic region of CorS would make immunodetection of CorS difficult and selecting peptides from within the conserved histidine kinase domain or further downstream C-terminal regions would make the antibodies non-specific due to the high degree of sequence conservation among HPKs. Additionally, the chosen region showed the best surface probability and the best antigenic index when analyzed by the program PROTEAN (DNA-STAR, USA).

Two peptides (NH_2–CRATNSQRARQLAI–H and NH_2–CLQQLDRRARKTTED–H) were synthesized and used for polyclonal antibody production in rabbits (EUROGENTEC, Hestal, Belgium). The antisera were tested by Western blot analysis with cell extracts of 18°C-grown cells of PG4180, PG4180.N9 (pRK:*malE:corR*), and with *E. coli* membrane fractions containing overproduced CorS$_{Strep\text{-tag}}$. PG4180.N9 (pRK:*malE:corR*) allows overproduction of a translational fusion of CorR to a maltose-binding protein (Peñaloza-Vázquez *et al*., 1996). Overproduction of the response regulator CorR might lead to an enhanced biosynthesis of CorS since the CorRSP system undergoes autoinduction (Ullrich *et al*., 1995). According to the respective immunoblot with CorS peptide antibodies, CorS was not detected in *P. syringae* cells extracts, in spite of overproduction of CorR. Although cells from both early and late exponential growth phases at 18°C were subjected to Western blot analysis, a band of ca. 48 kDa related to CorS was not detected. However, when produced in *E. coli*, CorS$_{Strep\text{-tag}}$ was detected by these antibodies. A 48-kDa band possibly representing CorS was visible in

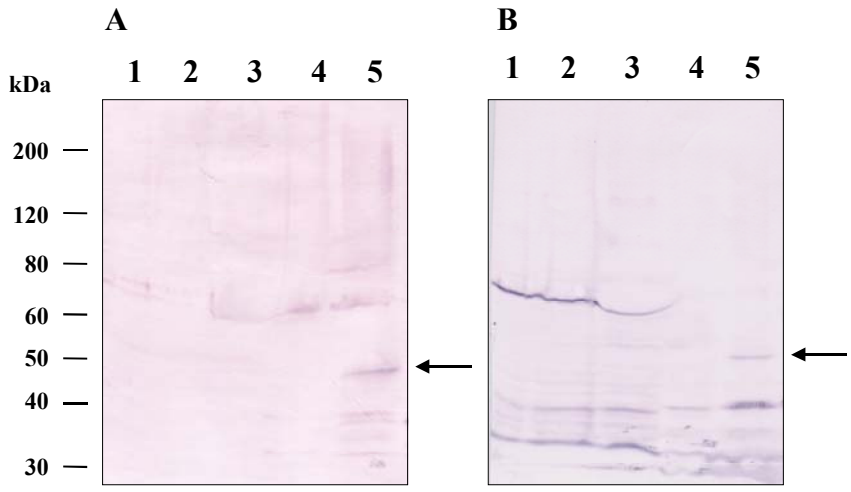

Fig. 26. Western blot analysis of CorS$_{Strep\text{-tag}}$ in cell extracts and membrane fraction of *P. syringae* and *E. coli*. The antibodies used were directed against CorS synthetic peptides (A). Streptavidin alkaline phosphatase conjugates were used to detect the *Strep*-tagII moiety (B). *P. syringae* cells were grown at 18°C. *E. coli* (pASK-IBA7corS) cells were grown at 28°C. The arrow indicates the detected CorS$_{Strep\text{-tag}}$ recombinant protein. Lanes: 1, PG4180 cell extract, OD$_{600nm}$= 0.9; 2, PG4180 cell extract, OD$_{600nm}$= 2.6; 3, PG4180.N9 (pRK:*malE*:*corR*) cell extract, CorR expression induced with IPTG; 4, *E. coli* (pASK-IBA7corS) cell extract, non-induced; 5, *E. coli* (pASK-IBA7corS) membrane fraction, CorS$_{Strep\text{-tag}}$ expression induced with anhydrotetracycline.

the membrane fraction of *E. coli* (pASK-IBA7:*corS*) when cells were induced and was absent from *E. coli* cell extracts of the non-induced culture (**Fig. 26A**). As a control, Western blot analysis with streptavidin alkaline phosphatase conjugates was carried out with the same samples (**Fig. 26B**). Because the same band of 48 kDa gave a signal in the control immunoblot, we concluded that both the streptavin alkaline phosphatase conjugate and the CorS peptide-specific antibodies detected CorS$_{Strep\text{-tag}}$.

5.7 Complementation analysis of PG4180 mutants defective in COR production

The CorSRP-system is crucial for COR biosynthesis as well as for the transcriptional activation of COR biosynthetic promoters. Previously, two Tn*5* mutants with a COR$^-$ CMA$^-$ CFA$^-$ phenotype, PG4180.F7 and PG4180.D4, were mapped to *corP* and *corR*, respectively (**Fig. 27**) (Ullrich *et al*., 1995). When the CorR regulatory protein was overproduced in mutant PG4180.D4, COR production was not restored to this mutant indicating that the Tn*5*-insertion in *corR* had a polar effect on *corS*. A marker exchange mutant of *corS*, PG4180.P1,

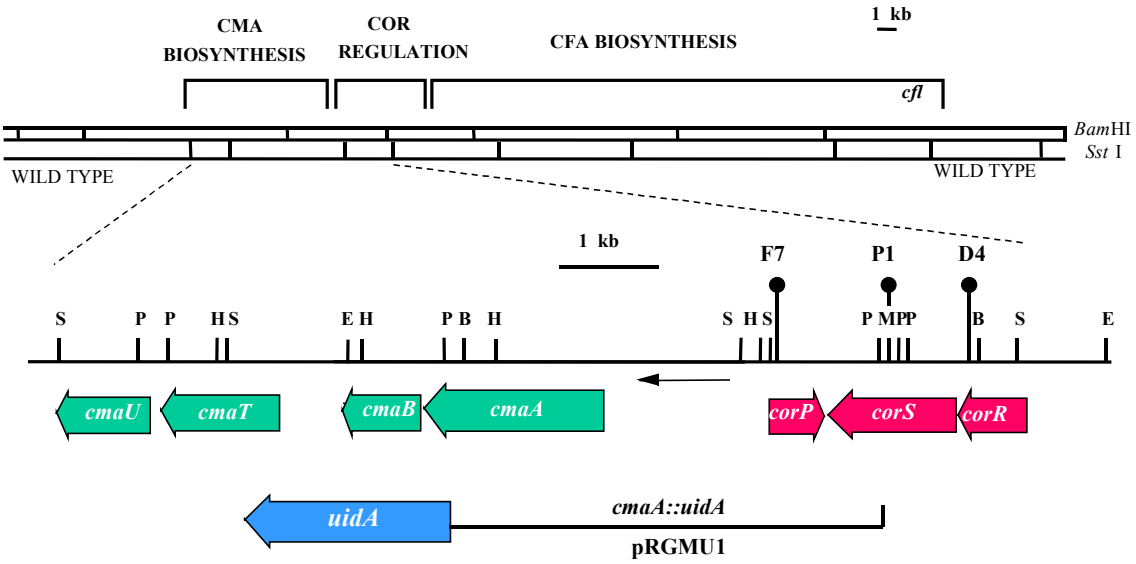

Fig. 27. Partial restriction map and genetic organisation of the 32.8-kb COR biosynthetic gene cluster, location of transposon and gentamycin cassette insertions in PG4180.D4, PG4180.F7, and PG4180.P1, respectively, and transcriptional fusion of a promoterless ß-glucuronidase (*uidA*) reporter gene to the *cmaABT* promoter in PG4180 (pRGMU1). Restriction enzymes: B, *Bam*HI; E, *Eco*RI; H, *Hin*dIII; M, *Msc*I; P, *Pst*I; S, *Sac*I.

was previously obtained by insertion of a gentamycin resistance gene into the *Msc*I site of *corS* (**Fig. 27**) (Ullrich *et al*., 1995). The low-copy number plasmid pMUH34 containing a 3.4-kb *Hin*dIII fragment with the three regulatory genes was able to restore COR production to mutants PG4180.D4, and PG4180.F7 and also restored *cmaABT* promoter activity to those mutants containing pRGMU1 (Ullrich *et al*., 1995). Plasmid pRGMU1 contains a promoterless ß-glucuronidase reporter gene (*uidA*) fused to a 2.9-kb *Pst*I fragment of the *cmaABT* promoter region (**Fig. 27**). The complementation analysis of these mutants was repeated. Plasmid pMUH34 was introduced into PG4180.D4 (pRGMU1), PG4180.F7 (pRGMU1), and PG4180.P1 (pRGMU1) (*corS*$^-$) by triparental mating and the *cmaABT* promoter activity or GUS expression was quantified in the new transconjugants. To verify that plasmid pMUH34 was introduced to the mutants, the plasmid profile of these transconjugants was analyzed. **Fig. 28** represents the native plasmid profiles of the new transconjugates compared to the plasmid profile of the wild type and plasmid pMUH34. According to this, pMUH34 was successfully conjugated into the recipients. The temperature-dependent GUS expression observed for the wild type was restored to transconjugants PG4180.D4 (pRGMU1; pMUH34), PG4180.F7 (pRGMU1; pMUH34), and PG4180.P1 (pRGMU1; pMUH34) (**Fig. 29C**). Additionally, there was a slightly elevated level of GUS expression in the transconjugants measured at 28°C.

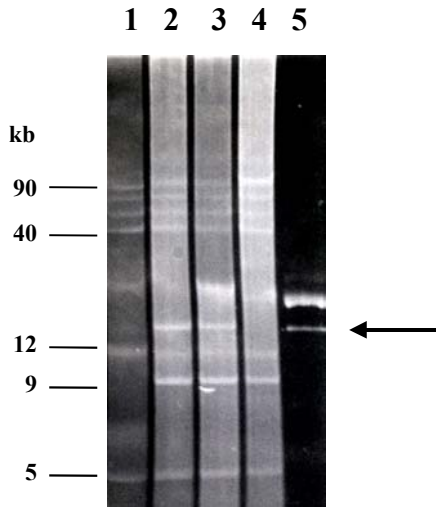

Fig. 28. Agarose gel electrophoresis of undigested plasmid DNA of PG4180, PG4180 regulatory mutants harboring plasmid pMUH34, and plasmid pMUH34. The arrow indicates plasmid pMUH34. Lanes: 1, PG4180; 2, PG4180. D4 (pRGMU1; pMUH34); 3, PG4180. F7 (pRGMU1; pMUH34); 4, PG4180. P1 (pRGMU1; pMUH34); 5, pMUH34.

According to the restriction analysis of pMUH34, the vector-borne *lac* promoter (P_{lac}) is orientated towards *corP* (**Fig. 29A**). Another plasmid, pRKH34R, which was formed by subcloning of the 3.4-kb *Hind*III fragment in the opposite orientation with respect to P_{lac}, was not able to complement any of the mutants. To check whether the plasmid's copy-number and the orientation of the insert affected mutant complementation, the 3.4-kb *Hin*dIII fragment was subcloned in both orientations with respect to P_{lac} in the medium-copy number vector, pBBR1MCS. The resulting plasmids, pBBRH34L and pBBRH34R, were subsequently conjugated into PG4180.D4 and PG4180.D4 (pRGMU1) and tested for COR production and *cmaABT* promoter activity. Quantitative estimation of GUS expression for the transconjugates demonstrated that pBBRH34R was able to complement PG4180.D4 (pRGMU1) (**Fig. 29D**). The temperature-dependent GUS expression was restored to the PG4180.D4 (pRGMU1; pBBRH34R) with slightly elevated GUS activities at 28°C as compared to the wild type. According to HPLC analysis, COR production at 18°C was restored to PG4180.D4 (pBBRH34R). The elevated COR promoter activity at 28°C resulted in minor COR production at this temperature (**Fig. 30**). In the 'R' orientation of plasmid pBBRH34 P_{lac} is not oriented towards *corP* as it is in the case of the 'L' orientation (**Fig. 29A**). This finding was in contradiction with results obtained with plasmid pMUH34. Additionally, plasmids pRKE70L and pRKE70R were used in the complementation analysis of PG4180.D4 (pRGMU1). These plasmids each contain a 7-kb *Eco*RI fragment from the COR gene cluster

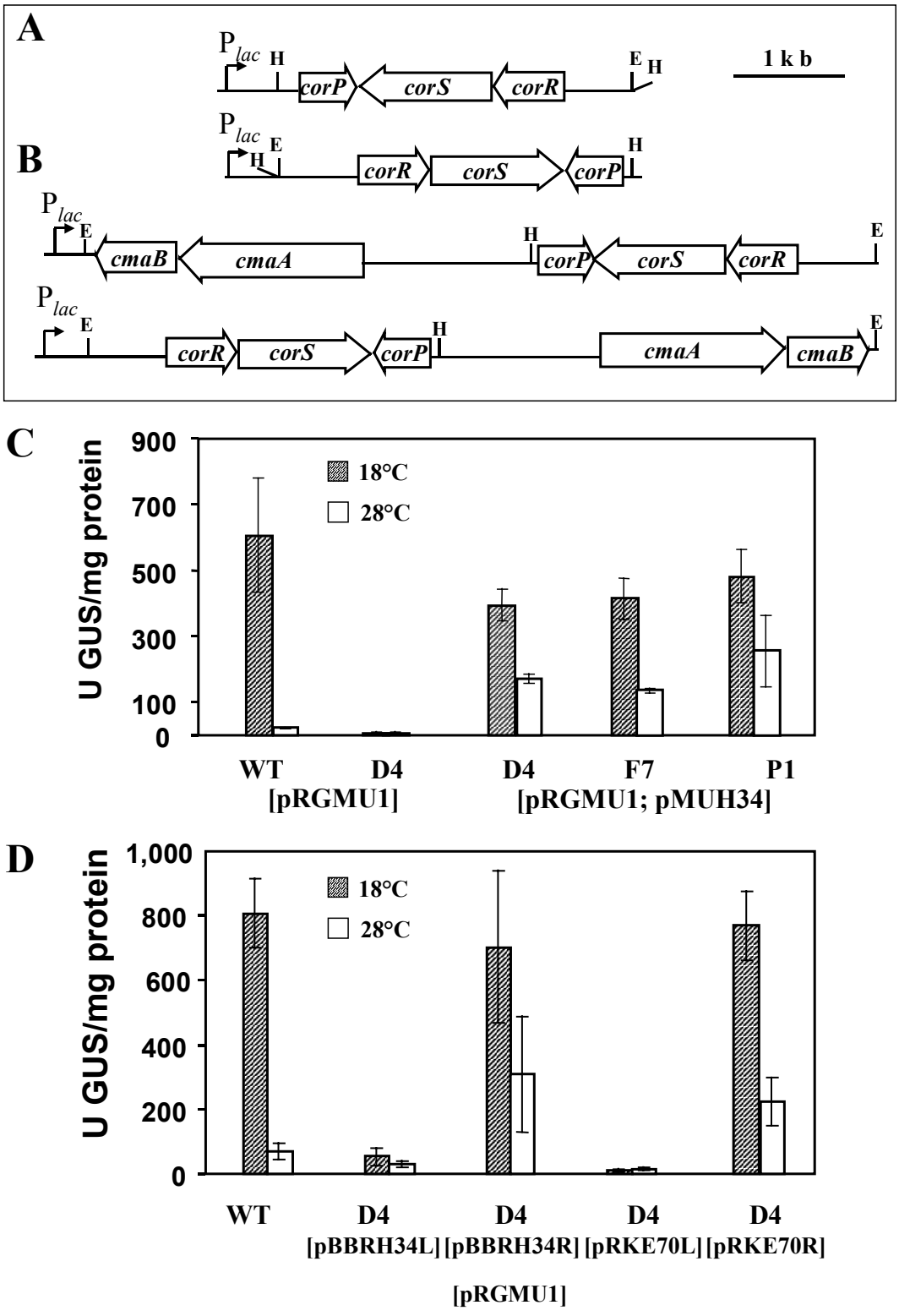

Fig. 29. Orientations of 3.4-kb *Hin*dIII (A) and 7.0-kb *Eco*RI (B) fragments towards P_{lac} in cloning vectors and complementation analysis of PG4180 regulatory mutants with plasmids pMUH34 (C), pBBRH34L, pBBRH34R, pRKE70L, and pRKE70R (D). *cmaABT::uidA* expression was determined in PG4180 (pRGMU1), PG4180.D4 (pRGMU1), and PG4180.D4 harboring pRGMU1 and plasmids mentioned above. Quantities represent the averages of three experiments with three replicates each.

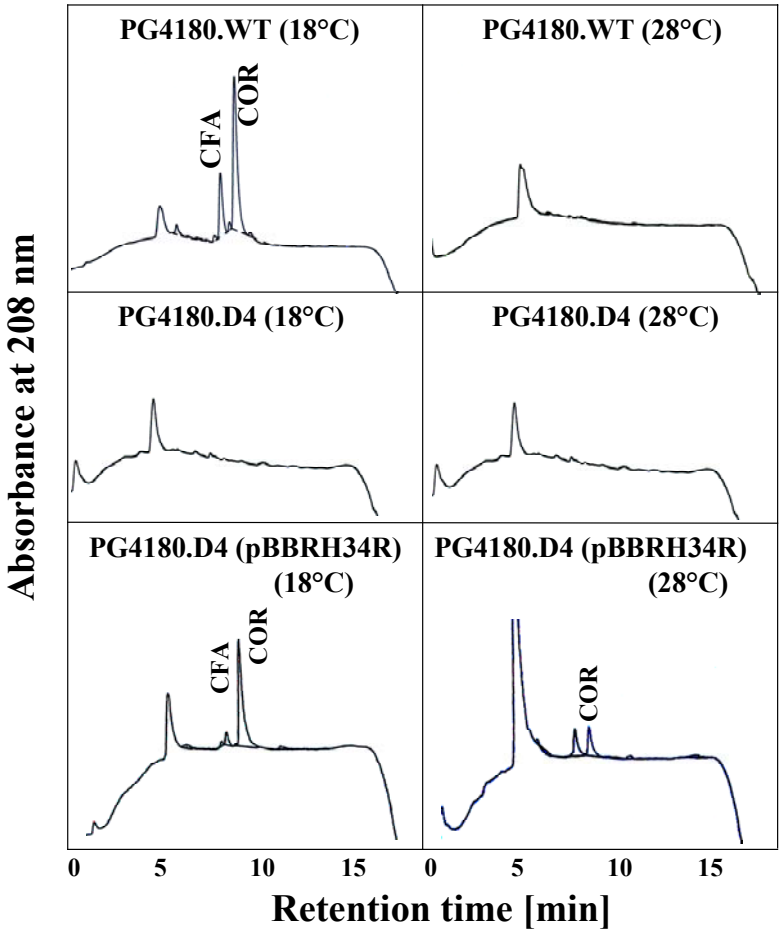

Fig. 30. HPLC analysis of COR and CFA production at 18°C and 28°C in PG4180, mutant PG4180.D4, and mutant PG4180.D4 harboring plasmid pBBRH34R.

in vector pRK415 in both orientations with respect to P_{lac} (**Fig. 29B**). According to the GUS assays, plasmid pRKE70R restored the temperature-dependent GUS expression to the wild-type level showing again a slightly elevated GUS expression at 28°C (**Fig. 29D**). Plasmid pRKE70L was inactive in the complementation analysis.

5.8 Genetic modifications of *corS*

5.8.1 Deletion analysis of the membrane-spanning region of CorS

The theoretical characterization of the CorS structure indicated that its highly hydrophobic N-terminus is the only structural feature which might be involved in temperature signal perception. According to the topological analysis, six transmembrane helices of CorS presumably span the inner membrane. To prove that the transmembrane region is important

for CorS's function as a temperature sensor, the respective region coding for either all six or the last four TMDs were subjected to an in-frame deletion analysis.

PCR amplification with *PfuTurbo* DNA polymerase (Stratagene) and the primers corSoutF, inSer22, corSoutR, corSinF, and corSinR (3.7) were used to generate deletion fragments. Plasmid pH34 was used as the template DNA for PCR. This plasmid contains a 3.4-kb *Hin*dIII fragment carrying *corR*, *corS*, and *corP*. For the deletion of all six TMDs, the first 1.5-kb PCR product (A) starts at the *Eco*RI site of plasmid pH34, at which the primer generated a *Sac*II site, and terminates at the codon for Ser-22, at which the primer generated an *Eco*RI site (**Fig. 31**). For the deletion of the last four TMDs, the second 1.7-kb PCR product (B) has the same 5' start but terminates at the codon for Thr-103, at which the primer generated an *Eco*RI site. The third 1.3-kb PCR product (C) was used for both deletion constructs. It starts at the codon for Ser-202, at which the primer generated an *Eco*RI site and terminates at the *Hin*dIII site of plasmid pH34, at which the primer generated a *Kpn*I site. The third PCR fragment (C) was cloned into pBluescript II SK, yielding plasmid pBKE14. Subsequently, both *Sac*II-*Eco*RI fragments (A and B) were separately cloned into pBKE14, resulting in constructs pSEEKS22 and pSEET103 (**Fig. 31**). pSEEKS22 contains a deletion of a 0.5-kb DNA region from *corS*, and pSEEKT103 contains a 0.3-kb deletion. Both constructs were sequenced. DNA sequence analysis indicated that the two deletions within *corS* were in-frame and that PCR amplification altered neither the sequence of *corS* aside of the deletion nor the sequences of *corR* and *corP*.

Subsequently, the two inserts of pSEEKS22 and pSEEKT103 were subcloned into pRK415, which is able to replicate in *P. syringae*. To do so, the *Eco*RI site of pRK415 was deleted, resulting in pRK415-E-B. A 3.0-kb *Sac*II-*Kpn*I fragment was derived from plasmid pSEEKT103 and blunt-ended with T4 DNA polymerase, whereas pRK415-E-B was cleaved with *Hin*dIII and blunt-ended with Klenow Fragment DNA polymerase. After subsequent ligation of vector and insert, transformants for both orientations of the insert with respect to P_{lac} were selected. Successful cloning resulted in plasmids pRKΔT103L and pRKΔT103R. Both plasmids were used in complementation analysis of mutant PG4180.D4 (pRGMU1). Because of difficulties in separating the 2.8-kb *Sac*II-*Kpn*I fragment from pSEEKS22 by electrophoresis, this fragment was PCR amplified as a 2.8-kb *Hin*dIII fragment using the Expand High Fidelity PCR System (Roche) and primers T3H and T7H (3.7). The PCR product was cloned into pRK415-E-B which had been linearized by *Hin*dIII treatment, yielding plasmid pRKΔS22L. Plasmid pRKΔS22R was selected following digestion of pRKΔS22L with *Hin*dIII and religation. This plasmid contains the 2.8-kb *Hin*dIII PCR

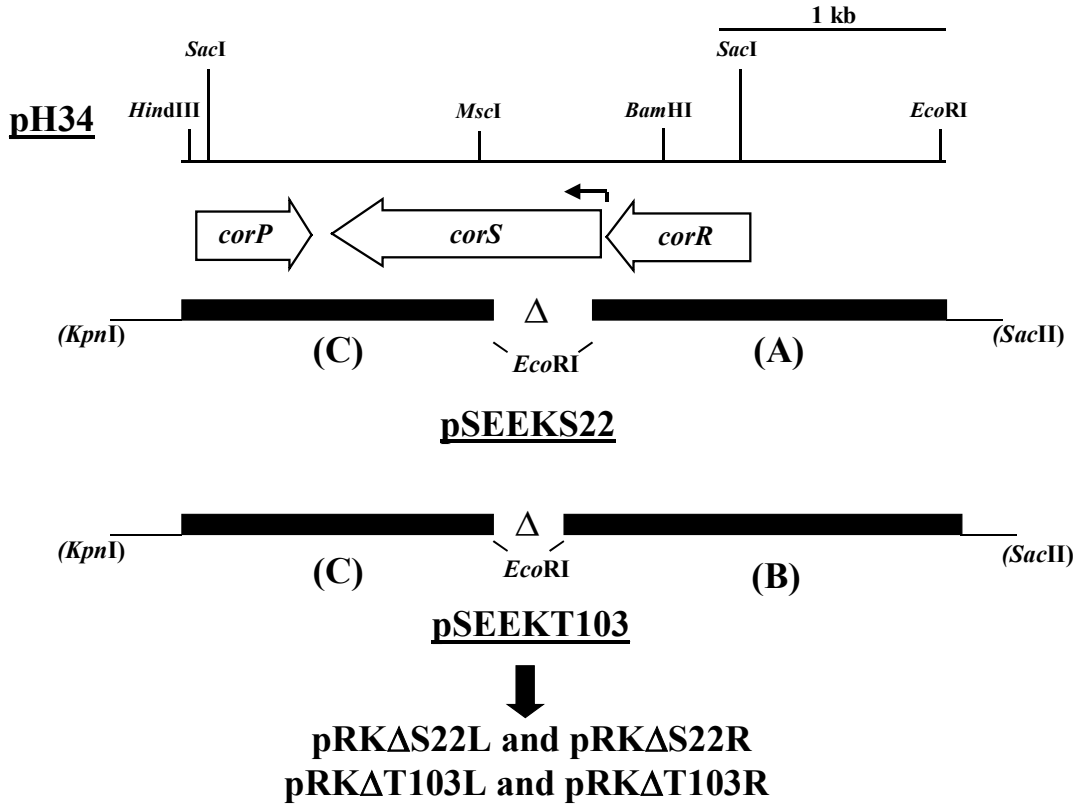

Fig. 31. Schematic representation of in-frame deletions in the *corS* gene. The PCR products (A), (B), and (C) and the plasmids containing the in-frame deletions are indicated. 'L' corresponds to the orientation of an insert where P_{lac} is oriented towards *corP*. 'R' is opposite to 'L' in the orientation of an insert. Restriction sites relevant for the construction of plasmids pSEEKS22 and pSEEKT103 are given. Restriction sites destroyed in the course of subsequent cloning steps are shown in brackets.

fragment in reverse orientation. Plasmids pRKΔS22L and pRKΔS22R were used further for complementation analysis of mutant PG4180.D4 (pRGMU1).

Plasmids pRKΔS22L, pRKΔS22R, pRKΔT103L, and pRKΔT103R were conjugated to PG4180.D4 (pRGMU1) by triparental mating. The presence of these plasmids in PG4180.D4 (pRGMU1) was proved by native plasmid electrophoresis. The truncated *corS* gene in pRKΔT103L and pRKΔT103R encodes a protein with two TMDs, whereas in pRKΔS22L and pRKΔS22R it presumably encodes a soluble protein. None of the plasmids containing truncated versions of *corS* gene complemented the PG4180.D4 (pRGMU1) with respect to *cmaABT* promoter activity. The GUS expression of the respective transconjugants remained at basal levels, whereas control plasmid pMUH34 containing an intact *corS* gene was able to complement the mutant and consequently restored temperature-dependent GUS expression (**Fig. 32A, B**). These results led to the conclusion that CorS lacking its TMDs is a non-functional protein.

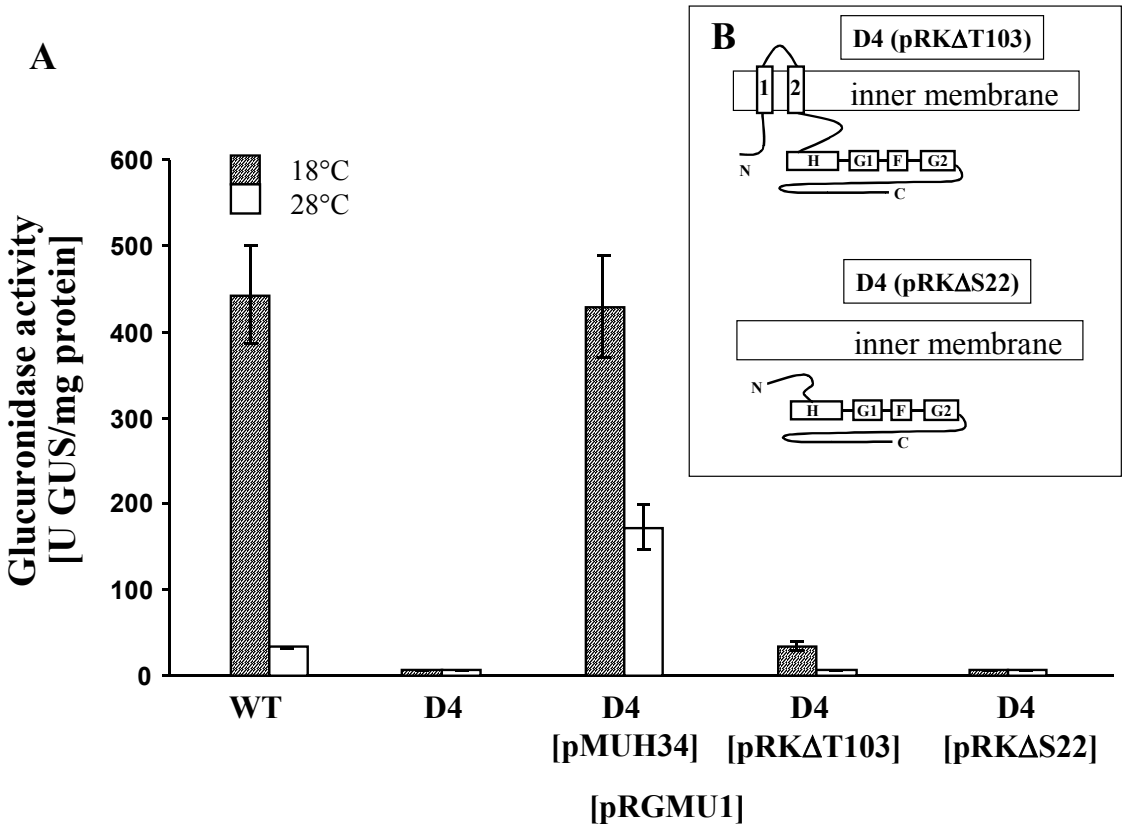

Fig. 32. Complementation analysis of mutant PG4180.D4 (*corS*⁻ *corR*⁻) with plasmid pMUH34 and plasmids containing in-frame deletions of *corS* (A) and schematic representation of truncated CorS proteins resulting from the in-frame deletions (B). *cmaABT::uidA* expression was determined in PG4180 (pRGMU1), PG4180.D4 (pRGMU1), and PG4180.D4 (pRGMU1) derivatives harboring plasmids pMUH34, pRKΔS22, and pRKΔT103L. Quantities represent the averages of two experiments with three replicates each.

5.8.2 Topological analysis of CorS

5.8.2.1 Construction of translational fusions of CorS to alkaline phosphatase (PhoA) and ß-galactosidase (LacZ)

To prove the predicted the topological membrane arrangement of CorS, a genetic approach was used based on the construction of translational fusions between C-terminally truncated versions of CorS and either alkaline phosphatase (PhoA) or ß-galactosidase (LacZ). Alkaline phosphatase is enzymatically active only when it is translocated to the periplasm, whereas ß-galactosidase is active only in the cytoplasm. Thus, PhoA shows activity when fused to periplasmic loops of membrane proteins and enzymatic activity of LacZ is observed when it is fused to cytoplasmic regions of a protein (Manoil & Beckwith, 1986; Alexeyev & Winkler,

1999). The combined use of PhoA and LacZ reporter proteins provides a reliable system for the analysis of the membrane topology of a protein.

PCR amplification with *PfuTurbo* DNA polymerase and the primers corSoutF and Thr27 to ArgcytphoA (3.7) were used to generate DNA fragments starting at the *Eco*RI site of plasmid pH34, at which the primer generated a *Sac*II site, and terminating at codons for certain amino acids located either in the putative periplasmic or cytoplasmic loops of CorS, at which the primer generated a *Kpn*I site (**Fig. 33**). All fragments contain the native *corS* promoter and the *corS* ribosome binding site. *Sac*II-*Kpn*I PCR fragments were cloned in pBluescript II SK, and subsequently were fused in this vector to a 2.6-kb *Kpn*I fragment containing a promoterless *phoA* gene, which lacks a ribosome-binding site as well as the signal peptide sequence. The *Kpn*I fragment containing the *phoA* gene was derived from plasmid pPHO7 (Guttierrez & Devedjian, 1989). It resulted in constructs bearing translational *corS::phoA* fusions under control of the *corS* promoter (**Fig. 33**). Precise in-frame fusion of all fragments to the *phoA* gene was verified by DNA sequence analysis of the junction region with primer phoA354rev derived from the *phoA* sequence (3.7). Subsequently, *Sac*II-*Pst*I fragments containing *corS::phoA* translational fusions were cloned into the broad-host-range vector pBBR1MCS which replicates in *P. syringae* (**Fig. 33**).

To generate *corS::lacZ* translational fusions, the 2.6-kb *Kpn*I fragment containing *phoA* was substituted by a 3.0-kb *Kpn*I fragment encoding the *lacZ* gene in all *corS::phoA* fusions in pBBR1MCS (**Fig. 33**). The DNA fragment encoding *lacZ* was PCR amplified using the Expand High Fidelity PCR System (Roche), primers lacZF and lacZR (3.7), and plasmid pMC-1871 (Amersham-Pharmacia Biotech) which contains an intact *lacZ* gene without its ribosome–binding site and without the first eight non-essential codons.

Plasmids harboring the translational *corS::phoA* and *corS::lacZ* fusions were conjugated to PG4180 by a triparental mating. The presence of the introduced plasmids in PG4180 was verified by native plasmid electrophoresis as well as by PCR with the primers corSoutF/phoAfusTrev and corSout/lacZfusTrev (3.7) (**Fig. 34**).

5.8.2.2 CorS-PhoA and CorS-LacZ fusion activities on substrate-containing agar plates

Minimal MG medium plates containing the substrates for either alkaline phosphatase (X-Phos) or ß-galactosidase (X-Gal) were used for the visual estimation of differential expression of CorS-PhoA and CorS-LacZ fusion proteins, respectively. The plates were

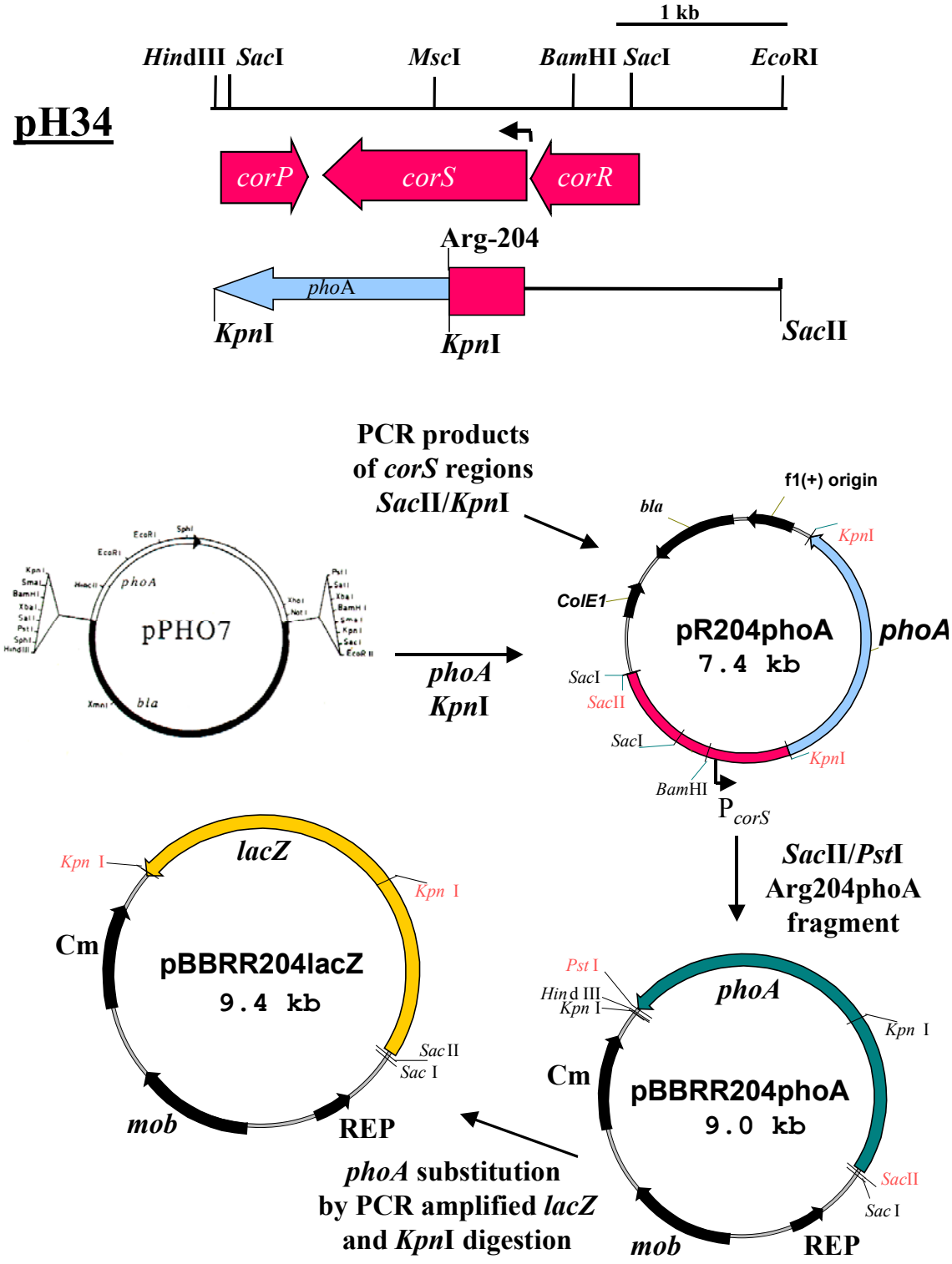

Fig. 33. Construction of translational fusions of CorS at residue Arg-204 to alkaline phosphatase (PhoA) and ß-galactosidase (LacZ) reporter genes. Restriction sites relevant to plasmid pH34 and for the construction of plasmids bearing the translational fusions are indicated.

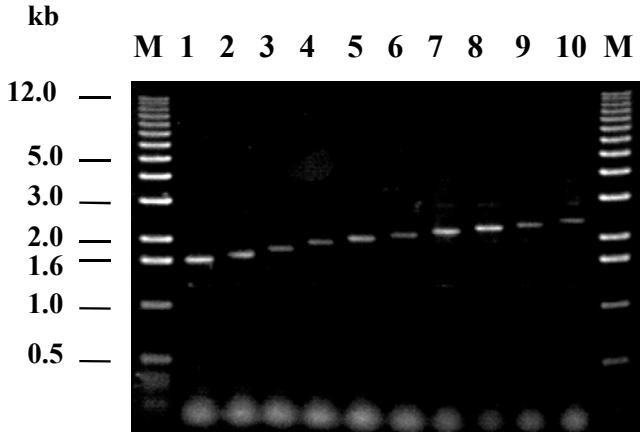

Fig. 34. PCR screening of PG4180 derivatives harboring *corS::phoA* translational fusions. Lanes: M, molecular size marker; 1, PG4180 (pBBRT27phoA); 2, PG4180 (pBBRA51phoA); 3, PG4180 (pBBRY85phoA); 4, PG4180 (pBBRL125phoA); 5, PG4180 (pBBRL151phoA); 6, PG4180 (pBBRV177phoA); 7, PG4180 (pBBRR204phoA); 8, PG4180 (pBBRD227phoA); 9, PG4180 (pBBRL249phoA); 10, PG4180 (pBBRQ281phoA).

incubated at 18°C and 28°C. PhoA fusions to amino acid residues Ala_{51}, Leu_{125}, and Val_{177} exhibited a clear $PhoA^+$ phenotype (blue colonies), whereas PhoA fusions to amino acid residues Thr_{27}, Tyr_{85}, Leu_{151}, and Arg_{204} gave rise to a $PhoA^-$ phenotype (white colonies) at 18°C (**Fig. 35**). The $PhoA^+$ phenotypes of PhoA fusions to Ala_{51}, Leu_{151}, and Val_{177} indicated that these amino acids are located in periplasmic loops of CorS, whereas the $PhoA^-$ phenotype of the other fusions implied that amino acids Thr_{27}, Tyr_{85}, Leu_{151}, and Arg_{204} are located in the cytoplasm. In close agreement with these results were results obtained with the respective CorS-LacZ fusions. LacZ fusions to amino acid residues Thr_{27}, Tyr_{85}, Leu_{151}, and Arg_{204} exhibited a $LacZ^+$ phenotype (blue colonies), thus supporting the assumption of their cytoplasmic location. LacZ fusions to Ala_{51} and Leu_{125} showed a $LacZ^-$ phenotype (white colonies) (**Fig. 35**). This proved their periplasmic location. However, the LacZ fusions to amino acid residue Val_{177} showed a $LacZ^+$ phenotype which contradicts the result obtained for the Val_{177}-PhoA fusion exhibiting a $PhoA^+$ phenotype.

Although the transcriptional fusion of the *corS* promoter to a promoterless *uidA* gene *(uidA::corS)* was shown to be thermoresponsive (Ullrich *et al*., 1995), translational *corS::phoA* fusions which were expressed under control of the *corS* promoter were not affected by temperature. Most cells harboring CorS-PhoA fusions with $PhoA^+$ phenotypes and cells carrying CorS-LacZ fusions with $LacZ^+$ phenotypes formed blue colonies on MG plates at both temperatures and consequently, cells harboring CorS-PhoA fusions with $PhoA^-$

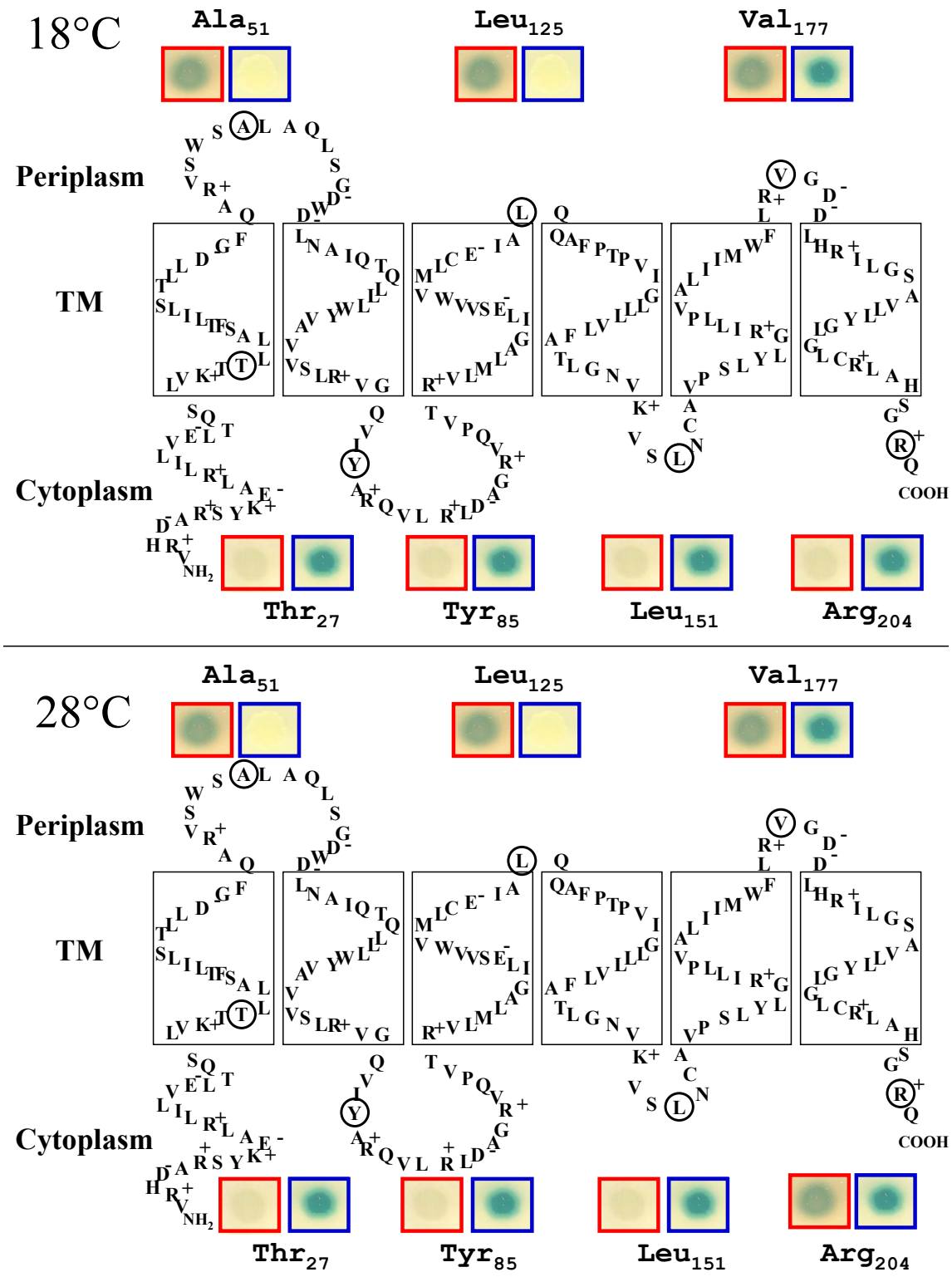

Fig. 35. Schematic representation of the topological structure of CorS derived from hydrophobicity, prediction analyses and experimental phenotypic characterization of CorS-PhoA and CorS-LacZ translational fusions on substrate-containing agar plates at 18°C (top) and 28°C (bottom). Red rectangles show the observed phenotypes for CorS-PhoA fusions and blue rectangles for CorS-LacZ fusions. Circles indicate the residues of CorS fused to PhoA and LacZ. The charged residues are indicated with '+' and '-'.

phenotypes and cells containing CorS-LacZ fusions with LacZ$^-$ phenotypes formed white colonies at both temperature. However, one fusion of PhoA to the amino acid residue Arg_{204} showed a temperature-dependent phenotype. Cells harboring this fusion formed a white colony at 18°C and a blue colony at 28°C (**Fig. 35**).

Expression of corS-PhoA fusions was also tested on IM medium plates. However, this minimal medium was not suitable for this particular test since all fusions tested formed blue color on these plates. The same test with complex KB medium plates demonstrated clearly distinguishable differences in the phenotypes between CorS-PhoA fusions. Cells harboring the PhoA$^+$ fusions to amino acid residues Ala_{51}, Leu_{125}, and Val_{177} formed intense blue colonies whereas cells harboring the PhoA$^-$ fusions to the other amino acid residues remained white. The temperature-dependent phenotype of the Arg_{204}-PhoA fusion was not pronounced on KB plates. At both temperatures the cells harboring this fusion remained white. Thus, the observed phenotype of a temperature dependence for the Arg_{204} fusion to PhoA is also medium-dependent and occurs only in cells grown in specific minimal medium such as MG.

5.8.2.3 Construction of additional CorS-PhoA fusions and their phenotypic characterization

Based on the results described above, CorS possesses six TMDs. This confirms the membrane topology prediction. However, the 6th TMD (aa 181-201) exhibited the lowest hydrophobicity of all TMDs. In addition, **TopPred 2** predicted a 7th TMD (aa 257-277). This 7th TMD was predicted to be located in the conserved His-domain, which is the conserved site of autophosphorylation for HPKs. Interestingly, a temperature-dependent phenotype of the PhoA fusion at Arg_{204} is located downstream of the 6th TMD. This combination of theoretical and experimental results raises the hypothesis that this TMD is translocated into the periplasm at 28°C, whereas it would be embedded in the membrane at 18°C.

To test this hypothesis, additional CorS-PhoA fusions were generated to amino acid residues Asp_{227} and Leu_{249} located upstream of the His-domain, and to amino acid residue Gln_{281} located downstream of the His-domain. This time the *Sac*II-*Kpn*I PCR fragments were cloned directly into pBBR1MCS and later fused to the 2.6-kb *Kpn*I fragment containing *phoA*, yielding *corS::phoA* translational fusions. Plasmids harboring these translational fusions were conjugated to PG4180 by triparental mating. The presence of these recombinant plasmids in PG4180 was verified by native plasmid electrophoresis and by PCR using primers corSoutF/phoAfusTrev (3.7) (**Fig. 34**). Subsequently, cells carrying these fusions were

screened on MG plates containing X-Phos. Interestingly, the Asp_{227}-PhoA fusion led to the same temperature-dependent phenotype observed for the Arg_{204}-PhoA fusion. Cells formed blue colonies at 28°C, whereas colonies remained white at 18°C. Cells harboring the fusions Leu_{249}-PhoA and Gln_{281}-PhoA remained white at both temperatures (**Fig. 36**).

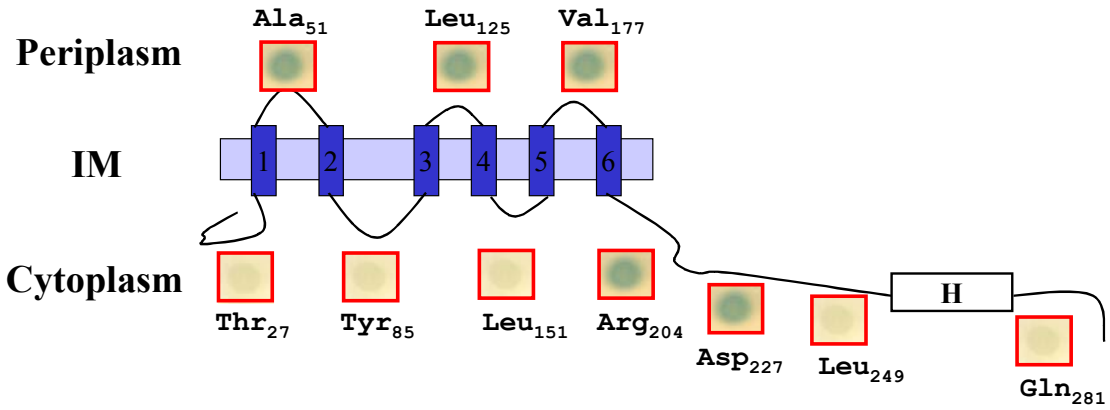

Fig. 36. Schematic representation of the CorS structure and phenotypic characterization of CorS-PhoA translational fusions on substrate-containing agar plates at 28°C. The conserved histidine kinase domain is indicated by a boxed H.

3.8.2.4 Quantitation of specific alkaline phosphatase activities for the CorS-PhoA fusion proteins

PG4180 cells harboring the diverse CorS-PhoA fusions were grown in minimal HSC medium at 18°C and at 28°C. Enzymatic activity was measured for cells derived from cultures reaching ODs_{600nm} of 2.4-2.7 and permeabilized by SDS and chloroform. As a control for enzymatic measurements, wild-type cells lacking a recombinant PhoA were used. The enzymatic activity of none of the fusion proteins analyzed was temperature-dependent (**Fig. 37A**). Approximately equal levels of PhoA activities were measured at both temperatures for the periplasmic CorS-PhoA fusion proteins. PhoA fusions to amino acid residues Ala_{51}, Leu_{125}, and Val_{177} showed high levels of specific activities (1-2.5 units) compared to significantly lower levels for the cytoplasmic fusion proteins (0.1-0.4 units) (**Fig. 37A**). Thus, quantitative estimation of PhoA activities proved the periplasmic location of amino acids Ala_{51}, Leu_{125}, and Val_{177} and cytoplasmic location of the other amino acids. Specific PhoA activities of 28°C-samples for fusions Arg_{204}-PhoA and Asp_{227}- PhoA, which had exhibited a temperature-dependent phenotype on solid medium, were not distinguishable

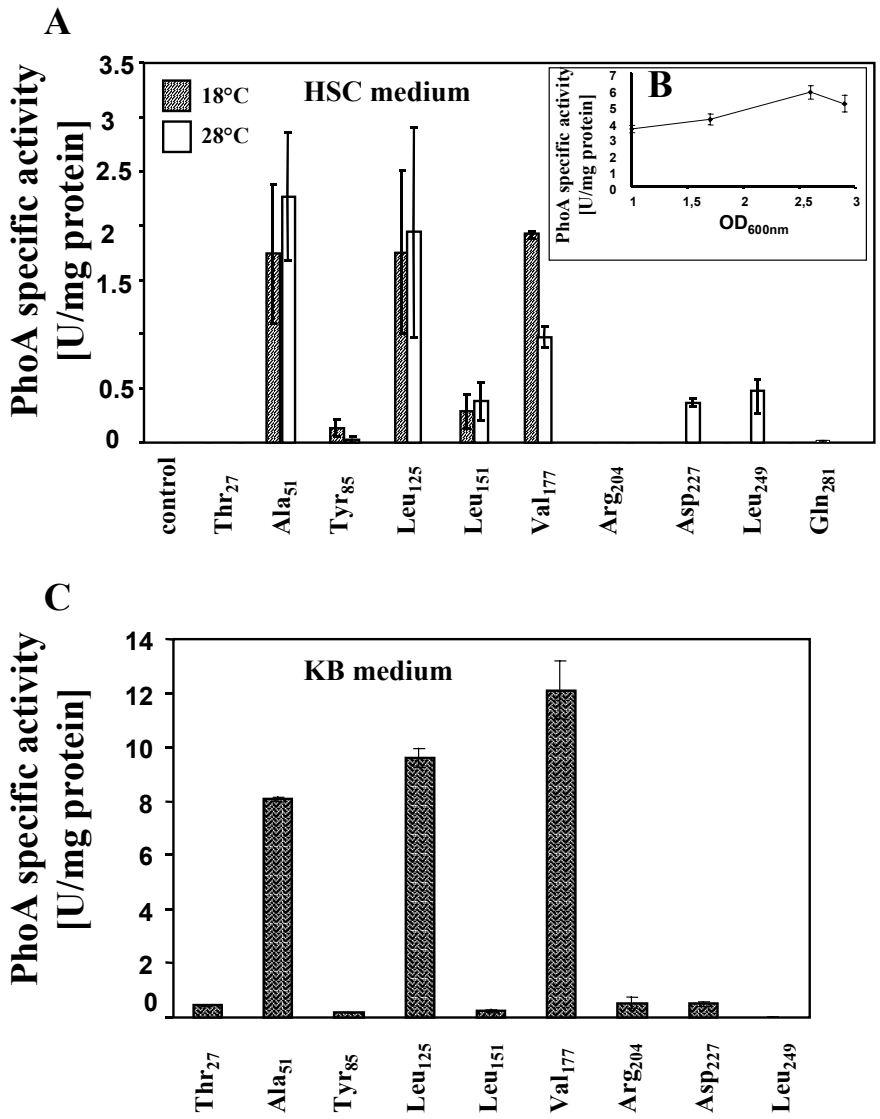

Fig. 37. Quantitative estimation of specific alkaline phosphatase activities for CorS-PhoA translational fusions at 18°C and 28°C for PG4180 cells grown in HSC medium (A) and KB medium (C), dependence of the specific activity for the PhoA fusion to the Leu-125 residue of CorS on cell density (B) measured for PG4180 cells grown in HSC medium at 28°C. Wild-type PG4180 cells were used as a control. Quantities represent the averages from five experiments with three replicates each.

from specific activities of cytoplasmic CorS-PhoA fusions, suggesting that this interesting temperature-dependent phenotype could not be reproduced in liquid medium.

Additionally, enzymatic activities were quantified for cells derived from different growth phases. Samples from the same culture were taken in a range of OD_{600nm} from 1.0 to 2.9 (**Fig. 37B**). The enzymatic activity of CorS-PhoA fusion proteins was cell density-dependent and was more pronounced when the cells reached the late exponential phase (OD_{600nm} of 2.6). Interestingly, wild type cells reaching the stationary phase also showed an elevated level of PhoA activity. This result might indicate that PG4180 contains an indigenous enzyme similar

to alkaline phosphatase which might be expressed in response to phosphate starvation in the stationary phase. Taking this into account, all subsequent measurements were performed for before cells reached the stationary phase (OD_{600nm} of 2.4-2.7).

Quantitation of specific PhoA activities in cells grown in IM minimal medium indicated that the difference between the expression of periplasmic and cytoplasmic CorS-PhoA fusion proteins was negligible (data not shown). However, the difference between periplasmic and cytoplasmic fusion proteins was more pronounced for cells grown in complex KB medium than for cells incubated in HSC medium (**Fig. 37C**). In KB medium a high level of the PhoA activity (8-12 units) was measured for Ala_{51}-PhoA, Leu_{125}-PhoA, and Val_{177}-PhoA fusions as compared to a significantly lower level of the PhoA activity (0.2-0.5 units) for the other fusions.

5.8.2.5 Quantitation of specific ß-galactosidase activities for the CorS-LacZ fusion proteins

PG4180 cells harboring CorS-LacZ fusions were grown in minimal HSC-medium at 18°C and at 28°C to an OD_{600nm} of 3.0. Enzymatic activity was measured for cells permeabilized by SDS and chloroform (**Fig. 38**). As a control, wild-type cells lacking a recombinant LacZ were used. The $LacZ^+$ phenotypes of LacZ fusions to the amino acid residues Thr_{27}, Tyr_{85}, Leu_{151}, and Arg_{204} on MG plates corresponded to high levels of specific activities for these fusion proteins (34-157 units). Thus, the quantitative estimation of LacZ activities proved

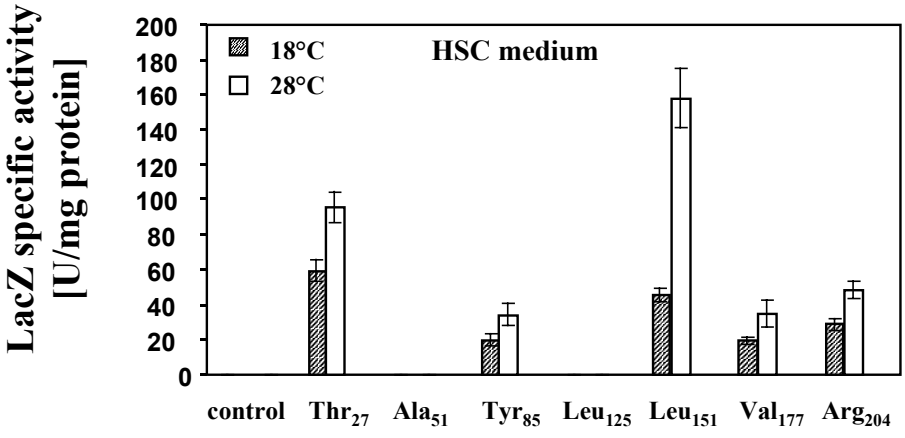

Fig. 38. Quantitative estimation of specific ß-galactosidase activities for CorS-LacZ translational fusions at 18°C and 28°C for PG4180 cells grown in HSC medium. Wild-type PG4180 cells were used as control. Quantities represent the averages from two experiments with three replicates.

the cytoplasmic location of these amino acids. An elevated level of LacZ activity for the Val_{177}-LacZ fusion contradicted the high level of PhoA activity for the corresponding PhoA fusion. As observed on MG plates, active fusion proteins were expressed at both temperatures and quantitation of LacZ activities revealed negligible temperature differences in the CorS-LacZ activities. However, for the fusion Leu_{151}-LacZ the activity of 18°C-grown cells was 3-fold less than the activity of 28°C-grown cells (**Fig. 38**).

5.8.2.6 Immunological estimation of the expression of CorS-PhoA and CorS-LacZ hybrid proteins

To demonstrate that differences in the enzymatic activities of various hybrid proteins were not the result of different levels of protein expression, immunoblot analyses for CorS-PhoA and CorS-LacZ hybrid proteins with antibodies raised against either PhoA or LacZ were performed. Samples of the same *P. syringae*-cultures that were used for measurement of the enzymatic activities were used for Western blotting. PG4180 cells expressing CorS-PhoA fusions were fractionated to generate spheroplasts. The spheroplasts were lysed in the presence of SDS and TritonX-100. The lysate containing solubilized proteins was used to monitor the expression of CorS-PhoA by Western blot analysis with antisera against PhoA. For Western blot analysis proteins were separated by SDS-10%-PAGE, transferred to nitrocellulose membranes, and immunostained with a rabbit anti-PhoA IgG. Representative results are shown in **Fig. 39A**. The actual expression levels for the hybrid proteins do not account for differences observed for the respective PhoA activities. Western blot analysis for all CorS-PhoA fusions furthermore demonstrated that hybrid proteins of the expected molecular size were produced. However, some degree of protein instability was observed: for all chimeras, a band of ca. 48 kDa was detected, which corresponds to the size of the PhoA moiety.

For CorS-PhoA fusions, the periplamic or cytoplasmic localization of the respective hybrid proteins was also verified by protease sensitivity assays. If a hybrid protein is translocated into the periplasm it becomes protease-resistant due to intramolecular disulfide bond formation. In the cytoplasm it remains protease-sensitive (Rutz *et al*., 1999). Upon protease treatment, solubilized CorS-PhoA hybrid proteins should be cleaved to the molecular size of the PhoA protein (48 kDa), if the PhoA portion reaches the periplasm. In contrast, the hybrid protein should be completely digested if the PhoA portion is located in the cytoplasm. To test

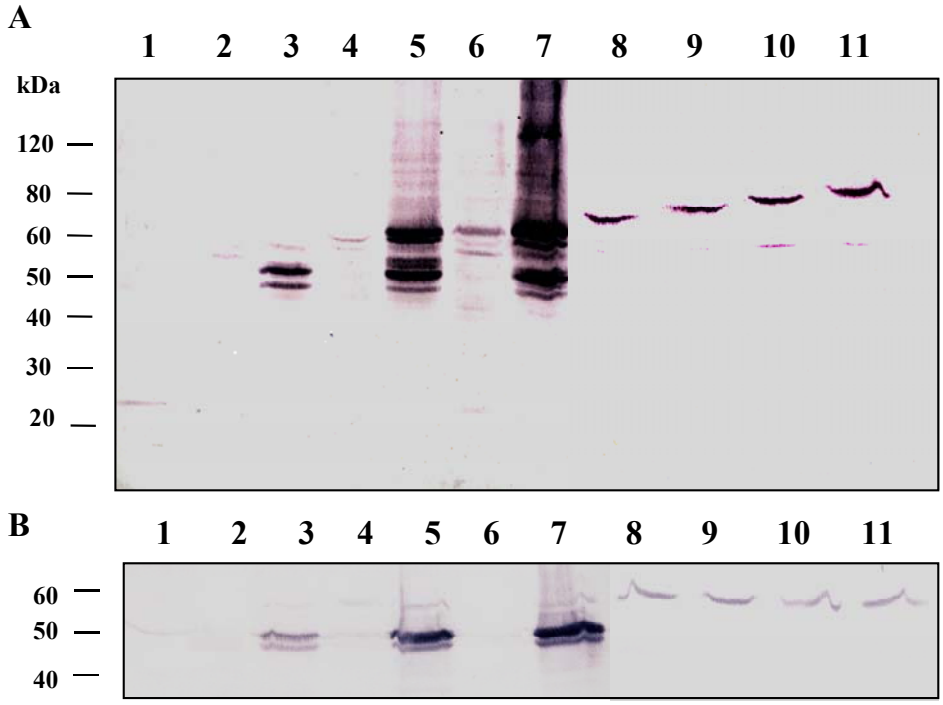

Fig. 39. Western blot analysis of the CorS-PhoA hybrid proteins (A) and their protease sensitivity assay (B). Equal amounts of solubilized proteins from spheroplasts (A) and solubilized proteins treated with 1µg/ml trypsin (B) were resolved by SDS-10%-PAGE and immunoblotted with anti-alkaline phosphatase antiserum. Solubilized proteins from wild-type PG4180 cells were used as control. Lanes: 1, control; 2, Thr_{27}PhoA; 3, Ala_{51}PhoA; 4, Tyr_{85}PhoA; 5, Leu_{125}PhoA; 6, Leu_{151}PhoA; 7, Val_{177}PhoA; 8, Arg_{204}PhoA; 9, Asp_{227}PhoA; 10, Leu_{249}PhoA; 11, Gln_{281}PhoA.

this, the lysate containing solubilized proteins was treated with trypsin. Upon trypsin treatment, a band of ca. 48 kDa was detected for those hybrid proteins which showed high PhoA activities (**Fig. 39B**). The protease resistance of PhoA in these cases confirmed that PhoA was exposed to the periplasm. Whenever the hybrid proteins were located in the cytoplasm, they were cleaved by protease and the 48-kDa signal could not be detected.

Whole cell extracts of PG4180 expressing CorS-LacZ hybrid proteins were separated by SDS-6%-PAGE, transferred to nitrocellulose membranes, and immunostained with mouse monoclonal anti-LacZ (*E. coli*) IgG. As a control, whole cell extract of *E. coli* cells bearing plasmid pMC-1871 (*lacZ*$^+$) was used. Signals corresponding to CorS-LacZ hybrid proteins were hardly visible in the immunoblot, whereas a band corresponding to the normal LacZ protein of ca. 130 kDa was clearly visible in the *E. coli* control sample. Thus, it was not possible to immunologically estimate the expression of CorS-LacZ hybrid proteins in *P. syringae* cells.

5.8.3 Pentapeptide mutagenesis of the N-terminal region of CorS

Deletion analysis of the membrane-spanning N-terminus of CorS proved that its TMDs are required for the function of CorS. In order to elucidate how CorS functions in temperature signal perception and what particular alterations of the TMD of CorS make it insensitive to temperature signals, a random *in vitro* mutagenesis approach was used.

According to the restriction map of the *corS* gene and its upstream DNA, a 0.8-kb *Aat*II-*Mcs*I fragment comprises the N-terminal region of the *corS* gene. Plasmid pMA8 harboring this *Aat*II-*Mcs*I fragment was subjected to an *in vitro* mutagenesis. Plasmid pMA8 was generated by three successive steps. First, the vector pBluescript II SK had to be equipped with a *Msc*I and an *Aat*II recognition site. These sites were introduced into the *Bam*HI site of pBluescript II SK by insertion of a 42-kb synthetic double-stranded oligonucleotide comprising the *Msc*I and *Aat*II sites, yielding plasmid pBlueMA (**Fig. 40A**). According to the mutagenesis principle used, a *Not*I site must be the unique site for mapping a 15-bp insertion in each individual mutant. Because pBlueMA contained a *Not*I site, the latter one had to be deleted by digestion of pBlueMA with *Not*I and *Xba*I, end repair with Klenow Fragment polymerase, and blunt-end self-ligation of pBlueMA. Finally, a 0.8-kb *Aat*II-*Mcs*I fragment derived from plasmid pBSB24 was cloned into pBlueMA, yielding plasmid pMA8 (**Fig. 40A)**.

The *in vitro* transposition reaction was performed with a modified mini-Mu transposon as the donor DNA, plasmid pMA8 as the target DNA, and purified MuA transposase as reported previously (Haapa *et al*., 1999; Taira *et al*., 1999). Following the formation of a transposition complex, the mini-Mu transposon was randomly inserted into the target DNA (**Fig. 40B**). Transposition reaction products were randomly analyzed by electrophoresis. The transposition plasmid pool was introduced to *E. coli* MC1061 by electroporation and selected for ampicilin (150 µg/ml) and chloramphenicol (5 µg/ml) resistance. Transformation resulted in ~32,000 colonies. Plasmid DNA was then isolated from this mutant pool. To exclude mutant clones containing mini-Mu insertions in the vector, plasmid DNA was digested with *Kpn*I and *Sac*I, and the *Kpn*I-*Sac*I inserts containing mini-Mu insertions were subsequently cloned into a non-affected vector DNA. Ligations were electroporated to *E. coli* MC1061 and selected for ampicilin (150 µg/ml) and chloramphenicol (5 µg/ml) resistance. Transformation resulted in ~80,000 colonies which were pooled together, and plasmid DNA was isolated from this pool. Next the transposons were deleted from the pooled mutated insert DNAs by *Not*I digestion

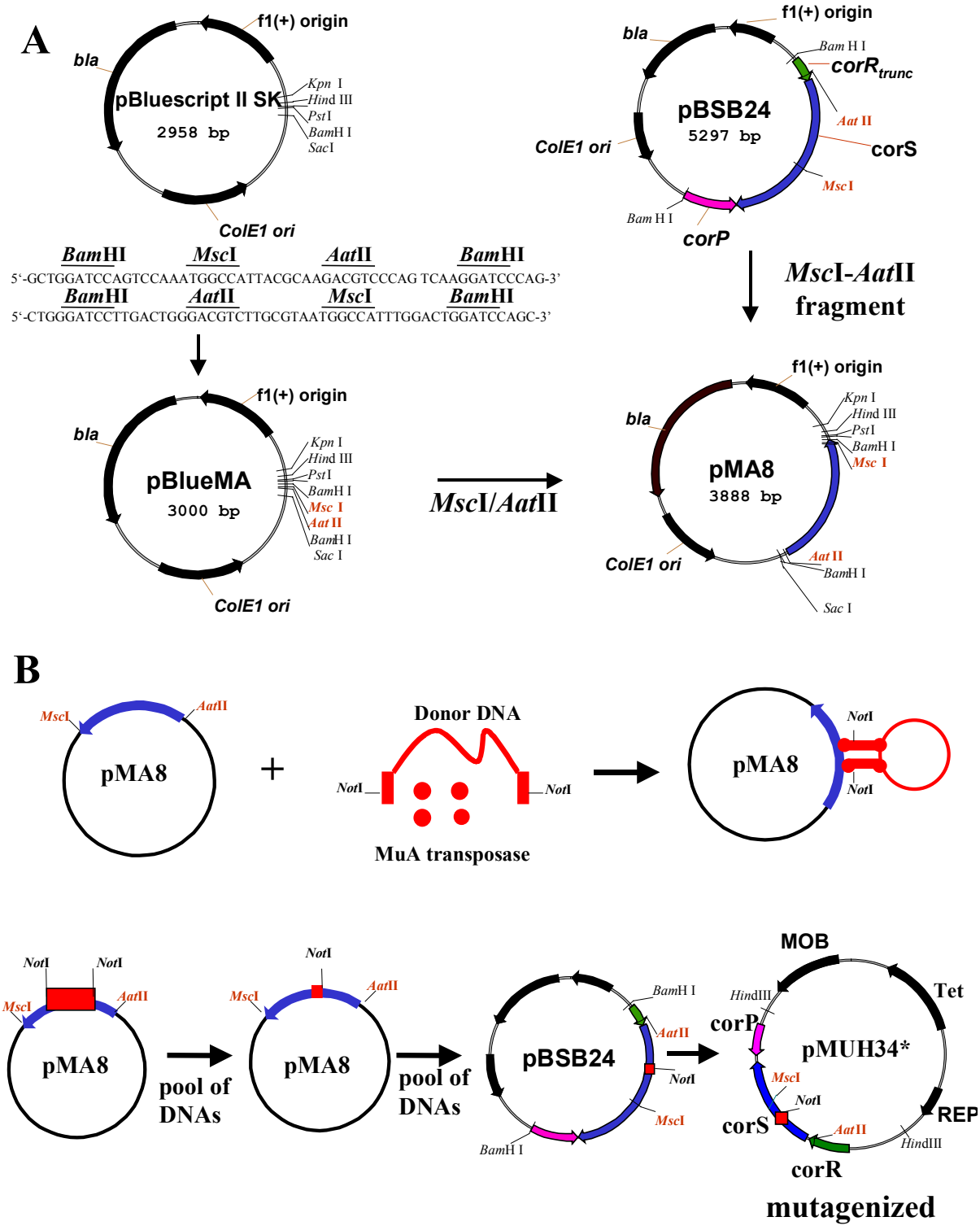

Fig. 40. Construction of plasmid pMA8 containing a 0.8-kb *Msc*I-*Aat*II fragment which encodes the transmembrane region of CorS (A) and a simplified scheme for the *in vitro* mutagenesis of plasmid pMA8 and subsequent subcloning steps to yield mutagenized plasmid pMUH34* (B). The sequences of oligonucleotides used for the generation of *Msc*I and *Aat*II sites are indicated. Restriction sites relevant for plasmids used in the course of cloning and restriction analysis as well as a unique *Not*I site in the entranceposon are indicated.

and self-ligation of the plasmid pool. Ligations were subsequently electroporated to *E. coli* MC1061 and selected for ampicilin (150 µg/ml) resistance and chloramphenicol (5 µg/ml) sensitivity. This resulted in 10^6 colonies which were ampicilin resistant and sensitive to chloramphenicol. Less than 1% of colonies were still ampicilin and chloramphenicol resistant. Colonies were pooled together. The mutant pool contained a mutant library of pMA8 in which each mutant harbored a unique 15-bp insertion with a unique *Not*I site. This 15-bp insertion encodes for five amino acid residues which were inserted in the CorS sequence at any given position. The plasmid DNA pool was isolated and tested by restriction analysis (**Fig. 41**). According to the restriction analysis, a *Not*I digestion of the pMA8 plasmid pool resulted in a fragment of 3.8-kb corresponding to the size of pMA8, while an *Aat*II-*Mcs*I double digestion yielded 0.8-kb *Aat*II-*Mcs*I and 3.0-kb fragments. A *Not*I-*Aat*II-*Mcs*I triple digestion resulted in a smear lower the 0.8-kb due to the presence of the *Not*I site at different distances to the insert ends. Subsequently, the mutagenized *AatII-McsI* fragments were introduced back into plasmid pBSB24. Ligations were transformed to *E. coli* DH5α. Then 2,000 colonies were pooled and the plasmid DNA pool was isolated. The pool of 2.3-kb *Hin*dIII-*Bam*HI fragments from the pBSB24 pool was subcloned into plasmid pRKBE11. Plasmid pRKBE11 contains a 1.1-kb *Bam*HI-*Eco*RI fragment derived from pMUH34 in pRK415. Thus the fusion of the pooled 2.3-kb *Hin*dIII-*Bam*HI fragment from pBSB24 to the 1.1-kb *Bam*HI-*Eco*RI fragment in pRKBE11 yielded a library of 3.4-kb *Hin*dIII-*Eco*RI fragments in pRK415 or – alternatively, a randomly mutagenized plasmid pMUH34*. After

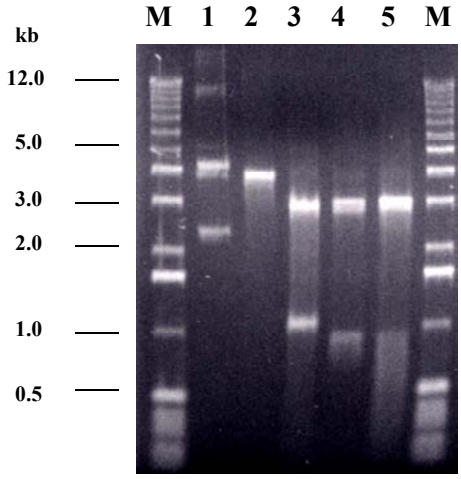

Fig. 41. Restriction enzyme analysis of the mutagenized plasmid pool of pMA8. Lanes: M, molecular size marker; 1, undigested pooled DNA; 2, digestion with *Not*I; 3, digestion with *Msc*I and *Aat*II; 4, digestion with *Kpn*I and *Sac*I; 5, digestion with *Msc*I, *Aat*II and *Not*I.

ligation, the mix was transformed to *E. coli* DH5α, and single colonies were kept for subsequent steps. 34 colonies containing mutagenized pMUH34* plasmids were screened by PCR with fcsB/rcsB primers (3.7). A 1.4-kb PCR fragment corresponding to the size of *corS* was amplified from all of these. The PCR products were subsequently digested with *Not*I to determine the diversity of mutants. According to the *Not*I restriction analysis, 28 mutants of 34 tested differed from each other. Additionally, one of the plasmids was sequenced. The DNA sequence analysis demonstrated that the 15-bp (5 amino acids) insertion was located between the codons for Leu-211 and Lys-212 of CorS (**Fig. 42**).

Finally, 28 mutagenized pMUH34 plasmids harboring different mutations in the N-terminus of CorS and one non-mutagenized pMUH34 plasmid were separately conjugated to PG4180.D4 (pGMU1) by triparental mating. The presence of the plasmids in *P. syrinage* was confirmed by native plasmid electrophoresis. All resulting transconjugants were screened for GUS expression at 18°C and 28°C on X-Gluc-containing MG plates. Simultaneously, GUS activities were quantified in the fluorescence assay. None of the introduced mutagenized plasmids restored the temperature-dependent GUS expression to PG4180.D4 (pRGMU1) (*corS*$^-$ *corR*$^-$). In contrast, the control non-mutagenized pMUH34 plasmid restored the thermoresponsive GUS expression to PG4180.D4 (pRGMU1). All transconjugants containing a mutated pMUH34 plasmid showed a GUS$^-$ phenotype on MG plates.

CorS mutant	**HSGRQRLVKQLCGRKLKRQLLLDETTKRARRDL**
CorS wild type	**HSGRQRLVKQL----------KRQLLLDETTKRARRDL**

Fig. 42. Comparison of the amino acid sequences of wild type CorS and one CorS mutant ranging from amino acid residues 201 to 228 of the wild type CorS sequence.

6 DISCUSSION

With currently ongoing genome sequencing projects and mutational analyses of microorganisms, more and more two-component regulatory systems have been identified controlling a wide variety of pathways in response to biotic and abiotic environmental signals. Even though some of them are already well studied, it is still impossible to draw concrete conclusions about the function for most of the HPKs of two-component regulatory systems solely based on sequence homology to a few well-characterized bacterial HPKs. Divergence of environmental signals is likely to reflect the divergence of mechanisms in signal perception and transduction. Nothing is known about how temperature signals activate sensor kinases and there is still very limited knowledge about the mechanism of phosphotransfer between a sensor kinase and a response regulator. It is important to understand those questions, especially because bacterial two-component regulatory systems are often involved in pathogenicity.

In the frame of this work, we attempted to elucidate the mechanism of signal perception by the HPK CorS which responds to a temperature change and initiates a signal transduction pathway resulting in the coordinated regulation of the production of the phytotoxin coronatine by the plant pathogen *P. syringae*. Our initial assumption that fluidity of the bacterial membrane might influence the function of this membrane-associated protein was supported by the finding that the fatty acid composition of *P. syringae* membranes differed at 18°C and at 28°C with respect to the proportions of unsaturated, saturated, and cyclo fatty acids. In addition, the transcriptional activation of COR biosynthetic genes at 18°C was suppressed by addition of a membrane fluidizer. It is likely that the physical state of the membrane at 28°C might promote conformational changes of CorS which may lead to its inactive state. Thermoresponsive phenotypes of two CorS-PhoA translational fusions downstream of the last predicted TMD supported the assumption that topological changes might be involved in signal perception.

6.1 Effect of the plasmid copy-number and the orientation of the insert on the complementation phenotype for regulatory COR$^-$ mutants

Biosynthesis of COR in *P. syringae* is regulated by temperature at the transcriptional level. Previously, it was demonstrated that mutants PG4180.D4 (*corR*$^-$ *corS*$^-$), PG4180.F7 (*corP*$^-$), and PG4180.P1 (*corS*$^-$) did not produce COR and that the temperature-dependent activation of

cmaABT was completely abolished as a consequence of these mutations (Ullrich *et al*., 1995). Furthermore, a 3.4-kb *Hin*dIII fragment containing the three regulatory genes, *corR*, *corS*, and *corP*, could restore thermoresponsive COR production to these mutants (Ullrich *et al*., 1995). Analysis of this fragment revealed that P_{lac} was oriented towards *corP*. In the reverse orientation, the DNA fragment did not complement the regulatory mutants. It was suggested that *corP* devoid of its promoter region within this DNA fragment might require P_{lac} to be transcribed. Interestingly, mutants complemented with pMUH34 showed an elevated level of *cmaABT* promoter activity. This might be explained by the presence of additional copies of each of the regulatory genes. In this study, effects on the complementation of mutant PG4180.D4 were investigated with plasmids pBBRH34R and pBBRH34L, pRKE70R and pRKE70L. Plasmids pMUH34 and pRKE70 are low-copy plasmids, whereas the two pBBRH34 derivatives are medium-copy plasmids. It turned out that inserts in pBBRH34(R/L) were able to complement mutations in the *corR*$^-$ *corS*$^-$ mutant PG4180.D4 in the orientation where P_{lac} is oriented towards *corR*, but not when it was driving *corP* as it was in the case of pMUH34. Obviously, the copy number of the plasmid affected the complementation phenotype. In addition, an elevated level of *cmaABT* promoter activity at 28°C in the complemented mutant resulted in minor COR production at 28°C. The *corP* gene was present in multiple copies in pBBRH34. This might give rise to an elevated level of transcriptional activation. This finding raised the question about the role of CorP in the regulatory cascade of the CorRSP system. Previously, it was demonstrated that CorR overproduced in the *corP*$^-$ mutant PG4180.F7 was inactive in DNA-binding assays (Wang *et al*., 1999) suggesting that CorP is essential for initiation of the transcriptional activation mediated by the binding of CorR to its target DNA. The presence of multiple copies of CorP might disrupt the coordinated temperature-dependent regulation of this system.

Complementation analysis with plasmids pRKE70R and pRKE70L revealed that only pRKE70R was able to complement the mutant PG4180.D4. Since these plasmids contain a 7-kb *Eco*RI fragment from the COR gene cluster with all three regulatory genes plus their promoter sequences, there is no need for P_{lac} to drive either *corP* or *corR*. Both plasmids should have led to complementation of the mutant PG4180.D4. Interestingly, only pRKE70R complemented PG4180.D4 whereas pRKE70L did not. Since pRKE70R was the initial plasmid used for subcloning of the 3.4-kb *Hin*dIII fragment in pMUH34, we assume that pRKE70L possesses point mutations in one of the regulatory genes abolishing its expression.

6.2 Temperature-dependent expression of COR biosynthetic proteins

Transcriptional fusions of the *cmaABT* and *cfl*/CFA biosynthetic operons with a promoterless *uidA* gene showed maximal transcriptional activation at 18°C (Ullrich & Bender, 1994; Budde *et al*., 1998; Liyanage *at al*., 1995b). In this respect, we aimed to identify with 2-DE biosynthetic proteins as well as regulatory proteins such as CorS expressed differentially under conditions optimal for the COR synthesis. All our attempts to identify CorS using this technique failed so far. Because CorS is a membrane-associated protein as demonstrated in the course of this work, it might not have been properly solubilized by the standard sample preparation technique used (Molloy *et al*., 1998) or its abundance might simply have been too low. In addition, CorS is a rather basic protein (pI 9.1) making it difficult to resolve by 2-DE. In contrast, the cytoplasmic protein CmaB involved in the biosynthesis of the COR precursor CMA was identified by 2-DE as a protein expressed in a temperature-dependent manner. Previously, it had been demonstrated by Western blot analysis that CmaB accumulated in the late stationary phase of *P. syringae* cultures grown at 18°C and that its stability was more pronounced at 18°C than at 28°C (Budde et al., 1998). This result was confirmed by 2-DE in this study. In addition, it was shown that expression of CmaB depended on a functional CorRSP system. This protein was shown to be not expressed when protein fractions of the *corR*$^{-}$ *corS*$^{-}$ mutant PG4180.D4 were arrayed by 2-DE.

The temperature-dependent expression of large proteins (>200 kDa) of PG4180 was demonstrated using conventional SDS-PAGE. The fact that these proteins were not expressed in a Tn*5* mutant mapped to the *cfa6* gene (PG4180.AG28) of the CFA biosynthetic operon (Palmer *et al*., 1997) led to the conclusion that these proteins are involved in the biosynthesis of COR precursor, CFA, and might be related to polyketide synthases. Previously, it was shown that polyketide synthases involved in the CFA biosynthesis were expressed in *P. syringae* under conditions favorable for COR production (Rangaswamy *et al*., 1998b). In the current study, it was demonstrated that the expression of these proteins depended on the CorRSP system since they were not expressed in fractions of the *corR*$^{-}$ *corS*$^{-}$ mutant PG4180.D4. Interestingly, these usually cytoplasmic proteins were found in the membrane fractions of *P. syringae*. In agreement with our finding, the cytoplasmic proteins EntE, EntF, and EntB/G, which are *E. coli* enzymes necessary for the final stage of enterobactin synthesis, were found to be associated with membrane fractions (Hantash & Earhart, 2000). Components of the polyketide synthase of *Streptomyces glaucescens* involved in the production of the antibiotic tetracenomycin C were demonstrated to be membrane-bound by

Western blot analysis of cytoplasmic and membrane fractions of *S. glaucescens* (Gramajo *et al*., 1991). In this study it was not particularly investigated whether CFA polyketide synthases are indeed associated with the membrane. However, since they were always found in the membrane fractions, it is tempting to speculate that these proteins might be either indeed associated with the membrane or might fractionate with membrane components due to their large molecular mass.

6.3 Heterologous expression and imunological detection of CorS

One of the objectives of this study was to overproduce CorS in amounts that allow the generation of antibodies directed against CorS and that would enable us to characterize CorS enzymatically. The histidine protein kinase CorS was overproduced in *E. coli* as an N-terminal $CorS_{\textit{Strep}\text{-tag}}$ fusion protein. One significant advantage of the *Strep*-tagII system is the fast and easy detection method of recombinant proteins with streptavidin alkaline phosphatase conjugates. Although the expression level of $CorS_{\textit{Strep}\text{-tag}}$ was low, the protein was detected by Western blot analysis. $CorS_{\textit{Strep}\text{-tag}}$ was found in the membrane fraction of *E. coli* cells, thereby confirming that it is a membrane-associated protein. The fact that heterologous expression of $CorS_{\textit{Strep}\text{-tag}}$ led to membrane insertion of $CorS_{\textit{Strep}\text{-tag}}$ might have accounted for the low protein expression level, since any disturbances of the bacterial membrane disrupt its normal function. Thus, the presence of a recombinant protein such as $CorS_{\textit{Strep}\text{-tag}}$ in the membrane might be highly toxic for *E. coli* cells. Taking into account that a number of membrane proteins such as the betaine transporter BetP from *Corynebacterium glutamicum* (Rübenhagen *et al*., 2000), the sugar phosphate transporter from *E. coli* (Tamai *et al*., 1997), and eukaryotic cytochrome P450 2B4 (Saribas *et al*., 2001) were overproduced in *E. coli* and later solubilized from *E. coli* membrane fractions, we also attempted to solubilize the overproduced $CorS_{\textit{Strep}\text{-tag}}$ from membrane fractions with TritonX-100. However, the solubilization procedure needs to be optimized in future experiments to increase the protein yield.

Antibodies raised against synthetic peptides derived from CorS within this study were effective in the detection of recombinant $CorS_{\textit{Strep}\text{-tag}}$ but failed to detect the native CorS protein from *P. syringae* cell extracts. Possibly, the epitopes for these antibodies were more accessible in $CorS_{\textit{Strep}\text{-tag}}$ than in native CorS due to different folding properties of CorS in *E. coli* and *P. syringae*. Additionally, native CorS might be very low in abundance in *P. syringae.*

6.4 Does the membrane fluidity influence the mode of action of CorS?

In this study a membrane-associated status of CorS was proven by its topological analysis. Since temperature affects the fluidity of the bacterial membrane, we assumed that CorS functions as a 'temperature sensor' via sensing the fluidity of the *P. syringae* membrane. According to GC analysis of FAME extracted from whole cells or from phospholipid fractions, *P. syringae* membranes exhibit the classical type of thermoadaptation by increasing the content of unsaturated fatty acids at the expense of saturated ones at 18°C. Another characteristics of thermoadaptation in *P. syringae* is the occurrence of a cyclo fatty acid at 28°C. In order to maintain a correct physical state of the membrane, which is required for optimal membrane structure and function, the main gel-to-liquid phase transition temperature of lipids in biological membranes must be below the environmental temperature (Annous *et al*., 1997). In such a way lipids are maintained in the fluid, liquid-to-crystalline state. As the growth temperature decreases, lower-melting-point unsaturated fatty acids are incorporated into lipids, which have a lower phase transition temperature. Another function of unsaturated fatty acids is believed to be the disruption of the ordered acyl chain packing to ensure fluidity of the biological membrane (Cronan *et al*., 1987). In contrast, when the growth temperature increases, high-melting-point saturated fatty acids are incorporated into lipids and in addition, *cis*-unsaturated fatty acids are converted by a putative cyclo fatty acid synthase into cyclo fatty acids which reduce the effects of temperature on membrane fluidity and restrict the propagation of motion from one end of the acyl chain to the other (Grogan & Cronan, 1997).
Changes which affect the fluidity of the membrane might have an impact on the topology and function of the membrane-associated protein CorS. To test this, we aimed to artificially simulate the physical state of a '18°C-membrane' in cells grown at 28°C, by external addition of unsaturated fatty acids. When PG4190 cultures were fed with unsaturated fatty acids, *cis* (18:1ω9 and 16:1ω7), at 28°C, the conversion of naturally occurring *cis*-16:1ω7 fatty acid to its *trans* isomer was observed in the extracted FAME. Obviously, addition of 18:1ω9 and 16:1ω7 resulted in an artificial increase of fluidity, and to reduce the membrane fluidity to non-lethal levels, bacteria might have used the mechanism of isomerization of the naturally present *cis*-16:1ω7 fatty acid. This might be due to the fact that phospholipids containing a *trans* instead of a *cis* unsaturated fatty acid exhibit increases in the phase transition temperature (Okuyama *et al*., 1990). In addition, the longer, extended steric structure of the *trans* configuration of such an unsaturated fatty acid is able to insert itself into the membrane

at a rate similar to the incorporation rate of saturated fatty acids, which are mostly in their all-*trans* configurations (Heipieper *et al*., 1992). *cis-trans* isomerization was reported in *Pseudomonas putida* to be an adaptive response in the presence of toxic compounds such as phenols (Heipieper *et al*., 1992, 1994). Occurrence of *trans* unsaturated fatty acids was reported for a phychrophilic bacterium, *Vibrio* sp. and was required for adaptation to growth at elevated temperatures (Okuyama *et al*., 1990). Isomerization of *cis*-16:1ω7 in *P. syringae* coincided with a dramatic decrease in the production of the 17:0 cyclo fatty acid at 28°C since the content of the *cis*-unsaturated fatty acid, which is a substrate for the cyclo fatty acid synthase, decreased as well. Because of this isomerization phenomenon, all attempts to alter membrane fluidity by addition of unsaturated fatty acids, in order to simulate 18°C-conditions for 28°C-growing cells, failed. The addition of these particular unsaturated fatty acids did not affect the *cmaABT* promoter activity and thus might not have affected CorS activity in *P. syringae*.

The membrane fluidity can also be modulated by addition of higher alcohols such as benzyl alcohol which are known as membrane-perturbing agents (Konopásek *et al*., 2000). Addition of 10 mM benzyl alcohol to cells of PG4180 (pRGMU1) prior to a temperature shift from 28°C to 18°C had a dramatic effect on the *cmaABT* promoter activity. Following the temperature down-shift GUS activity of the benzyl alcohol treated culture at 18°C remained at levels comparable to those observed at 28°C, whereas GUS activity of the untreated control culture reached the expected 18°C-values. Although the bacterial growth was slightly inhibited upon addition of benzyl alcohol, cells grew well and accumulated proteins. Since GUS activities were normalized to the protein concentration, the effects on growth can be neglected. Previously, it had been proposed that benzyl alcohol could induce membrane perturbation in a manner analogous to that of heat shock (Vígh *et al*., 1998). Taking this into account, we suggested that the fluidizing effect of benzyl alcohol on *P. syringae* membranes led to simulation of 28°C-conditions for cells growing at 18°C. Possibly, this physical state of the membrane had an impact on the topology and/or activity of CorS which then was not able to respond to a temperature change.

6.5 Structural and functional similarities of CorS with other HPKs

The conversion of saturated to *cis*-unsaturated fatty acids at low temperatures is mediated by the enhanced expression of genes coding for acyl-lipid desaturases (Macartney *et al*., 1994). Since the expression of such desaturases might depend on two-component regulatory systems,

it is tempting to speculate that HPKs exist which sense temperature changes and therefore are required for desaturase expression. Recently, an extensive mutagenesis of putative genes coding for HPKs in the genome of the cyanobacterium *Synechocystis* sp PCC 6803 was carried out (Suzuki *et al*., 2000). It showed that a membrane-associated HPK, Hik33, and a soluble HPK, Hik19, were involved in the signal perception and transduction of a low-temperature signal that regulates the induction of genes coding for ω3 and Δ6 acyl-lipid desaturase and RNA helicase. The authors assumed that temperature-induced changes in the membrane fluidity might be mediated by the membrane-bound HPK Hik33. Thus, Hik33 might be another example for a 'temperature sensor' in bacterial systems. Subsequent analysis of desaturase and global gene expression in a Hik33$^-$ mutant using DNA arrays revealed that Hik33 regulated the expression of some cold-inducible genes in *Synechocystis*, and a Hik33-independent group of cold-inducible genes is regulated by an as yet unidentified additional cold sensor (Suzuki *et al*., 2001).

Does CorS respond to a temperature change in a similar way as Hik33 does? Comparison of the primary structures and membrane topology predictions of both kinases revealed that they are significantly different from each other. The HPK Hik33 showed only 23% similarity to CorS over the entire amino acid sequence. Hik33 has two hydrophobic helices that might span the membrane, and a long periplasmic loop which is typical for HPKs that bind extracellular signal substrates (**Fig. 43**). **Pfam** structural analysis of Hik33 revealed that it additionally has a PAS domain which might sense change in the redox potential of the membrane (**Fig. 43**). In contrast, CorS has six TMDs with very short periplasmic loops. CorS does not possess a PAS domain. This indicates that CorS probably senses neither oxygen nor the redox potential of the membrane. This assumption was confirmed by experimental data when effects of the growth rate on COR synthesis and on *cmaABT* promoter activity were estimated. Since there was an optimum in the growth rate below and above which *cmaABT* promoter activity and COR production were inhibited, oxygen might not exhibit a direct regulatory effect on the CorRSP system. Experiments with temperature shifts from 28°C to 18°C demonstrated that temperature-inducible *cmaABT* expression was not a rapid process and was not cold-shock dependent in *P. syringae*. Upon the temperature shift and following a lag phase, the *cmaABT* promoter activity increased steadily and reached 18°C-values within a couple of hours. However, in order to maintain the membrane fluidity, the expression of desaturase genes should be induced shortly after the temperature change. In *Synechocystis* the relative level of mRNA of the *desA* gene encoding a Δ12-desaturase increased within 30-60 min after a temperature shift from 36°C to 22°C (Vígh *et al*., 1998). Thus, the expression of desaturase

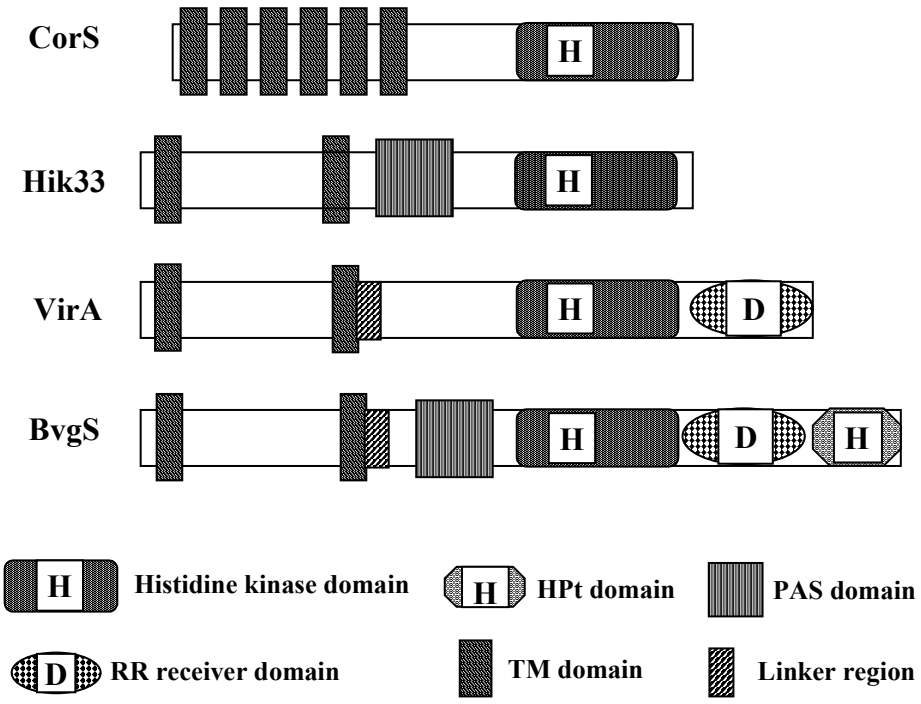

Fig.43. Schematic representation of structures of histidine protein kinases which respond to a temperature change.

genes is rapid and cold-shock inducible. In order to regulate the expression of the genes coding for ω3 and Δ6 desaturase, Hik33 must respond rapidly to a temperature change. Obviously, in comparison to Hik33 CorS might be a 'slow temperature sensor'. Whether this significant difference is due to indirect effects or general differences in the desaturases of *Synechosystis* and *P. syringae* remains an open question. In this respect, it is important to realize that homologies for membrane-bound desaturases of *Synechosystis* have not been identified in gram-negative bacteria such as *E. coli* and *P. syringae*. Therefore, the adaptive processes during cold acclimation might differ between cyanobacteria and bacteria such as *P. syringae*.

Other examples for HPKs which may respond to temperature changes are BvgS from *Bordetella pertussis*, and VirA from *Agrobacterium tumefaciens* which are involved in the regulation of virulence gene expression. However, both HPKs are distantly related to CorS with respect to their structures. BvgS and VirA are complex proteins containing multiple domains involved in signaling (Miller *et al*., 1992; Uhl & Miller, 1996; Chang & Winans, 1992). Both proteins have only two transmembrane helices separated by a large periplasmic domain. The respective N-terminal periplasmic domains are linked by the second transmembrane-spanning helix to the C-terminal cytoplasmic linker region, the transmitter,

and the receiver domains (**Fig. 43**). BvgS also has a PAS and a HPt domain (**Fig. 43**). This complexity mediates sensing diverse environmental signals. BvgS responds to environmental signals such as sulfate, nicotinate, and temperature (Melton & Weiss, 1989; Manetti *et al*., 1994). VirA of *A. tumefaciens* responds primary to phenolic compounds such as acetosyringone (AS) and hydroxy-AS produced by wounded plants (Toyoda-Yamamoto *et al*., 2000). It also responds to certain amounts of glucose, to a monosaccharide that potentiates the induction by AS (Cangelosi *et al*., 1990; Peng *et al*., 1998), as well as to pH and temperature (Chang & Winans, 1992; Jin *et al*., 1993). For both, BvgS and VirA, the actual temperature sensing mechanism has not been resolved yet. In contrast to these HPKs, only one environmental signal, temperature, has been demonstrated to control activity of CorS.
In summary, it is possible to assume that the temperature sensing mechanism may be different from one system to the other. This assumption argues for the hypothesis that CorS and its N-terminally structural homologs such as DivJ of *Caulobacter crescentus*, VsrB of *Ralstonia solanacearum*, and a *Pseudomonas stutzeri* HPK (**Fig. 4**) might all respond to changes in the physical state or the fluidity of the bacterial membrane. These changes might be induced by a variety of environmental signals such as temperature.

6.6 Potential role of the membrane-spanning domains for CorS function

Plasmids containing deletions of the DNA regions encoding the last four or all TMDs in *corS* did not complement the *corR*$^-$ *corS*$^-$ mutant PG4180.D4. Possibly, the mutant CorS proteins exhibited a constitutively negative phenotype. Thus, deletion analysis of CorS indicated that the TMDs are important for either the signal perception or for the overall structure of CorS. Essentially, this kind of deletion could also lead to a constitutively positive phenotype as it was the case when the N-terminal receiver domain of the bifunctional HPK for nitrogen regulation, NtrB, was deleted (Kramer & Weiss, 1999). However, since the function and structure of both, NtrB and CorS, are very different, deletions of the N-terminal receiver domain might have divergent effects on the enzyme functions. Our data indicated that deletion of a given N-terminus of an HPK can influence the overall function or structure of this type of enzyme. Additional deletions of distinct TMDs might indicate the role for each of those in the activity of CorS.
To generate mutant proteins of CorS with a constitutively positive phenotype, the method of pentapeptide mutagenesis was used. 28 mutants of CorS with a random 15-bp insertion all showed a negative phenotype in the complementation analysis with mutant PG4180.D4.

However, the results of the mutagenesis approach are not conclusive and it will be necessary to screen more mutants and to analyze these 28 mutants in more detail. It could also be assumed that any insertions in any of the TMDs of CorS might disrupt the stabilizing effects of van-der-Waals interactions on the tertiary and quaternary structure of CorS and therefore lead to a non-functional protein. This is the first time the pentapeptide mutagenesis approach was applied to a membrane protein. Previously, this approach was used successfully for mutational analysis of the *P. syringae hrpA* gene encoding a Hrp pilus subunit (Taira *et al*., 1999). In general, there are no examples for random mutagenesis of transmembrane regions of HPKs to compare our results with previous ones. Site-directed mutagenesis was used to analyze the role of the negatively charged glutamate residues within putative membrane-spanning domains of the HPK VirS from *Clostridium perfringens* (Cheung & Rood, 2000). Changes of these glutamates to alanine, aspartate or glutamine resulted in non-functional VirS proteins. It was suggested that these mutations interfered with the ability of VirS to undergo a conformational change in the transmembrane domain that is required for signal transfer between the N-terminal receiver domain of VirS and the C-terminal kinase domain.

6.7 Topological membrane organization of CorS

Obviously, the conformational and topological information about the membrane association of CorS revealed in this study will be helpful to determine protein segments that might play a role in the signal perception. It is well established that the distribution of positively charged residues in the regions flanking hydrophobic TMDs is the most important determinant for the membrane topology of a given HPK. Strong support for this has come from protein engineering experiments which demonstrated that the membrane topology can be changed dramatically by moving positively charged residues from cytoplasmic to extra-cytoplasmic regions of the protein (Monne *et al*., 1998; Rutz *et al*., 1999). The prediction of the protein's membrane structure is based on combining a hydrophobicity analysis with a subsequent charge-bias analysis that ranks all possible structures on the basis of their conformity with the so-called positive-inside rule (von Heijne, 1992). The topological analysis of CorS with two topology prediction programs indicated that six TMDs presumably span the membrane and that the N-and C-termini of the protein are located in the cytoplasm. Uncertain topological information was derived by this analysis for a putative sixth TMD showing a relatively low hydropathy index and a putative seventh TMD predicted to be in the conserved histidine kinase domain. An experimental approach based on the generation of translational fusions

between C-terminally truncated CorS portions and either PhoA or LacZ was used to establish the topological assignments of all TMDs. The activities of hybrid fusion proteins were determined in qualitative and quantitative assays. Their expression levels in *P. syringae* were furthermore analyzed by immunoblotting. High activities of PhoA fusions at amino acid residues Ala_{51}, Leu_{125} and Val_{177} indicated their periplasmic location. LacZ fusions at these residues showed the expected lack of activity for Ala_{51} and Leu_{125}, whereas an elevated LacZ activity level was observed for the fusion at residue Val_{177}. According to the previous topological studies of various membrane proteins, it was known that LacZ is a less reliable reporter enzyme than PhoA (Hennesssey & Broome-Smith, 1993; Bartsevich & Pakrasi, 1999). It was suggested that ß-galactosidase fused to periplasmic domains sometimes exhibits high activity because of disruption of the membrane integration of the fusion protein by this large-sized reporter enzyme (Hennesssey & Broome-Smith, 1993). In contrast, a PhoA fusion requires active translocation of the reporter enzyme moiety through the cytoplasmic membrane for activity. Since the PhoA fusion at Val_{177} showed high specific activity in a quantitative assay, and in addition, the Western blot analysis and protease sensitivity assay clearly demonstrated its periplasmic location, we concluded that this site was indeed periplasmic. Absence of PhoA activities and presence of LacZ activities for fusions at amino acid residues Thr_{27}, Tyr_{85}, and Leu_{151} indicated their cytoplasmic location and in addition, showed that N-and-C-termini of CorS were located in the cytoplasm. Western blot analysis for PhoA fusions demonstrated some instability of most of the hybrid proteins. In most cases the bands for cytoplasmic hybrid proteins showed weaker signals than the bands of periplasmic hybrid proteins. This result is probably attributable to a proteolytic degradation of the hybrid proteins as reported earlier (Haardt & Bremer, 1996; Guan *et al*., 1999; Ouchane & Kaplan, 1999). Our experimental data confirmed the predicted topology of CorS with six TMDs and cytoplasmic locations for the N- and C-terminus. However, since two PhoA fusions at amino acid residues Arg_{204} and Asp_{227} showed a temperature-dependent phenotype on MG-indicator plates, we assume that the CorS topology might be thermoresponsive in this particular protein region. Colonies harboring PhoA fusions at Arg_{204} and Asp_{227} showed a $PhoA^+$ phenotype at 28°C, whereas a $PhoA^-$ phenotype was observed for both fusions at 18°C. This indicates that the sixth TMD of CorS might be translocated into the periplasm at 28°C. Thus, the putative seventh TMD which represents the histidine kinase domain might be embedded into the membrane at this temperature (**Fig. 44**). The PhoA fusions at Leu_{249} and Gln_{281} located in close proximity upstream and downstream of the histidine kinase domain, respectively, both showed a $PhoA^-$ phenotype indicating their clearly cytoplasmic location. As

yet, it has been impossible to confirm the temperature-sensitive phenotype of those fusions in a quantitative assay. To complicate things, the PhoA phenotypes are generally medium-dependent. There was no difference in PhoA phenotypes between cytoplasmic and periplasmic fusions in minimal IM liquid and agar medium. This difference was well pronounced on minimal MG medium agar plates. However, minimal HSC medium optimized for COR production was used for bacterial growth in liquid culture because *P. syringae* does not grow well in MG liquid medium. In HSC medium, a quantitative difference between PhoA activities for fusions Arg_{204} and Asp_{227} was not possible. Both fusions showed a constitutively negative phenotype in this medium. The reason for this remains obscure. Complex KB medium was the best medium to differentiate periplasmic and cytoplasmic fusions in liquid culture as well as on agar plates. However, there is no detectable COR production by *P. syringae* in KB medium. In this study, experiments with temperature shifts from 28°C to 18°C demonstrated that temperature-inducible *cmaABT* expression was completely abolished for cells grown in KB medium. Thus, this medium can not be used in order to study temperature-dependent phenomena mediated by CorS.

Topological information derived from computer predictions and experimental data, which argued for a change in the topology of membrane proteins, was reported previously. Different approaches were used to analyze the topology of the mammalian multidrug transporters, P-glycoproteins (Germann & Chambers, 1998). However, for this system conflicting data have been reported on the number of TMDs, and on the orientation of a subset of TMDs and their connecting loops relative to the plasma membrane. Zhang *et al*. (1996) speculated that alternative topological forms of P-glycoprotein may be expressed in different cell types and that different topological forms of P-glycoprotein may exhibit different biological functions. The same hypothesis was proposed in a study of the membrane topology of the lactococcal bacteriocin ABC transporter LcnC (Franke *et al*., 1999). Such topological alteration is thought to mediate the bacteriocin secretion process. Computer analysis of the membrane-localized redox-responsive sensor kinase PrrB from *Rhodobacter sphaeroides* showed that it has six TMDs, and the C-terminus contains a seventh TMD located in proximity to the conserved histidine residue which is the site of autophosphorylation (Ouchane & Kaplan, 1999). PhoA fusion analyses supported a cytoplasmic C-terminal location of PrrB. The authors speculated that the putative seventh TMD could serve to interact with other proteins. Unfortunately, the PrrB linker region between the last TMD and the conserved histidine residue was not analyzed by a reporter gene fusions approach. In the case of CorS, the thermoresponsive PhoA fusions were located in this linker region. Moreover, this linker region showed the best

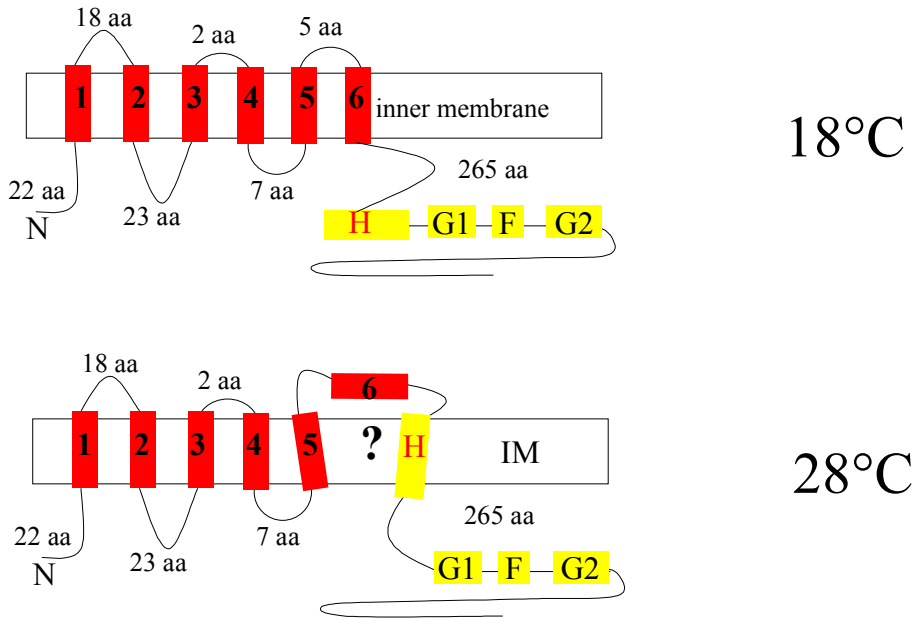

Fig. 44. Model for the topological organization of CorS at 18°C and 28°C. It shows a topological change of CorS resulting in different abilities for CorS to be autophosphorylated at the conserved His^{254} residue with respect to temperature.

surface probability index using the PROTEAN program. This allows us to speculate that the linker region between the last TMD and the histidine kinase domain is involved in a temperature-dependent conformational change affecting autophosphorylation of the conserved histidine residue (**Fig. 44**). According to our hypothesis, at 18°C CorS might be fixed in the membrane with six TMDs. The linker region and the histidine kinase domain would be located in the cytoplasm. In such a case, the conserved His^{254} residue of CorS can be efficiently autophosphorylated and subsequently initiates the signal transduction pathway via phosphorylation of CorR. In contrast, at 28°C, due to the possible translocation of the sixth TMD and the linker region into the periplasm, the histidine kinase domain is embedded in the membrane, which makes the His^{254} residue inaccessible for autophosphorylation. This model is supported by our previous findings that there was no detectable COR production at 28°C and that the CorS-dependent RR CorR was inactive in DNA-binding assays when it was overproduced at 28°C in *P. syringae* (Wang *et al*., 1999).

Generally, conformational changes of proteins require an energy input. The energy required for a conformational change of CorS may be released when temperature increases from 18°C to 28°C. More importantly, the fatty acid composition of the membrane might directly or

indirectly influence this conformational change. Thus, the proposed model may explain the temperature signal perception mediated by CorS. It may also shed light on how CorS senses the fluidity of the bacterial membrane.

6.8 Outlook

To elucidate whether the proposed model indeed explains a mechanism of signal perception by CorS, it is necessary to generate additional fusions in the linker region between the last TMD and the conserved histidine kinase domain. It is also imperative to confirm the temperature-dependent phenotypes of the respective PhoA fusions in the linker region by a quantitative assay. If the proposed model really applies, increases of the hydrophobicity of the 6^{th} TMD by site-directed mutagenesis would generate a temperature-insensitive constitutive derivative of CorS. In this respect, screening of more entranceposon mutants of CorS would also lead to the detection of temperature-insensitive derivatives of CorS and would help to identify which particular amino acids or segments of CorS are involved in signal perception by CorS. Finally, specific protease accessibility experiments could prove the proposed model. Ultimately, future experiments will lead to the complete understanding of the temperature sensing process in *P. syringae*.

7 REFERENCES

Alarcón-Chaidez, F.J., Peñaloza-Vázquez, A., Ullrich, M., & Bender, C.L. (1999). Characterization of plasmids encoding the phytotoxin coronatine in *Pseudomonas syringae. Plasmid* **42**: 210-220.

Alexeyev, M.F., & Winkler, H.H. (1999). Membrane topology of the *Rickettsia prowazekii* ATP/ADP translocase revealed by novel dual *pho-lac* reporters. *J. Mol. Biol*. **285**: 1503-1513.

Anderson, J., Forst, S.A., Zhao, K., Inouye, M., & Delihas, N. (1989). The function of *micF* RNA. *J. Biol. Chem.* **264**: 17961-17970.

Annous, B.A., Becker, L.A., Bayles, D.O., Labeda, D.P., & Wilkinson, B.J. (1997). Critical role of anteiso-$C_{15:0}$ fatty acid in the growth of *Listeria monocytogenes* at low temperatures. *App. Environ. Microbiol.* **63**(10): 3887-3894.

Banta, L.M., Bohne, J., Lovejoy, S.D., & Dostal, K. (1998). Stability of the *Agrobacterium tumefaciens* VirB10 protein is modulated by growth temperature. *J. Bacteriol.* **180**(24): 6597-6606.

Bartsevich, V.V., & Pakrasi, H.B. (1999). Membrane topology of MntB, the transmebrane protein component of an ABC transporter system for manganese in the cyanobacterium *Synechocystis* sp. strain PCC 6803. *J. Bacteriol.* **181**(11): 3591-3593.

Barzic, M.R. (1999). Persicomycin production by strains of *Pseudomonas syringae* pv. persicae. *Physiol. Mol. Plant. Pathol.* **55**(4): 243-250.

Bender, C.L. (1999). Chlorosis-inducing phytotoxins produced by *Pseudomonas syringae. Eur. J. Plant Pathol.* **105**: 1-12.

Bender, C.L., Alarcón-Chaidez, F., & Gross, D.C. (1999). *Pseudomonas syringae* phytotoxis: mode of action, regulation, and biosynthesis by peptide and polyketide sythetases. *Micrbiol. Mol. Biol. Rev.* **63**(2): 266-292.

Bender, C.L., & Cooksey, D.A. (1986). Indigenous plasmids in *P. syringae* pv. tomato: Conjugative transfer and role in copper resistance. *J. Bacteriol.* **165**: 534-541.

Bender, C.L., Young, S.A., & Mitchell, R.E. (1991). Conservation of plasmid DNA sequences in coronatine-producing pathovars of *Pseudomonas syringae. Appl. Environ. Microbiol.* **57**(4): 993-999.

Bender, C.L., Palmer, D., Peñaloza-Vázquez, A., Rangaswamy, V., & Ullrich, M. (1996). Biosynthesis of coronatine, a thermoregulated phytoxin produced by the phytopathogen *Pseudomonas syringae*. *Arch. Microbiol*. **166**: 71-75.

Berlutti, F., Casalino, M., Zagaglia, C., Fradiani, P.A., Visca, P., & Nicoletti, M. (1998). Expression of the virulence plasmid-carried apyrase gene (*apy*) of enteroinvasive *Escherichia coli* and *Shigella flexneri* is under the control of H-NS and the *virF* and *virB* regulatory cascade. *Infect. Immun.* **66**(10):4957-4964.

Bilwes, A.M., Alex, L.A., Crane, B.R., & Simon, M.I. (1999). Structure of CheA, a signal-transducing histidine kinase. *Cell* **96**: 131-141.

Bjellqvist, B., Ek, K., Righetti, P.G., Gianazza, E., Görg, A., Westermeir, R., & Postel, W. (1982). Isoelectric focusing in immobilised pH gradients: Principle, methodology and some applications. *J. Biochem. Biophys. Methods* **6**: 317-339.

Blake, M.S., Johnston, K.H., Russel-Jones, G.J., & Gotschlich, E.C. (1984). A rapid, sensitive method for detection of alkaline phosphatase-conjugated antibody on Western blots. *Anal. Biochem*. **136**: 175-179.

Bott, M. (1997). Anaerobic citrate metabolism and its regulation in enterobacteria. *Arch. Microbiol*. **167**: 78-88.

Boyd, D., Manoil, C., & Beckwith, J. (1987). Determinants of membrane protein topology. *Proc. Natl. Acad. Sci. USA* **84**: 8525-8529.

Bradford, M.M. (1976). A rapid and sensitive method for the quantitation of microgram quantities of protein utilizing the principle of protein dye binding. *Analyt. Biochem*. **72**: 248-254.

Budde, I.P., Rohde, B.H., Bender, C., & Ullrich, M.S. (1998). Growth phase and temperature influence promoter activity, transcript abundance, and protein stability during biosynthesis of the *Pseudomonas syringae* phytotoxin coronatine. *J. Bacteriol.* **180**(6): 1360-1367.

Cangelosi, G.A., Ankenbauer, R.G., & Nester, E.W. (1990). Sugars induce the *Agrobacterium* virulence through a periplasmic binding protein and a transmembrane signal protein. *Proc. Natl. Acad. Sci. USA* **87**: 6708-6712.

Castelli, M.E., Garcia, V.E., & Fernando, S.C. (2000). The phosphatase activity is a the target for Mg^{2+} regulation of the sensor protein PhoQ in *Salmonella*. *J. Biol. Chem*. **175**(30): 22948-22954.

Chang, C-H., & Winans, S.C. (1992). Functional roles assigned to the periplasmic, linker and receiver domains of the *Agrobacterium tumefaciens* VirA protein. *J. Bacteriol.* **174**: 7033-7039.

Cheung, J.K., & Rood, J.I. (2000). Glutamate residues in the putative transmembrane region are required for the function of the VirS sensor histidine kinase from *Clostridium perfringens*. *Microbiology* **146**: 517-525.

Collmer, A., Badel, J.L., Charkowski, A.O., Deng, W-L., Fouts, D.E., Ramos, A.R., Rehm, A.H., Anderson, D.M., Schneewind, O., van Dijk, K., & Alfano, J.R. (2000). *Pseudomonas syringae* Hrp type III secretion system and effector proteins. *Proc. Natl. Acad. Sci. USA* **97**(16): 8770-8777.

Craig, E.A., & Gross, C.A. (1991). Is hsp70 the cellular thermometer? *Trends Biochem. Sci.* **16**: 135-140.

Cronan. J.E., Jr., Gennis, R.B., & Maloy, S.R. (1987). The cytoplasmic membrane, p.31-35. *In* Neidhardt, F.C., Ingraham, J.L., Low, K.B., Magasanik, B., Schaechter, M., & Umbarger, H.E. (ed), *Eschrerichia coli* and *Salmonella typhimurium*: cellular and molecular biology, vol.1. American Society for Microbiology, Washington, D.C.

Dagert, M., & Ehrlich, S.D. (1979). Prolonged incubation in calcium chloride improves the competence of *E. coli* cells. *Gene* **6**: 23-28.

de Philip, P., Batut, J., & Boistard, P. (1990). *Rhizobium meliloti* FixL is an oxygen sensor and regulates *R. meliloti nifA* and *fixK* genes differently in *Eschrerichia coli*. *J. Bacteriol.* **174**: 1726-1733.

Diep, D.B., Håvarstein, L.S., Nissen-Meyer, J., & Nes, I.F. (1994). The gene encoding plantaricin A, a bacteriocin from *Lactobacillus plantarum* C11, is located on the same transcription unit as an *agr*-like regulatory system. *Appl. Environ. Microbiol*. **60**(1): 160-166.

Dutta, R., Qin, L., & Inouye, M. (1999). Histidine kinases: diversity of domain organization. *Mol. Microbiol*. **34**(4): 633-640.

Ethier, J., & Boyd, J.M. (2000). Topological analysis and role of the transmembrane domain in polar targeting of PilS, a *Pseudomonas aeruginosa* sensor kinase. *Mol. Microbiol*. **38**(4): 891-903.

Falconi, M., Colonna, B., Prosseda, G., Micheli, G., & Gualerzi, C.O. (1998). Thermoregulation of *Shigella* and *Escherichia coli* EIEC pathogenicity. A temperature-dependent structural transition of DNA modulates accessibility of *virF* promoter to transcriptional repressor H-NS. *EMBO J.* **17**(23): 7033-7043.

Figurski, D.H., & Helsinki, D.R. (1979). Replication of an origin-containing derivative of plasmid RK2 dependent on a plasmid function provided *in trans*. *Proc. Natl. Acad. Sci. USA* **76**(4): 1648-1659.

Folch, J., Less, M., & Stanly, G.M.S. (1957). A simple method for the isolation and purification of total lipids from animal tissues. *J. Biol. Chem*. **226**: 497-509.

Franke, C.M., Tiemersma, J., Venema, G., & Kok, J. (1999). Membrane topology of the lactococcal bacteriocin ATP-binding cassette transporter protein LcnC. *J. Biol. Chem*. **274**(13): 8584-8490.

Fukunaga, N., Sahara, T., & Takada, Y. (1999). Bacterial adaptation to low temperature: implications for cold-inducible genes. *J. Plant Res.* **112**(1106): 263-272.

Fullner, K.J., & Nester, E.W. (1996). Temperature affects the T-DNA transfer machinery of *Agrobacterium tumefaciens. J. Bacteriol.* **178**(6): 1498-1504.

Gamer, J., Multhaup, G., Tomoyasu, T., McCarty, J.S., Rädiger, S., Schönfeld, H.-J., *et al*. (1996). A cycle of binding and release of the DnaK, DnaJ and GrpE chaperones regulates activity of the *Escherichia coli* heat shock transcription factor σ^{32}. *EMBO J*. **15**: 607-617.

Garcia, V.E., Youhna, A.M., Enrico, Di C., & Groisman, E.A. (1997). Characterization of the bacterial sensor protein PhoQ: evidence for distinct binding sites for Mg^{2+} and Ca^{2+}. *J. Biol. Chem.* **272**(3): 1440-1443.

Gardan, K.H., Shafik, H., Belouin, S., Broch, R., Grimont, F., & Grimont, P.A.D. (1999). DNA relatedness among pathovars of *Pseudomonas syringae* and description of *Pseudomonas tremae* sp. nov. and *Pseudomonas cannabina* sp. nov. (ex Sutic & Dowson 1959). *Int. J. System. Bacteriol*. **49**: 469-478.

Germann, U.A., & Chambers, T. (1998). Molecular analysis of the mutidrug transporter, P-glycoprotein. *Cytotechnology* **27**: 31-60.

Gibbon, M.J., Sesma, A., Canal, A., Wood, J.R., Hidalgo, E., Brown, J., Vivian, A., & Murillo, J. (1999). Replication regions from plant-pathogenic *Pseudomonas syringae* plasmids are similar to ColE2-related replicons. *Microbiology* **145**: 325-334.

Golby, P., Davies, S., Kelly, D.J., Guest, J.R., & Andrews, S.C. (1999). Identification and characterization of a two-component regulatory sensor-kinase and response-regulator system (DcuSR) controlling gene expression in response to C_4-decarboxylates in *Escherichia coli. J. Bacteriol.*. **181**: 1238-1248.

Golby, P., Kelly, D.J., Guest, J.R., & Andrews, S.C. (1998). Transcriptional regulation and organization of the *dcuA* and *dcuB* genes, encoding homologous anaerobic C_4-dicarboxylate transporters in *Escherichia coli. J. Bacteriol.*. **180**: 6586-6596.

Göransson, M., Sonden, B., Nilsson, P., Dagberg, B., Forsman, K., Emanuelsson, K., & Uhlin B.E. (1990). Transcriptional silencing and thermoregulation of gene expression in *Escherichia coli. Nature* **344**: 682-685.

Görg, A., Postel, W., & Günther, S. (1988). The current state of two-dimensional electrophoresis with immobilized pH gradients. *Electrophoresis* **9**: 531-546.

Gramajo, H.C., White, J., Hutchinson, R., & Bibb, M.J. (1991). Overproduction and localization of components of the polyketide synthase of *Streptomyces glaucescens* involved in the production of the antibiotic tetracenomycin C. *J. Bacteriol.* **173**(20): 6475-6483.

Graumann, P., & Marahiel, M.A. (1996). Some like it cold - response of microorganisms to cold shock. *Arch. Microbiol*. **166**(5): 293-300.

Grogan, D.W., & Cronan, J.E., Jr. (1997). Cyclopropane ring formation in membrane lipids of bacteria. *Microbiol. Mol. Biol. Rev*. **61**: 429-441.

Guan, L., Ehrmann, M., Yoneyama, H., & Nakae, T. (1999). Membrane topology of the xenobiotic-exporting subunit, MexB, of the MexA,B-OprM extrusion pump in *Pseudomonas aeruginosa. J. Biol. Chem.* **274**(15): 10517-10522.

Guttierrez, C., & Devedjian, J.C. (1989). A plasmid facilitating *in vitro* construction of *phoA* gene fusions in *Escherichia coli*. *Nucleic Acids Res*. **17**(10): 3999.

Haake, D.A. (2000). Spirochaetael lipoproteins and pathogenesis. *Microbiol.* **146**: 1491-1504.

Haapa, S., Taira, S., Heikkinen, E., & Savilahti, H. (1999). An efficient and accurate integration of mini-Mu transposons *in vitro*: a general methodology for functional genetic analysis and molecular biology applications. *Nucleic Acids Res*. **27**(13): 2777-2784.

Haardt, M., & Bremer, E. (1996). Use of *phoA* and *lacZ* fusions to study the membrane topology of ProW, a component of the osmoregulated ProU transposrt bsystem of *Escherichia coli*. *J. Bacteriol.* **178**(18): 5370-5381.

Hantash, F.M., & Earhart, C.F. (2000). Membrane association of the *Escherichia coli* enterobactin synthase proteins EntB/G, EntE, and EntF. *J. Bacteriol.* **182**(6): 1768-1773.

Harlocker, S.L., Rampersaud, A., Yang, W., & Inouye, M. (1993). Phenotypic revertant mutations of a new *ompR2* mutant (V203Q) of *Escherichia coli* lie in *envZ* gene, which encodes the OmpR kinase. *J. Bacteriol.* **175**: 1956-1960.

Heipieper, H-J., Diefenbach, R., & Keweloh, H. (1992). Conversion of *cis* unsaturated fatty acids to *trans*, a possible mechanism for the protection of phenol-degrading

Pseudomonas putida P8 from substrate toxicity. *Appl. Environ. Microbiol*. **58**(6): 1847-1852.

Heipieper, H-J., & de Bont, J.A.M. (1994). Adaptation of *Pseudomonas putida* S12 to ethanol and toluene at the level of fatty acid composition of membranes. *Appl. Environ. Microbiol.* **60**(12): 4440-4444.

Hellingwerf, K.J., Crielaard, W.C., de Mattos, M.J.T., Hoff, W.D., Kort, R., Verhamme, D.T., & Avignone-Rossa, C. (1998). Current topics in signal transduction in bacteria. *Antonie von Leeuwenhoek* **74**: 211-227.

Hendrickson, E.L., Guevera, P., Peñaloza-Vázquez, A., Shao, J., Bender, C.L., & Ausubel, F.M. (2000). Virulence of the phytopathogen *Pseudomonas syringae* pv. maculicola is *rpoN* dependent. *J. Bacteriol.* **182**: 3498-3507.

Hennessey, E.S., & Broome-Smith, J.K. (1993). Gene-fusion techniques for determining membrane-protein topology. *Curr. Opin. Struct. Biol*. **3**: 524-531.

Hettwer, U., Jaeckel, F.R., Boch, J., Meyer, M., Rudolph, K., & Ullrich, M.S. (1998). Cloning, nucletide sequence, and expression in *Escherichia coli* of levansucrase genes from the plant pathogens *Pseudomonas syringae* pv. glycinea and *P. syringae* pv. phaseolicola. *Appl. Environ. Microbiol.* **64**(9): 3180-3187.

Hoch, J.A. (2000). Two-component and phosphorelay signal transduction. *Curr. Opin. Microbiol*. **3**: 165-170.

Hoe, N.P., & Goguen, J.D. (1993). Temperature sensing in *Yersinia pestis*: translation of the LcrF activator protein is thermally regulated. *J. Bacteriol.* **175**: 7901-7909.

Horváth, I., Glatz, A., Varvasovszki, V., Török, Z., Páli, T., Balogh, G., Kovács, E., Nádasdi, L., Benkö, S., Joó, F., & Vígh, L. (1998). Membrane physical state controls the signaling mechanism of the heat shock response in *Synechocystis* PCC 6803: Identification of *hsp17* as a "fluidity gene". *Proc. Natl. Acad. Sci. USA* **95**: 3513-3518.

Hrabak, E.M., & Willis, D.K. (1992). The *lemA* gene required for pathogenicity of *Pseudomonas syringae* pv. syringae on bean is a member of a family of two-component regulators. *J.Bacteriol*. **174**: 3011-3020.

Hsing, W., Russo, F.D., Bernd, K.K., & Silhavy, T. (1998). Mutations that alter the kinase and phosphatase activities of two-component sensor EnvZ. *J. Bacteriol.* **180**(17): 4538-4546.

Huang, J., Denny, T.P., & Schell, M.A. (1993). VsrB, a regulator of virulence genes of *Pseudomonas solanacearum*, is homologous to sensors of the two-component regulatory family. *J. Bacteriol.* **175**(19): 6169-6178.

Hugouvieux-Cotte-Pattat, N., Dominguez, H., & Robert-Baudouy, J. (1992). Environmental conditions affect transcription of pectinase genes of *Erwinia chrysanthemi* 3937. *J. Bacteriol.* **174**(23): 7807-7818.

Hurme, R., Bernt, K.D., Normark, S.J., & Rhen, M. (1997). A proteinaceous gene regulatory thermometer in *Salmonella. Cell* **90**: 55-64.

Hurme, R., & Rhen, M. (1998). Temperature sensing in bacterial gene regulation – what it all boils down to. *Mol. Microbiol*. **30**(1): 1-6.

Hutchison, M.L, Tester, M.A., & Gross, D.C. (1995). Role of biosurfactant and ion channel-forming activities of syringomycin in transmembrane ion flux: A model for the mechanism of action in the plant-pathogen interaction. *Mol. Plant-Microbe Interact*. **8**: 610-620.

Huynh, T.V., Dahlbeck, D., & Staskawicz, B.J. (1989). Bacterial blight of soybean: regulation of a pathogen gene determining host cultivar specificity. *Science* **245**: 1374-1377.

Jackson, A.P., & Maxwell, A. (1993). Identifying the catalytic residue of the ATPase reaction of DNA gyrase. *Proc. Natl. Acad. Sci. USA* **90**: 11232-11236.

Jefferson, R.A., Burgess, S.M., & Hirsh, D. (1986). ß-Glucuronidase from *Eschrerichia coli* as a gene fusion marker. *Proc. Natl. Acad. Sci. USA* **86**: 8447-8451.

Jiang, P., Atkinson, M.R., Srisawat, C., Sun, Q., & Ninfa, A.J. (2000). Functional dissection of the dimerization and enzymatic activities of *Eschrerichia coli* nitrogen regulator II and their regulation by the PII protein. *Biochemistry* **39**: 13433-13449.

Jin, A.J., Edidin M., Nossal, R., & Gershfeld, N. L. (1999). A singular state of membrane lipids at cell growth temperatures. *Biochemistry* **38**: 13275-13278.

Jin, S., Song, Y-N., Deng, W-Y., Gordon, M.P., & Nester, E.W. (1993). The regulatory VirA protein of *Agrobacterium tumefaciens* does not function at elevated temperatures. *J. Bacteriol.* **175**(21): 6830-6835.

Jourlin, C., Bengrine, A., Chippaux, M., & Mejean, V. (1996). An unorthodox sensor protein (TorS) mediates the induction of the *tor* structural genes in response to trimethylamine N-oxide in *Eschrerichia coli. Mol. Microbiol.* **20**(6): 1297-1306.

Jung, K., & Altendorf, K. (1998). Truncation of amino acids 12-128 causes deregulation of the phospatase activity of the sensor kinase KdpD of *Escherichia coli*. *J. Biol. Chem.* **273**: 17406-17410.

Kado, C.I., & Liu, S.T. (1981). Rapid procedure for detection and isolation of large and small plasmids. *J. Bacteriol.* **145**(3): 1365-1373.

Kaspar, S., Perozzo, R., Reinelt, S., Meyer, M., Pfister, K., Scapozza, L., & Bott, M. (1999). The periplasmic domain of the histidine autokinase CitA functions as a highly specific citrate receptor. *Mol. Microbiol*. **33**(4): 858-872.

Katz, L., & Donadio, S. (1993). Polyketide synthesis: prospects for hybrid antibiotics. *Annu. Rev. Microbiol*.**47**: 875-912.

Keane, P.J., Kerr, A., & New, P.B. (1970). Grown gall of stone fruit. II. Identification and nomenclature of *Agrobacterium* isolates. *Aust. J. Biol. Sci*. **23**: 585-595.

Keen, N.T., Tamaki, S., Kobayashi, D., & Trollinger, D. (1988). Improved broad-host-range plasmid for DNA cloning in gram-negative bacteria. *Gene* **70**: 191-197.

King, E.O., Ward, M.K., & Raney, D.E. (1954). Two simple media for the demonstration of pyocyanin and fluorescein. *J. Lab. Clin. Med*. **44**: 301-307.

Kleinkauf, H., & von Döhren, H. (1996). A non-ribosomal system of peptide biosynthesis. *Eur. J. Biochem.* **236**: 335-351.

Knapp, S., & Mekalanos, J.J. (1988). Two *trans*-acting regulatory genes (*vir* and *mod*) control antigenic modulation in *Bordetella pertussis. J. Bacteriol.* **170**: 5059-5066.

Konopásek, I., Strzalka, K., & Svobodova, J. (2000). Cold shock response in *Bacillus subtilis*: different effects of benzyl alcohol and ethanol on the membrane organization and cell adaptation. *Biochim. Biophys. Acta* **1464**: 18-26.

Kovach, M.E., Phillips, R.W., Elzer, P.H., Roop, R.M., 2nd, & Peterson, K.M. (1994). pBBR1MCS: a broad-host-range cloning vector. *Biotechniques* **16**(5): 800-802.

Kramer, G., & Weiss, V. (1999). Functional dissection of the transmitter module of the histidine kinase NtrB in *Escherichia coli. Proc. Natl. Acad. Sci. USA* **96**: 604-609.

Kropinski, A.M.B., Lewis, V., & Berry, D. (1987). Effect of growth temperature on the lipids, outer membrane proteins, and lipopolysaccharides of *Pseudomonas aeruginosa* PAO. *J. Bacteriol.* **169**: 1960-1966.

Kyte, J., & Doolittle, R.F. (1982). A simple method for displaying the hydropathic character of a protein. *J. Mol. Biol*. **157**: 105-132.

Laemmli, U.K. (1970). Cleavage of structural proteins during assembly of the head of bacteriophage T4. *Nature* **227**: 680-685.

Lai, E-M., & Kado, C.I. (1998). Processed VirB2 is the major of the promiscuous pilus of *Agrobacterium tumefaciens*. *J. Bacteriol.* **180**(10): 2711-2717.

Lanham, P.G., McIlravey, K.I., & Perombelon, M.C. (1991). Production of the cell wall dissolving enzymes by *Erwinia carotovora* subsp. atroseptica *in vitro* at 27°C and 30,5°C. *J. Appl. Bacteriol.* **70**: 20-24.

Lee, A.I., Delgado, A., & Gunsalus, R.P. (1999). Signal-dependent phosphorylation of the membrane-bound NarX two-component sensor-transmitter protein of *Escherichia coli. J. Bacteriol.* **181**(17): 5309-5316.

Lei, S.P., Lin, H.C., Heffernan, L., & Wilcox, G. (1985). Cloning of the pectate lyase genes from *Erwinia carotovora* and their expression in *Escherichia coli. Gene* **35**(1-2): 63-70.

Levit, M.N., Liu, Y., & Stock, J.B. (1998). Stimulus response coupling in bacterial chemotaxis: receptor dimers in signalling arrays. *Mol. Microbiol*. **30**(3): 459-466.

Li, H., & Ullrich, M.S. (2001). Characterization and mutational analysis of three alleic *lsc* genes encoding levansucrase in *Pseudomonas syringae. J. Bacteriol.* **183**(11): 3282-3292.

Liyanage, H., Penfold, C., Turner, J., & Bender, C.L. (1995a). Sequence, expression and transcriptional analysis of the coronafacate ligase-encoding gene required for coronatine biosynthesis by *Pseudomonas syringae*. *Gene* **153**: 17-23.

Liyanage, H., Palmer, D.A., Ullrich, M., & Bender, C.L. (1995b). Characterization and transcriptional analysis of the gene cluster for coronafacic acid, the polyketide component of the phytotoxin coronatine. *Appl. Environ. Microbiol*. **61**: 3843-3848.

Macartney, A., Maresca, B., & Cossins, A.R. (1994). Acyl-CoA desaturases and the adaptive regulation of membrane lipid composition, p. 129-139. *In* Cossins, A.R. (ed), Temperature adaptation of biological membranes. Portland Press, London.

Mandel, M., & Higa, A. (1970). Calcium dependent bacteriophage DNA infection. *J. Mol. Biol*. **53**: 154-162.

Manetti, R., Aricò, B., Rappuoli, R., & Scarlato, V. (1994). Mutations in the linker region of BvgS abolish response to environmental signals for the regulation of the virulence factors in *Bordetella pertussis. Gene* **150**: 123-127.

Manoil, C., & Beckwith, J. (1986). A genetic approach to analyzing membrane protein topology. *Science* **233**: 1403-1408.

Mekalanos, J.J. (1992). Environmental signals controlling expression of virulence determinants in bacteria. *J. Bacteriol.* **174**(1): 1-7.

Melton, A.R., & Weiss, A.A. (1989). Environmental regulation of expression of virulence determinants in *Bordetella pertussis. J. Bacteriol.* **171**: 6206-6512.

Meyers, J.A., Sanchez, D., Elwell, L.P., & Falkow, S. (1976). Simple agarose gel electrophoretic method for the identification and characterization of plasmid deoxyribonucleic acid. *J. Bacteriol.* **127**(3): 1529-1537.

Miller, J., Johnson, S.A., Black, W.J., Beattie, D.T., Mekalanos, J.J., & Falkow, S. (1992). Constitutive sensory transduction mutations in *Bordetella pertussis bvgS* gene. *J. Bacteriol.* **174**(3): 970-979.

Mitchell, R.E. (1982). Coronatine production by some phytopathogenic pseudomonads. *Physiol. Plant. Pathol*. **20**. 83-89.

Mitchell, R.E. (1985). Norcoronatine and N-coronafacoyl-L-valine, phytotoxin analogues of coronatine produced by a strain *Pseudomonas syringae* pv. glycinea. *Phytochemistry* **24**: 1485-1488.

Mitchell, R.E., & Bieleski, R.L. (1977). Involvement of phaseolotoxin in halo blight of beans. Transport and conversion to functional toxin. *Plant Physiol*. **60**: 723-729.

Mitchell, R.E., & Ford, K.L. (1998). Chlorosis-inducing products from *Pseudomonas syringae* pathovars: new N-coronafacoyl compounds. *Phytochemistry* **49**(6): 1579-1583.

Mitchell, R.E., & Young, H. (1985). N-coronafacoyl-L-isoleucine and N-coronafacoyl-L-*allo*isoleucine, potential biosynthetic intermediates of the phytotoxin coronatine. *Phytochemistry* **24**: 2716-2717.

Mitchell, R.E., Young, H., & Liddell, M.J. (1995). Isolation and structural characterization of 2-[1-oxo-2-cyclopenten-2-ylmethyl]-butanoic acid, a polyketide product of coronatine-producing *Pseudomonas* spp. *Tetrahedron*. *Lett*. **36**(18): 3237-3240.

Molloy, M.P., Herbert, B.R., Walsh, B.J., Tyler, M.I., Traini, M., Sanchez, J-C., Hochstrasser, D.F., Williams, K.L., & Gooley, A. A. (1998). Extraction of membrane proteins by differential solubilization for separation using two-dimensional gel electrophoresis. *Electrophoresis* **19**: 837-844.

Monne, M., Nilsson, I., Johansson, M., Elmhed, N., & von Heijne (1998). Positively and negatively charged residues have different effects on the position in the membrane of a model transmembrane helix. *J. Mol. Biol*. **284**: 1177-1183.

More, M.I., Pohlman, R.F., & Winans, S.C. (1996). Genes encoding the pKM101 conjugal mating pore are negatively regulated by the plasmid-encoded KorA and KorB proteins. *J. Bacteriol.* **178**: 284-293.

Morita, M., Kanemori, M., Yanagi, H., & Yura, T. (1999). Heat-induced synthesis of σ^{32} in *Escherichia coli*: structural and functional dissection of *rpoH* mRNA secondary structure. *J. Bacteriol.* **181**(2): 401-410.

Nakahigashi, K., Ron, E.Z., Yanagi, H., & Yura, T. (1999). Differential and independent roles of a σ^{32} homolog (RpoH) and an HrcA repressor in the heat shock response of *Agrobacterium tumefaciens*. *J. Bacteriol.* **181**(24): 7509-7515.

O'Farrell, P.H. (1975). High resolution two-dimensional electrophoresis of proteins. *J. Biol. Chem.* **250**: 4007-4021.

Ohta, N., Lane, T., Ninfa, E.G., Sommer, J.M., & Newton, A. (1992). A histidine protein kinase homologue required for regulation of bacterial cell division and differentiation. *Proc. Natl. Acad. Sci. USA* **89**: 10297-10301.

Okuyama, H., Sasaki, S., Higashi, S., & Murata, N. (1990). A *trans*-unsaturated fatty acid in a psychrophilic bacterium, *Vibrio* sp. strain ABE-1. *J. Bacteriol.* **172**(6): 3515-3518.

Osborn, M.J., Gander, J.E., Parisi, E., & Carson, J. (1972). Mechanism of assembly of the outer membrane protein of *Salmonella typhimurium*. *J. Biol. Chem.* **247**: 3962-3972.

Ouchane, S., & Kaplan, S. (1999). Topological analysis of the membrane-localized redox-responsive sensor kinase PrrB from *Rhodobacter sphaeroides*. *J. Biol. Chem*. **274**(24): 17290-17296.

Palmer, D.A., & Bender, C.L. (1993). Effects of environmental and nutritional factors on production of the polyketide phytotoxin coronatine by *Pseudomonas syringae* pv. glycinea. *Appl. Environ. Microbiol*. **59**: 1619-1626.

Palmer, D.A., & Bender, C.L. (1995). Ultrastructure of tomato leaf tissue treated with the pseudomonad phytotoxin coronatine and comparison with methyl jasmonate. *Mol. Plant-Microbe Interact*. **8**: 683-692.

Palmer, D.A., Bender, C.L., & Sharma, S. (1997). Use of Tn*5-gusA5* to investigate environmental and nutritional effects on gene expression in the coronatine biosynthetic gene cluster of *Pseudomonas syringae* pv. glycinea. *Can. J. Microbiol*. **43**: 517-525.

Park, H., & Inouye, M. (1997). Mutational analysis of the linker region of EnvZ, an osmosensor in *Escherichia coli*. *J. Bacteriol.* **179**: 4382-4390.

Parry, R.J., Lin, M.T., Walker, A.E., & Mhaskar, S. (1991). Biosynthesis of coronatine: investigation of the biosynthesis of coronamic acid. *J. Am. Chem. Soc*. **113**: 1849-1850.

Parry, R.J., Mhaskar, S.V., Lin, M.T., Walker, A.E., & Mafoti, R. (1994). Investigation of the biosynthesis of the phytotoxin coronatine. *Can. J. Chem*. **72**: 86-99.

Peñaloza-Vázquez, A., & Bender, C.L. (1998). Characterization of CorR, a transcriptional activator which is required for biosynthesis of the phytotoxin coronatine. *J. Bacteriol.* **180**: 6252-6259.

Peñaloza-Vázquez, A., Rangaswamy, V, Ullrich, M., Bailey, A.M., & Bender, C.L. (1996). Use of translational fusions to the maltose-binding protein to produce and purify proteins in *Pseudomonas syringae* and assess their activity *in vivo*. *Mol. Plant-Microbe Interact*. **9**: 637-641.

Peñaloza-Vázquez, A., Preston, G., Collmer, A., & Bender, C.L. (2000). Regulatory interactions between the Hrp type III protein secretion system and coronatine biosynthesis in *Pseudomonas syringae* pv. tomato DC3000. *Microbiology* **146**: 2447-2456.

Peng, W-T., Lee, Y-W., & Nester, E. W. (1998). The phenolic recognition profiles of the *Agrobacterium tumefaciens* VirA protein are broadened by a high level of the sugar binding protein ChvE. *J. Bacteriol.* **180**(21): 5632-5638.

Perraud, A-L., Weiss,V., & Gross, R. (1999). Signalling pathways in two-component phosphorelay systems. *Trends Microbiol*. **7**(3): 115-120.

Raleigh, E.A., Lech, K., & Brent, R. (1989) in *Current Protocols in Molecular Biology* eds. Ausbel, F.M. *et al*. Publishing Associates and Wiley Interscience; New York. Unit 1.4.

Rangaswamy, V., Mitchell, R., Ullrich, M., & Bender, C.L. (1998a). Analysis of genes involved in biosynthesis of coronafacic acid, the polyketide component of the phytotoxin coronatine. *J. Bacteriol.* **180**(13): 3330-3338.

Rangaswamy, V., Jiralerspong, S., Parry, R., & Bender, C.L. (1998b). Biosynthesis of the *Pseudomonas* polyketide coronafacic acid requires monofunctional and multifunctional polyketide synthase proteins. *Proc. Natl. Acad. Sci. USA* **95**: 15469-15474.

Rowley, K.B., Clements, D.E, Mandel, M., Humphreys, T., & Patil, S.S. (1993). Multiple copies of a DNA sequence from *Pseudomonas syringae* pathovar phaseolicola abolish thermoregulation of phaseolotoxin production. *Mol. Microbiol*. **8**: 625-635.

Rowley, K.B., Xu, R., & Patil, S.S. (2000). Molecular analysis of thermoregulation of phaselotoxin-resistant ornithine carbamoyltransferase (argK) from *Pseudomonas syringae* pathovar phaseolicola. *Mol. Plant-Microbe Interact*. **13**(10): 1071-1080.

Rübenhagen, R., Rönsch, H., Jung, H., Krämer, R., & Morbach, S. (2000). Osmosensor and osmoregulator properties of the betaine carrier BetP from *Corynebacterium glutamicum* in proteoliposomes. *J. Biol. Chem*. **275**(2): 735-741.

Rudolph, K., & Sonnenberg, B. (1997). Role of exopolysaccharides from *Pseudomonas syringae* pathovars in pathogenesis, p.265-270. *In* Rudolph, K., Burr, T.J., Mansfield,

J.W., Stead, D., Vivian, A., & von Kietzell, J. (ed), *Pseudomonas syringae* pathovars and related pathogens, Kluwer Academic Publishers, Dordrecht, The Netherlands.

Rutz, C., Rosenthal, W., & Schülein, R. (1999). A single negatively charged residue affects the orientation of a membrane protein in the inner membrane of *Escherichia coli* only when it is located adjacent to a transmembrane domain. *J. Biol. Chem*. **274**(47): 33757-33763.

Saiki, R.K., Gelfand, D.H., Stoffel, S., Scharf, S.J., Higuchi, R., Horn, G.T., Mullis, K.B., & Erlich, H.A. (1988). Primer-directed enzymatic amplification of DNA with thermostable DNA polymerase. *Science* **239**(4839): 487-491.

Sakai, R., Nishiyama, K., Ichihara, A., Shiraishi, K., & Sakamura, S. (1979). Studies on the mechanism of physiological activity of coronatine: Effect of coronatine on cell wall extensibility and expansion of potato tuber tissue. *Ann. Phytopathol. Soc. Japan* **45**: 645-653.

Sambrook, J., Fritsch, E.F., & Maniatis, T. (1989). Molecular cloning: a laboratory manual. Cold Spring Harbor Laboratory Press, Cold Spring Harbor, N.Y.

Saribas, A.S., Gruenke, L., & Waskell, L. (2001). Overexpression and purification of the membrane-bound cytochrome P450 2B4. *Protein Express. Purif*. **21**: 303-309.

Skerra, A. (1994). Use of the tetracycline promoter for the tightly regulated production of a murine antibody fragment in *Escherichia coli*. *Gene* **151**: 131-135.

Stachelhaus, T., & Marahiel, M.A. (1995). Modular structure of genes encoding multifunctional peptide synthetases required for non-ribosomal peptide synthesis. *FEMS Microbiol. Lett*. **125**: 3-14.

Stachel, S.E., & Zambryski, P.C. (1986). *virA* and *virG* control the plant-induced activation of the T-DNA transfer process of *A. tumefaciens*. *Cell* **46**: 325-333.

Starr, M.P., & Chatterjee, A.K. (1972). The genus *Erwinia*: enterobacteria pathogenic to plants and animals. *Annu. Rev. Microbiol*. **26**: 389-426.

Sundin, G.W., Kidambi, S.P., Ullrich, M., & Bender, C.L. (1996). Resistance to ultraviolet light in *Pseudomonas syringae*: sequence and functional analysis of the plasmid-encoded *rulAB* genes. *Gene* **177**: 77-81.

Surette, M.G., Levit, M., Liu, Y., Lukat, G., Ninfa, E.G., Ninfa, A., & Stock, J.B. (1996). Dimerization is required for the activity of the protein histidine kinase CheA that mediates signal transduction in bacterial chemotaxis. *J. Biol. Chem*. **271**(2): 939-945.

Suzuki, I., Los, A.D., Kanesaki, Yu, Mikami, K., & Murata, N. (2000). The pathway for perception and transduction of low-temperature signals in *Synechocystis*. *EMBO J.* **19** (6): 1327-1334.

Suzuki, I., Kanesaki, Yu, Mikami, K., Kanehisa, M., & Murata, N. (2001). Cold-regulated genes under control of the cold sensor Hik33 in *Synechocystis*. *Mol. Microbiol*. **40**(1): 235-244.

Swanson, R.V., Alex, L.A., & Simon, M.I. (1994). Histidine and aspartate phosphorylation: two-component systems and the limits of homology. *TIBS* **19**: 485-490.

Taira, S., Tuimala, J., Roine, E., Nurmiaho-Lassila, E-L., Savilahti, H., & Romantschuk, M. (1999). Mutational analysis of the *Pseudomonas syringae* pv. tomato *hrpA* gene encoding Hrp pilus subunit. *Mol. Microbiol*. **34**(4): 736-744.

Tang, J-L., Feng, J-X., Li, Q-Q., Wen, H-X., Zhou, D-L, Wilson, T.J.G., Dow, J.M., Ma, Q-S., & Daniels, M.J. (1996). Cloning and characterization of the *rpfC* gene of *Xanthomonas oryzae* pv. oryzae: involvement in exopolysaccharide production and virulence to rice. *Mol. Plant-Microbe Interact.* **9**(7): 664-666.

Tamai, E., Fann, M-C., Tsuchiya, T., & Maloney, P. (1997). Purification of UhpT, the sugar phosphate transporter of *Escherichia coli*. *Protein Express. Purif*. **10**: 275-282.

Taylor, B.L., & Zhulin, I.B. (1999). PAS domains: internal sensors of oxygen, redox potential, and light. *Microbiol. Mol. Biol. Rev*. **63**(2): 479-506.

Thomas, M.D., Langston-Unkefer, P.J., Uchytil, T.F., & Durbin, R.D. (1983). Inhibition of glutamine synthetase from pea by tabtoxinine-ß-lactam. *Plant Physiol*. **71**: 912-915.

Tomomori, C., Tanaka, T., Dutta, R., Park, H., Saha, S.K., Zhu, Y. *et al*. (1999). Solution structure of homodimeric core domain of *Escherichia coli* histidine kinase EnvZ. *Nat. Struct. Biol*. **6**: 729-734.

Toyoda-Yamamoto, A., Shimoda, N., & Machida, Y. (2000). Genetic analysis of the signal-sensing region of the histidine protein kinase VirA of *Agrobacterium tumefaciens*. *Mol. Gen. Genet*. **263**: 939-947.

Trevor, C.C., & Nester, E.W. (1993). A chromosomally encoded two-component sensory transduction system is required for virulence of *Agrobacterium tumefaciens. J. Bacteriol.* **175**(20): 6614-6625.

Turner, J.G., & Debbage, J.M. (1982). Tabtoxin-induced symptoms are associated with accumulation of ammonia formed during photorespiration. *Physiol. Plant Pathol*. **20**: 223-233.

Uhl, M.A., & Miller, J.F. (1996). Integration of multiple domains in a two-component sensor protein: the *Bordetella pertussis* BvgAS phosphorelay. *EMBO J*. **15**: 1028-1036.

Ullrich, M.S., & Bender, C.L. (1994). The biosynthetic gene cluster for coromanic acid, an ethylcyclopropyl amino acid, contains genes homologous to amino acid-activating enzymes and thioesterases. *J. Bacteriol.* **176**(24): 7574-7586.

Ullrich, M., Bereswill, S., Voelksch, B., Fritsche, W., & Geider, K. (1993). Molecular characterization of field isolates of *Pseudomonas syringae* pv. glycinea differing in coronatine production. *J. Bacteriol.* **139**: 1927-1937.

Ullrich, M.S., Peñaloza-Vázquez, A., Bailey, A.M., & Bender, C.L. (1995). A modified two-component regulatory system is involved in temperature-dependent biosynthesis of the *Pseudomonas syringae* phytotoxin coronatine. *J. Bacteriol.*. **177**: 6160-6169.

Ullrich, M.S., Schergaut, M., Boch, J., & Ullrich, B. (2000). Temperature-responsive genetic loci in the plant pathogen *Pseudomonas syringae* pv. glycinea. *Microbiol*. **146**: 2457-2468.

van Dijk, K., Fouts, D.E., Rehm, A.H., Hill, A.R., Collmer, A., & Alfano, J.R. (1999). The Avr (effector) proteins HrmA (HopPsyA) and AvrPto are secreted in culture from *Pseudomonas syringae* pathovars via the Hrp (type III) protein secretion system in a temperature- and pH-sensitive manner. *J. Bacteriol.* **181**(16): 4790-4797.

Vígh, L., Maresca, B., & Harwood, J.L. (1998). Does the membrane‘s physical state control the expression of heat shock and other genes? *TIBS* **23**: 369-374.

von Heijne, G. (1992). Membrane protein structure. Hydrophobicity analysis and the positive-inside rule. *J. Mol. Biol*. **225**: 487-494.

Voss, S., & Skerra, A. (1997). Mutagenesis of a flexible loop in streptavidin leads to higher affinity for the *Strep*-tag II peptide and improved performance in recombinant protein purification. *Protein Eng*. **10**: 975-982.

Wang, L., Bender, C.L., & Ullrich, M.S. (1999). The transcriptional activator CorR is involved in biosynthesis of the phytotoxin coronatine and binds to the the *cmaABT* promoter region in a temperature-dependent manner. *Mol.Gen.Genet*. **262**: 250-260.

Waukau, J., & Forst, S. (1999). Identification of a conserved N-terminal sequence involved in transmembrane signal transduction in EnvZ. *J. Bacteriol.* **181**(17): 5534-5538.

Wei, Z.M., Sneath, B.J., & Beer, S.V. (1992). Expression of *Erwinia amylovora hrp* genes in response to environmental stimuli. *J. Bacteriol.* **174**: 1875-1882.

Wei, Z.M., Kim, J.F., & Beer, S.V. (2000). Regulation of hrp genes and typeIII protein in *Erwinia amylovora* by HrpX/HrpY, a novel two-component system, and HrpS. *Mol. Plant-Microbe Interac.* **13**(11): 1251-1262.

Weingart, H., Völksch, B., & Ullrich, M.S. (1999). Comparison of ethylene production by *Pseudomonas syringae* and *Ralstonia solanacearum. Phytopathol*. **89**: 360-365.

Weingart, H., & Ullrich, M.S. Unpublished results.

Wilkinson, S.G. (1988). Gram-negative bacteria, p. 333-346. *In* Ratledge, C., & Wilkinson, S.G. (ed), Microbial lipids, v.1. Academic Press, Harcourt Brace Jovanovich, Publishers, London.

Williams, S.B., & Stewart, V. (1999). Functional similarities among two-component sensors and methyl-accepting chemotaxis proteins suggest a role for linker region amphipathic helices in transmembrane signal transduction. *Mol. Microbiol*. **33**(6), 1093-1102.

White-Zieger, C.A., Angus Hill, M.L., Braaten, B.A., van der Woude, M.W., & Low, D.A. (1998). Thermoregulation of pap transcription: H-NS is a temperature-dependent DNA methylation blocking factor. *Mol. Microbiol*. **28**: 1121-1137.

Zhang, M., Wang, G., Shapiro, A., & Zhang, J.T. (1996). Topological folding and proteolysis profile of P-glycoprotein in membranes of mutidrug-resistant cells: implications for the drug-transport mechanism. *Biochemistry* **35**: 9728-9736.

Zhou, H., Lowry, D.F., Swanson, R.V., Simon, M.I., & Dahlquist, F.W. (1995). NMR studies of the phosphotransfer domain of the histidine kinase CheA from *Escherichia coli*: assignments, secondary structure, general fold and backbone dynamics. *Biochemistry* **34**: 13858-13870.

Acknowledgments

This work was done under supervision of PD Dr. M.S. Ullrich in the Ecophysiology group of the Max-Plank Institute for terrestrial Microbiology (Marburg) from June, 1998 to June, 2001. The project was supported by grants from the Max-Plank-Gesellschaft and Deutsche Forschungsgemeinschaft.

I would like to thank:

PD Dr. M.S. Ullrich for giving me the chance to work on this project, for supporting me with ideas and advice, in order to solve efficiently all theoretical and experimental problems in a way for realization of the main goals of the project. I am especially grateful to Dr. Ullrich for his sincere help in all problems concerning my accommodation and living in Marburg.

Prof. Dr. R.K. Thauer for giving me the possibility to do this work in the MPI for terrestrial Microbiology and for taking over the supervision of the project.

Prof. Dr. R. Kahmann and Prof. Dr. U. Maier for taking part in the examination commission and discussion of the project.

Dr. S. Taira (University of Helsinki) for help in the mutagenesis approach.

Prof. Dr. E. Bremer and PD. Dr. U. Völker for stimulating discussion at all steps of the project.

All members of our Ecophysiology group who already left and who are working in the laboratory for help, stimulating discussions and good working atmosphere from the first steps of working on the project to the end of the Ph.D. work.

Stephan Aufhammer, Antje Burse, and Helge Weingart for help in reading of the manuscript and all critical notes about it.

Bettina Rohde and Ina Budde for teaching me the protein techniques and the HPLC method.

Nicol Rössel and Petra Roth for technical support in overexpression of CorS.

Reinhard Böcher and Dr. A. Titze for technical support in gas chromatography.

Alexander Schenk for solving computer problems.

Stephan Aufhammer for taking over the project and for enthusiastic work on it.

Peter Dunfield for moral support, reading of the manuscript and all critical notes about it.

All members of groups of Thauer, Bremer, Völker, Conrad and Buckel for advice concerning methods, techniques and instruments used during this work.